# A SURVEY OF OXYGEN-INDUCED RADICALS IN IRRADIATED UHMWPE

M. Shah Jahan[1*], Muhammad Fuzail[2†], Benjamin M. Walters[1]

*corresponding author: [1]Department of Physics, 216 Manning Hall, The University of Memphis, Memphis, TN 38152, USA; phone 901-678-2620, fax: 901-678-4733; e-mail: mjahan@memphis.edu.
[2]PINSTECH, Islamabad, Pakistan

**Introduction**

In irradiated (x-, gamma or e-beam radiation) ultra-high molecular weight polyethylene (UHMWPE), polyethylene radicals (alkyl/ally) decay in air via oxidative reaction. Following the decay, oxygen induced radicals (OIR) are formed which remain very stable for a very long time; 20 years in this laboratory. OIR, also known as residual or terminal radicals, may have long-term oxidation potential. Under normal operating condition, 1-2 mW microwave power and 1-5 G modulation amplitude at X-band (~9 GHz), electron spin resonance (ESR) spectrometer produces a single-line spectrum or a singlet with no apparent hyperfine structure for the OIR. The peak-to-peak width $\Delta$Hpp of the spectrum is 10 G and the g-value 2.0015, approximately. Most reports [1-4] attribute this singlet to a peroxy specie (POO$^{\cdot}$), because it is primarily observed in the presence of oxygen.

In recent studies Jahan and Durant[5] and Jahan and Fuzail [6] used power saturation technique at low temperature to reveal that the singlet due to the OIR was in fact made of two overlapping spectra: one due to a polyenyl radical R1 (-C$^{\cdot}$H-[CH=CH-]$_{m}$-) with number of conjugation m>3, and the other R2 (-CHO$^{\cdot}$-[CH=CH-]$_{m}$-), an oxygen-centered di- or tri-enyl radical (m=2 or m=3). The ESR spectrum of R1 is a singlet with $\Delta H_{pp}$ = 5G and g = 2.00434, and it is observed at low microwave power. The spectrum for R2 is observed at high microwave power, and its g-value is 2.0056 and has 6 weakly-resolved hyperfine lines with line spacing of 4.8 G, approximately. Based on the annealing experiment, it was further speculated that R1 resided in the crystalline environment and R2 stretched out of or dangled at the crystalline regions. More speculatively, R2 resides in the voids or imperfections of the crystalline region [6].

While our laboratory is engaged in investigating the fate of the OIR in UHMWPE and their potential for oxidation, we present, in this report, ESR data of a representative group of UHMWPE samples which were shelf-aged in air for 1-20 years following irradiation with gamma or e-beam. The objective of this study is to determine: 1) whether or not R1 and R2 are independent radicals, and 2) the effect of sample history on their relative concentration.

**Materials and Methods**

UHMWPE used in this study were solid (ram extruded or compression molded) or powder GUR 4120, GUR 4150, Himont 1900, GUR 1020 and GUR 1050, and vitamin E (alpha-tocopherol)-blend powder and consolidated solid (GUR 1020). Retrieved acetabular cups and knee-joint plateaus (6-8 years in vivo and 13 years post-retrieval aging in air) were also included in this study. For irradiation/sterilization purpose gamma (60Co) or electron beam was used. Free radical measurements were conducted at room temperature using an X-band (~9.8 GHz) ESR spectrometer (Bruker EMX300). ESR spectra were recorded at microwave power 1-160 mW, and modulation amplitudes between 1.0 and 5.0 G.

**Results and discussion**

Figure 1 shows two ESR spectra per sample; one recorded at 1 mW and the other at 160 mW microwave power. As reported in the previous publications [5-7], OIR (in air-exposed samples) show a singlet at 1 mW and a multi-line spectrum at
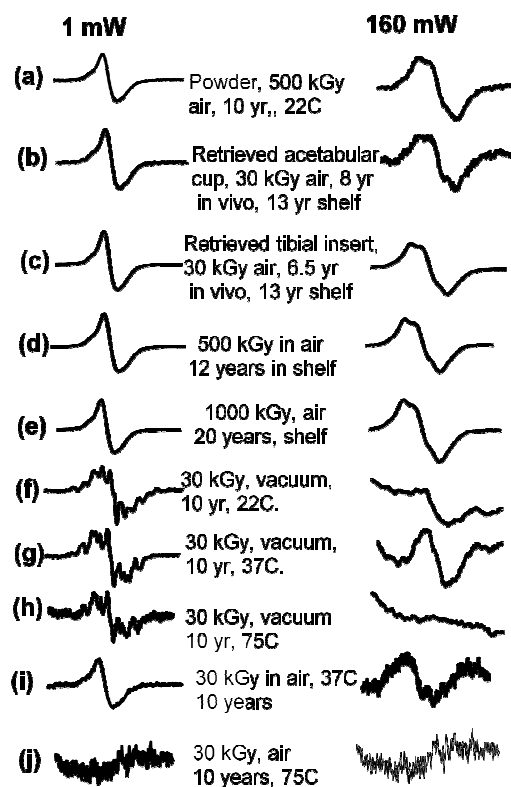


Fig. 1. ESR spectrum of irradiated UHMWPE plotted as a function of microwave power.

160 mW (spectra a-e in Fig. 1). Similar behavior is observed for OIRs present in vitamin E-containing UHMWPE (not shown). For clarity, a representative multi-line spectrum of R2 is shown in Fig. 2 (see ref. 6). Fig. 1 also shows spectra of vacuum-sealed samples which were aged for 10 years at room temperature (22$^{\circ}$C (f)), 37$^{\circ}$C (g) or 75$^{\circ}$C (h). At 1 mW, each of these samples shows ESR spectrum characteristic of primary alkyl/allyl radicals, and at 160 mW, no resolvable spectrum was detected because of microwave-power saturation of the ESR signals of the same carbon-centered radicals. This test does confirm the lack or absence of OIR in the vacuum-sealed samples. When heated at 75$^{\circ}$C for 10 years in the presence of oxygen (air), no radicals could be present for detection. But at 37$^{\circ}$C for the same duration, a weak signal due to R1 and a much weaker one due to R2 were observed. Similar test may provide an answer to the question whether or not R1 and R2 would decay independently.
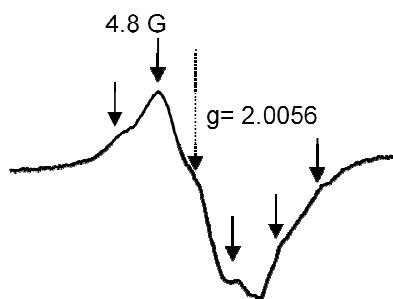


Fig. 2. ESR spectrum of radical R2 recorded at -133$^{\circ}$C using microwave power 10 mW and modulation amplitude 1 G. Arrows showing positions of the six lines with separation of 4.8 G, approximately.

## Summary
1) In irradiated UHMWPE, long-term oxidation in air produces a carbon-centered polyenyl radical (R1), detectable at low microwave power (1 mW, for example), and an oxygen-centered di- or tri-enyl radical (R2), detectable at high power (160 mW, for example).
2) In contrast, long-term storage in an inert environment (vacuum, for example) does not produce any OIR, R1 or R2, in irradiated UHMWPE.
3) In an inert environment the primary radicals are found to survive for more than 10 years (in this study) at 22$^{\circ}$C, 37$^{\circ}$C or 75$^{\circ}$C. It has to be emphasized that the primary radicals (carbon-centered) are detectable at low power only (1 mW, for example). High-power (160 mW) ESR

spectrum of each of these samples confirm the absence of OIR.
4) Analysis for determination of relative abundance of these two radicals R1 and R2 as a function of sample history is in progress.

## References
[1] P.O. Neill, Birkinshaw C. et al., Polymer Degradation and Stability 63 (1999) 31-39.
[2] M.S Jahan, C. Wang, G. Schwartz, J.A. David, Biomed. Mater. Res. 25 (1991) 1005.
[3] K. Nakamura, S. Ogata, Y. Ikada, Biomaterials, 19 (1998) 2341.
[4] L. Costa, M.P Luda, L. Trossarelli, E.M. Brach del Prever, M. Crova, P. Gallinaro, Biomaterials 19 (1998) 659.
[5] M.S. Jahan, J. Durant NIMB, 236 (2005) 166-171.
[6] Jahan, M. Shah, M. Fuzail, NIMB, 265 (2007) 67-71.
[7] J. Durant, M.S. Jahan, NIMB, 236 (2005) 160-165.

# INFLUENCE OF THE POLYETHYLENE STRUCTURE ON THE REACTIVITY OF THE RADICALS PRODUCED BY IRRADIATION

I. Carpentieri*[1], S. Bonomi[3], P. Bracco[1], E.M. Brach del Prever[2], V. Brunella[1], M.P. Luda[1], M.C. Paganini[1], M. Zanetti[1], L. Costa[1]

[1] *Dipartimento di Chimica IFM e NIS-Centre of Excellence, Università degli Studi di Torino, Via P. Giuria 7, 10125, Torino, Italy. e-mail: ilenia.carpentieri@unito.it*
[2]*Dipartimento di Traumatologia, Ortopedia e Medicina del Lavoro dell'Università di Torino, CTO, Torino, Italy*
[3]*Bioster S.p.A., Seriate (BG), Italy*

## Introduction

Irradiation of UHMWPE under inert gas leads to formation of radicals. UHMWPE is best regarded as a three-phase material which contains in addition to the fully crystalline and fully amorphous phases a significant interfacial all-trans phase [1]. Macro-alkyl radicals are formed upon irradiation in all three phases as major species, being the energy of the incident radiation some order of magnitude higher than that of the C-H bonds.

ESR studies showed that the formed macro-alkyl radicals decay in about ten hours, leaving an ESR signal, which has been attributed to macro-allyl radicals [2].

Vinyl double bonds and phenol groups of some antioxidants (i.e. Vitamin E) are consumed during irradiation [3]. These species are fixed on the polymer chain (double bonds) or allowed a very limited mobility, due to low diffusion coefficients (additives). Thus, a very high migration rate of the macro-alkyl radical must be hypothesized to justify the interaction between the radical and the reactive species, whose concentration is comparable to that of the radical itself (some mmol/l).

If irradiation occurs in the presence of oxygen, macro-alkyl radicals react with oxygen triggering the oxidation process.

Percentage of crystallinity, size of crystallites and mobility of the polymer chains in the amorphous phase can vary considerably among different polyethylenes.

The aim of the present study is to evaluate the influence of the polyethylene morphology on the evolution of the radiation-induced oxidation process. Moreover, it has also been attempted to determine in which phase the radicals produced by irradiation remain. E-beam has been used for irradiation, being a fast method to produce radicals.

## Materials and Methods

Different commercial polyethylenes were included in the study of the post-irradiation oxidation process: UHMWPE GUR1050 (Ticona), HDPE ML70U, LDPE FC20, LLDPE FF25 (Polimeri Europa), VLLDPE Engage 8842 (Dow).

150 microns thick films have been e-beam irradiated at 60 kGy, at RT, in air and in vacuum. All PE samples have been kept in liquid nitrogen until the measurement began.

Irradiated and unirradiated samples were characterized by DSC to obtain information on the crystal morphology, ESR spectroscopy to investigate the radical evolution and FTIR spectroscopy to follow post-irradiation oxidation at RT and crosslinking.

## Results and discussion

The DSC results show that the lamellae thickness is very different in the PEs considered. UHMWPE and HDPE show the thickest lamellae (respectively about 60 and 15 nm); LDPE and LLDPE have lamellae in the order of some nm and the VLLDPE is nearly completely amorphous.

In figure 1 the ESR spectra recorded at 0.1 mW for the PEs irradiated in vacuum are reported.
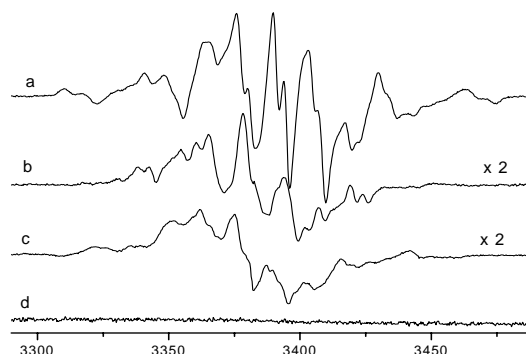


*Figure 1. ESR signal of : a) UHMWPE and HDPE 30 min after e-beam irradiation; b) UHMWPE and HDPE 24 h after e-beam irradiation; c) LDPE and LLDPE 30 min after e-beam irradiation; d) VLLDPE 30 min after e-beam irradiation*

Figure 1a shows the ESR spectrum obtained immediately after irradiation for UHMWPE and HDPE. This signal can be attributed to a macro-alkyl radical. As it can be observed in figure 1b, 24 h after irradiation the ESR spectrum of UHMWPE and HDPE changes, as reported in literature [2]. The new signal obtained can be attributed to macro-allyl radical, as mentioned before.

On the contrary, in LDPE and LLDPE the signal of the macro-allyl radicals was recorded immediately after irradiation (figure 1c).

No radicals at all have been detected after irradiation of the nearly completely amorphous VLLDPE (figure 1d).

Figure 2a and 2b show the build up of carbonyl products during the post-irradiation period in the PEs irradiated in air.
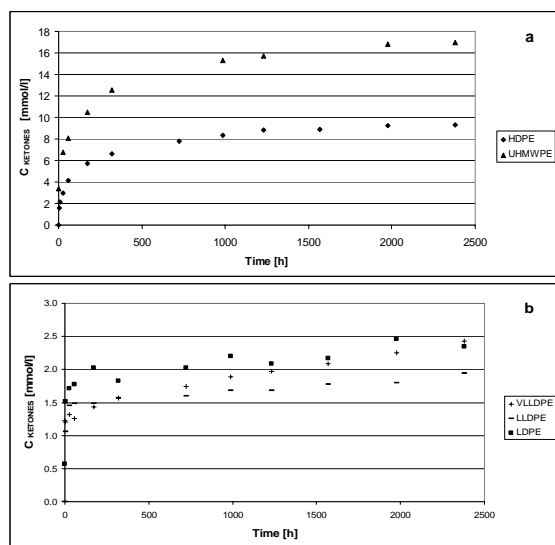


*Figure 2. Post-irradiation oxidation behaviour at RT of: a) HDPE and UHMWPE; b) LDPE, LLDPE and VLLDPE. Note the scale change on y-axes!*

The maximum oxidation level is reached in few hours for LDPE, LLDPE and VLLDPE (figure 2b), while it takes longer for UHMWPE and HDPE (figure 2a) and the overall level is higher in this case. Moreover, as it is shown in figure 3, the rate of oxidation is higher for HDPE than for UHMWPE.
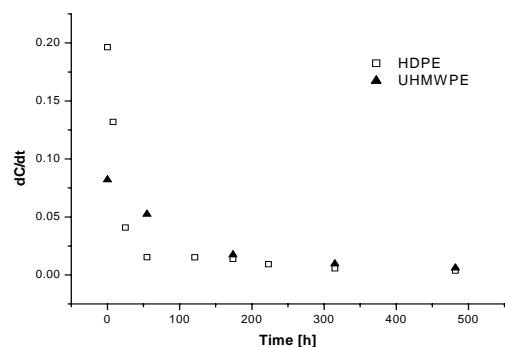


*Figure 3. Oxidation rate of UHMWPE and HDPE*

The oxidation kinetic is regulated by the concentration of radicals and that of oxygen. The oxygen solubility in the amorphous phase of PE is about 0.2 mmol/l [4].

In all the samples the oxidation level is higher than the oxygen concentration; this means that the oxygen diffuses in the polymer from the surrounding atmosphere.

Considering the nearly completely amorphous VLLDPE irradiated in vacuum, no radicals were detected. This can be explained assuming that the radicals formed in the amorphous phase decayed in very short time and cannot be detected in the timescale of our experiment. This justifies the very low level of oxidation found in this polymer; in fact, only the oxygen already present in the amorphous phase and that which diffuses in the polymer during the irradiation time is able to react with the very unstable macro-alkyl radicals in the amorphous phase.

Assuming that the radicals that we are able to detect are not in the amorphous phase, we can suppose that the post-irradiation oxidation is due to the migration of the radicals from the crystalline/all-trans phases to the amorphous one, where there is oxygen available. Therefore, the thickness of the lamellae plays a very important role in the oxidation level of the polymer.

In LDPE and LLDPE the post-irradiation oxidation level is very low and it is reached in a very short time, because the thickness of the lamellae is of some nm; this means that the time of migration of the radicals from the crystalline/all-trans amorphous phase to the amorphous one is very short. In fact we are not able to detect the macro-alkyl radicals in the ESR spectrum, but only the macro-allyl radicals present probably in the all-trans phase.

On the contrary, HDPE and UHMWPE show a high oxidation level reached in a long time in the post-irradiation period. This is due to the thick lamellae, the macro-alkyl radicals needing time to migrate in the amorphous phase; in fact in this polymers the signal of the macro-alkyl radicals in the crystalline/all-trans phase is present. Considering the dimensions of the lamellae, it is also explained the higher rate of oxidation of HDPE in comparison with UHMWPE; the smaller the lamellae, the faster is the post-irradiation oxidation process, being the macro-alkyl radicals faster to migrate in the amorphous phase.

**Conclusion**

The macroradicals detected after the irradiation process at RT, both with e-beam and gamma-rays, are those in the crystalline/all-trans phases.

The migration rate of the macro-alkyl radicals from the crystalline/all-trans phase to the amorphous one defines the oxidation level and the time to reach the maximum of oxidation during the post-irradiation period.

**References**
1. D. Barron, C. Birkinshaw, *Polymer*, 49, 3111-3115 (2008)
2. M. Dole, editor. *The radiation chemistry of macromolecules, Volume I* (1972)
3. L. Costa, I. Carpentieri, P. Bracco. Post e-beam irradiation oxidation of orthopaedic UHMWPE stabilized with vitamin E. *Polymer Degradation and Stability* (2009). In press
4. J. Pospìšil, P.P. Klemchuk, editors. *Oxidation inhibition in Organic Materials, Volume II.* (1990)

# IN VIVO OXIDATION, OXIDATION POTENTIAL, AND CLINICAL PERFORMANCE OF HIGHLY CROSSLINKED UHMWPEs IMPLANTED FOR UP TO 8 YEARS

Steven M. Kurtz*[1], Francisco Medel[1], Dan MacDonald[1], and Clare Rimnac[2]

[1] *Drexel University and Exponent, 3401 Market St. Suite 300, Philadelphia, PA 19104, USA, skurtz@drexel.edu*
[2] *School of Mechanical and Aerospace Engineering, Case Western Reserve University, Cleveland, OH, USA*

## Introduction

Highly crosslinked polyethylenes (HXLPEs) were clinically introduced in 1998. The hypothesis behind their use was that patients would experience reduced implant wear, which would mitigate loosening, osteolysis, and the subsequent need for revision. The relationship between clinical outcomes for THA and *in vivo* oxidation remains unclear. In this study we also tested the hypothesis that bearing surface oxidation, oxidation potential, and wear increase with implantation time in highly crosslinked liners.

## Methods

We analyzed oxidation, oxidation potential (hydroperoxide content), wear, and rim damage for 189 acetabular components revised at multiple centers between 2000-09. Liners were classified as annealed crosslinked (n=67; Crossfire); remelted crosslinked (n=90; Longevity and XLPE); or conventional gamma-inert sterilized (n=32). Annealed, remelted, and conventional liners were implanted for an average of 2.8y (range: 0.0–8.0y), 1.8y (range: 0.0–7.3y), and 5.5y (range: 0.0–13.8y), respectively. Femoral head penetration was directly measured from retrieved liners with a micrometer if they were implanted for >1y. Mechanical properties were measured using the small punch test. Oxidation, tranvinylene content, crystallinity and hydroperoxide content were determined using FTIR.

## Results

The most frequent reasons for revision were loosening (34%), instability (28%) and infection (21%) (Fig. 1). One annealed liner was revised with *in vivo* fracture of the rim. Annealed and remelted liners had comparable linear penetration rates (0.05, 0.04 mm/y, respectively, on average; p=0.3), and were significantly lower than conventional retrievals (0.12 mm/y; p≤0.01). Conventional and annealed acetabular liners showed elevated rim oxidation whereas remelted liners showed zero-to-low oxidation (Fig. 2). Elevated hydroperoxide content was observed at the rim of the conventional and annealed liners. Low but measurable oxidation potential was observed in the remelted liners (Fig. 3). According to logistic models, the reason for revision was not significantly related to polyethylene formulation (p=0.16), patient factors

(p≥0.1), penetration rate (p=0.14), or oxidation at the bearing surface (p>0.05).

## Discussion and Conclusions

This retrieval study including first-generation HXLPEs liners demonstrated lower wear than conventional polyethylene. While loosening remained the most prevalent reason for revision, we could not demonstrate a relationship between wear and loosening. The long-term clinical performance of first-generation HXLPEs remains promising, based on the mid-term outcomes of the components documented in this study.
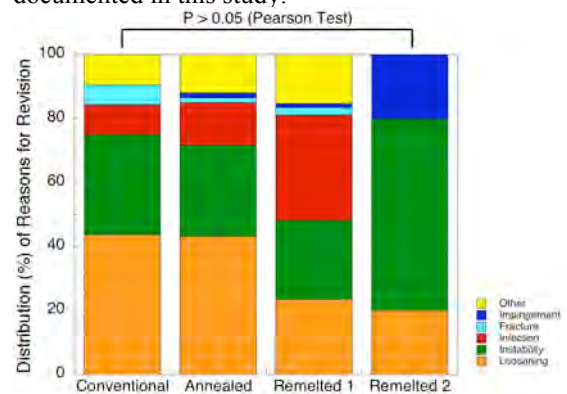


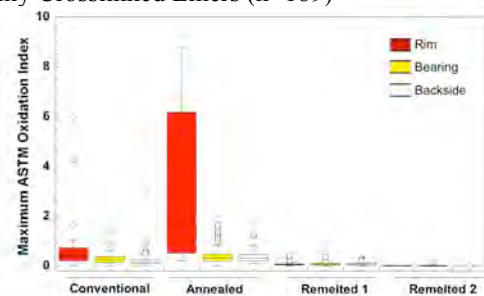Figure 1. Summary of Reasons For Revision in Highly Crosslinked Liners (n=189)



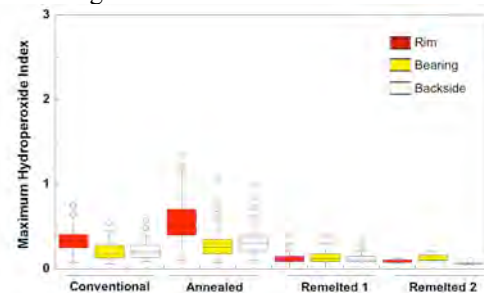Figure 2. Regional Oxidation in UHMWPE Liners.



Figure 3. Regional Oxidation Potential in UHMWPE liners.

# NITROXIDES AS FREE RADICAL SCAVENGERS IN UHMWPE

Marina K. Chumakov*[1], Joseph Silverman[2], and Mohamad Al-Sheikhly[2]

[1] *Fischell Department of Bioengineering, University of Maryland, College Park, MD 20742, USA*
[2] *Department of Materials Science & Engineering, University of Maryland, College Park, MD 20742, USA*
*\*chumakov@umd.edu*

## Introduction

Ultra-high molecular weight polyethylene (UHMWPE) has been the standard articulating lining material used in total joint arthroplasty for several decades. Yet, oxidation, premature aging and wear of the material and implant can cause a painful inflammation, bone resorption and loosening of the implant. Residual free radicals are a central concern because standard sterilization and crosslinking using $^{60}Co$ and electron beam produces alkyl free radicals in the polymer chain. These alkyl radicals can react to form bimolecular crosslinks at high dose rates, form long-lived allyl radicals, or react with oxygen at low dose rates to form the corresponding peroxyl radicals. These peroxyl radicals then produce hydroperoxides, more carbon-centered free radicals, and other oxidative degradation products. As an alternative to post-irradiation annealing, which allows radical recombination but reduces fatigue strength, antioxidants can be infused into the UHMWPE to act as radical scavengers. Nitroxides are stable organic compounds that have a strong paramagnetic signal and are very efficient in preventing lipid peroxidation and providing radioprotection in biological tissues[1, 2]. Nitroxides are also efficient carbon-centered free radical scavengers[3] *in vivo*. Through the electron transfer mechanism, radiolytically-produced carbon-centered free radicals in UHMWPE will combine with the nitroxide radical. This work aims to demonstrate the scavenging of residual alkyl and allyl free radicals in UHMWPE with nitroxide doping.

## Materials and Methods

The nitroxides used in this study were 2,2,6,6–Tetramethylpiperidine–1–oxyl (TEMPO) and 4-Hydroxy-2,2,6,6-Tetramethylpiperidine–1–oxyl (TEMPOL). Pellets of 1/8 in. diameter and 15 mm length were drilled from ultra high molecular weight polyethylene (UHMWPE) cylindrical disks (Biomet, Inc., Warsaw, IN.) with a custom plug cutter. Some of these pellets were then doped with TEMPO and TEMPOL, and some were left as virgin UHMWPE samples. Half the pellets were then packaged in Argon and the rest irradiated in air. Two $^{60}Co$ γ-ray sources and the 7 MeV electron linear accelerator (LINAC), at the University of Maryland radiation facilities, were used to irradiate and crosslink the UHMWPE samples. The dose rates used were 2.3 kGy h$^{-1}$, 20 kGy h$^{-1}$, and 650 kGy h$^{-1}$. Total irradiation doses consisted of 0 kGy, 30 kGy, and 100 kGy. After irradiation, samples were transferred to quartz EPR tubes in an Argon-filled glove bag. A Bruker ESP 300 Electron Paramagnetic Resonance (EPR) Spectrometer was used to detect the production of radiolytically-produced free radicals in UHMWPE, measure the consumption of the TEMPO and TEMPOL radical, and observe the interaction of nitroxide and UHMWPE free radicals. EPR parameters were set to 2 mW power, 1 G modulation amplitude, 163.84 ms time constant, and 100 kHz modulation frequency.

## Results and discussion

TEMPO and TEMPOL-doped UHMWPE exhibits a strong triplet structure observed with the EPR. The nitroxide signature triplet was quantified using a measure of the peak-to-peak heights. Naturally, the Argon packaged samples exhibited lower free radical concentrations. The virgin UHMWPE pellets demonstrated the characteristic allyl radical septet. The alkyl radical is not visible due to the fast conversion to allyl during the transfer time in the glove bag. As the nitroxide-doped UHMWPE pellets were irradiated with increasing doses using $^{60}Co$ γ-rays and electrons, the concentration of nitroxide radicals began to decrease, as shown in Figure 1.
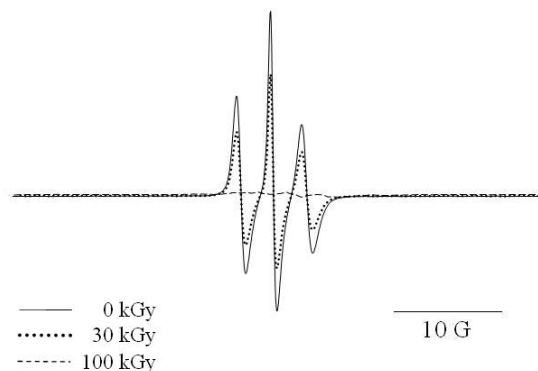


*Figure 1: EPR Spectra of TEMPO-Doped UHMWPE Irradiated to 0 kGy, 30 kGy, and 100 kGy showing consumption of nitroxide radical.*

Eventually, there is a complete consumption of the nitroxide, as the triplet structure gives way to minimal residual allyl free radicals. The initial nitroxide concentration is a function of the doping time. Two nitroxide concentrations, with peak-to-peak intensity measurements, as a function of dose, are shown in Figure 2. This plot demonstrates that by 100 kGy, all of the nitroxide has been

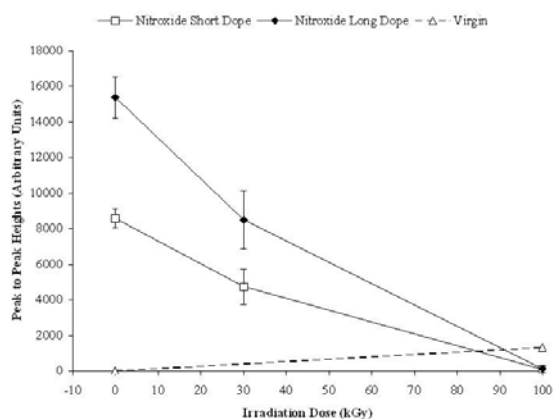consumed, through reaction with the free radicals produced by the 100 kGy dose.



*Figure 2: EPR Peak to Peak Heights with Irradiation Dose (Gy): TEMPO Central Triplet Peak Height in Doped UHMWPE and Allyl Radical Peak Height.*

If UHMWPE is doped with the nitroxide before irradiation, there would be a cross-linking inhibition, as has been cited with Vitamin E (α-tocopherol)[4]. The number of carbon-centered free radicals is dependent on the irradiation dose. Thus, if the residual free radical concentration is known just after crosslinking, the minimal amount of antioxidant can be infused into the polymer to scavenge the rest of the free radicals. By quantifying the concentration of nitroxides needed to scavenge a known concentration of alkyl, allyl, and peroxyl radicals, a very minimal quantity of foreign molecules would need to be used. Assuming that all of the nitroxide would be consumed through radical scavenging, the concern that there would be antioxidant elution out of the prosthesis would be reduced.

## Conclusion

Nitroxides have been shown to scavenge alkyl and allyl free radicals in UHMWPE, in addition to *in vivo*. Through a carefully calibrated quantification of nitroxide concentration and UHMWPE concentration in the EPR, it will be possible to estimate the needed antioxidant concentration to scavenge residual free radicals that may cause oxidation and wear in the long-term. Such a process will reduce the amount of additive infused in UHMWPE, reducing risk to the patient. This technique will be demonstrated with both TEMPO and TEMPOL, at varying concentrations, with a wide range of irradiation doses and dose rates.

## References
[1] B. P. Soule, The chemistry and biology of nitroxide compounds. *Free Radical Biology & Medicine* **42**, 1632-1650 (2007).
[2] A. Samuni, S. Goldstein, A. Russo, J. B. Mitchell, M. C. Krishna and P. Neta, Kinetics and Mechanism of Hydroxyl Radical and OH-Adduct Radical Reactions with Nitroxides and with Their Hydroxylamines. *Journal of the American Chemical Society* **124**, 8719-8724 (2002).
[3] A. L. J. Beckwith, V. W. Bowry and K. U. Ingold, Kinetics of nitroxide radical trapping. 1. Solvent effect. *Journal of the American Chemical Society* **114**, 4983-4992 (1992).
[4] E. Oral, K. K. Wannomae, N. Hawkins, W. H. Harris, O. K. Muratoglu. α-Tocopherol-doped irradiated UHMWPE for high fatigue resistance and low wear. *Biomaterials* **25** 5515 – 5522 (2004).

# HINDERED AMINE LIGHT STABILIZERS:
# A (BETTER) ALTERNATIVE FOR RADIATION CROSS-LINKED UHMWPE IMPLANTS

Pieter Gijsman*[1], Harold Smelt[2], Detlef Schumann[3]

[1] DSM Research, SRU PM-CT/TP, P.O. Box 18, 6160 MD Geleen, The Netherlands,
e-mail: pieter.gijsman@dsm.com
[2] DSM Dyneema, P.O. Box 1163, 6160 BD Geleen , The Netherlands
[3] DSM Biomedical, P.O. Box 18, 6160 MD Geleen, The Netherlands

## Introduction

To decrease wear, nowadays UHMwPE implants are cross-linked using γ or EB radiation [1]. However after radiating the polymer, long living radicals are still present, which can initiate the oxidation of the polymer and lead to a reduced life time [2,3]. This undesired process can be prevented in different ways. To reduce the residual radical concentration the polymer can be heated. To be effective it has to be heated to above its melting point, which results in a decrease of crystallinity and thus the properties. When the polymer is heated to just below its melting temperature not all radicals are trapped [1,4]. Another method to reduce the residual amount of radicals is by applying radical scavengers of which Vitamin E is the most well known. However, applying Vitamin E has several disadvantages. The main disadvantages is that this antioxidant already reacts with radicals during the cross-linking process leading to a reduced radiation efficiency and a consumption of (a part of) the dosed amount [4]. Another disadvantage of Vitamin E is that some of its conversion products are yellow to brown coloured [5]. In this presentation alternative stabilizers are presented that do not have these disadvantages.

## Experimental

### Materials

The UHMwPE used was MG003 from DSM, which has a molecular weight of 7.3 million g/mol. The stabilizers used are Vitamin E (from DSM Nutronal Products), Chimassorb® 944, Chimassorb® 119 and Tinuvin® NOR 371 (from Ciba Specialty Chemicals). For their chemical structure see Fig 1. Of these stabilizers Chimassorb 944 is FDA approved (up to 0.3wt %) to be used in polyethylene that is intended to come in contact with foodstuff. The stabilizers were added to the polymer by solution blending of the stabilizer in a for the stabilizer appropriate solvent.

### Sample preparation

All powders were compression moulded into sheets according to ISO 11542-2. These sheets were irradiated with 25, 75 and 150 kGy ray (at Beta-Gamma-Services GmbH). The samples dimensions needed for analyses were machined from the corresponding moulded samples. Colour measurements were done on 1 mm thick plaques. Tensile bars (Type ISO 527-5B) were punched from these 1 mm thick plaques. The cross-link density was determined using 5mm*5mm*5mm cubes
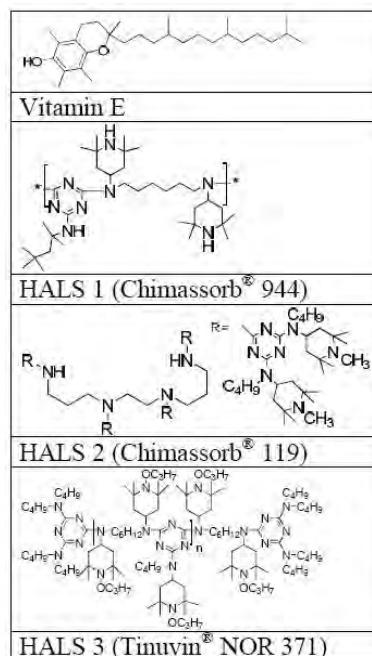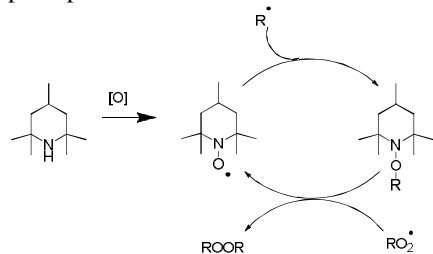


*Fig. 1. Chemical structure of used stabilizers*

### Ageing and analysis

All materials were aged during two weeks in an air venting oven (Binder FDL115) at 110°C. The cross-link density was determined according to ASTM F2214-02. Colour measurements were done according to ISO 7724-1-2-3 (CIELAB, D65, 10°, d8) The tensile tests (elongation at break and ultimate tensile strength) were done according to ISO 527, using sample specimens dimensions 5B. Oxidation indices were determined on coupes of about 100 µm, which were cut from cubes of 5*5*5 mm. according to ASTM F2102-06. The oxidation index was defined as the peak height at 1717 $cm^{-1}$ using a baseline drawn from 1680-1765 $cm^{-1}$.

## Results and discussion

The mechanism of action of HALS stabilizers is different from that of radical scavengers as Vitamin E. In scheme 1 a simplified mechanism of action of HALS stabilizers is given, for more detailed mechanisms see refs. 6-8. From this mechanism a high activity of HALS can be expected because it in principle is not consumed



*Scheme 1. Simplified radical scavenging mechanism of HALS Stabilizers*

As Vitamin E reacts with alkyl radicals it interferes in the cross-linking and it is (partly) consumed during irradiation of the sample. This results in a decreased cross-link density at given radiation dose (see Fig 2). HALS stabilizers themselves do not scavenge radicals; they first have to be converted into a nitroxide, which is the radical scavenger. As this does not happen during radiation, HALS stabilizer doe not have a negative influence on the cross-link density. (see Fig 3).
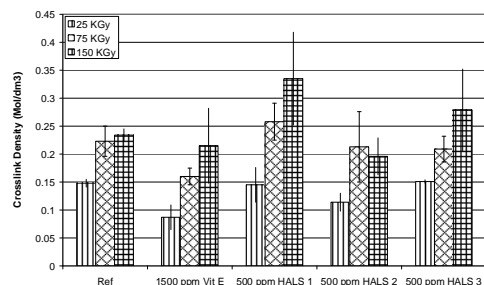


*Fig 2. Influence of stabilizer type on cross-link density after radiation with different doses.*

The conversion of Vitamin E leads to yellow coloured products (see Fig 3), which is not the case for HALS stabilized samples. This causes that the colour of the HALS stabilized samples are comparable to that of the unstabilized, while Vitamin E stabilized samples are much more coloured.

The effectivity of the stabilizers was determined by measuring the change in carbonyl absorbance due to ageing for two weeks at 110°C (Fig 4). For the unstabilized samples the carbonyl absorbance was over 10 (not shown). For all the other samples it was comparably low, showing that at a concentration of 500 ppm the used HALS stabilizers are as effective as Vitamin E at a concentration of 1500 ppm
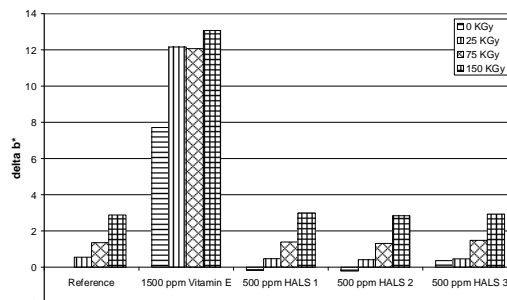


*Fig 3 Influence of stabilizer type on the yellowing after radiation with different doses (relative to not stabilized not irradiated sample)*
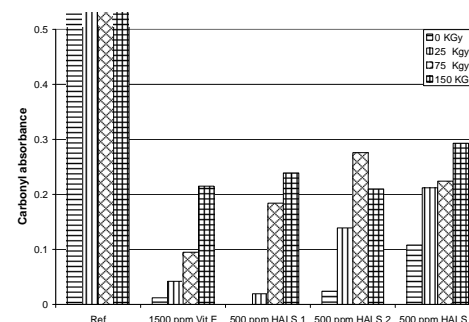


*Fig 4 Influence of stabilizer type on the carbonyl absorbance after two weeks at 110°C in an oven.*

## Conclusion

At the moment Vitamin E is the state of the art in stabilizing UHMwPE implants. However this stabilizer has some drawbacks. It has a negative influence on the cross-linking, leading to a lower cross-link density, a (partly) conversion and discoloration of Vitamin E. All these drawbacks can be overcome by using HALS stabilizers, which makes this class of stabilizer potentially better suitable for these applications.

## References

1 S. Kurtz, F.J. Medel, M. Manley, Current Orthopaedics 22 (2008) 392-399
2 L. Costa, I. Carpentieri, P. Bracco, Polymer Degaradation and Stability 93 (2008) 1695-1703
3 P. Bracco, V. Brunella, M.P. Luda, E.M. Brach del Prever, M. Zanetti, L. Costa, Polymer Degradation and Stability 91 (2006) 3057-3064
4 E. Oral, C. G. Beckos, A.S. Malhi, O.K. Muratoglu, Biomaterials 29 (2008) 3557-3560
5 S. Al-Malaika, S. Issenhuth, D. Burdick, Polymer Degradation and Stability 73 (2001) 491-503
6 P. Gijsman, M. Gitton Polymer Degradation and Stability 66 (1999) 365-371
7 P. Gijsman, M. Hamskog, Mechanism of action of Hindered Amines as Long Term Heat Stabilizers, ACS Symp Ser 978 (2007) 48-58
8 P.P. Klemchuk, M.E. Gande, E. Cordola Polymer Degradation and Stability, 27 (1990) 65-74

# LANTHANIDES AS STABILIZING AGENTS FOR UHMWPE

Luis A. Gallardo[1][2], Michel Laurent[1], Joachim Kunze[3] and Markus A. Wimmer[*][1][2]

[1]Department of Orthopedic Surgery, Rush University Medical Center, 726 Academic Facility, 1653 W. Congress Pkwy., Chicago, IL 60612, USA. (Markus_A_Wimmer@rush.edu)
[2]Bioengineering Department, University of Illinois at Chicago, USA
[3]Department of Analytical Chemistry, Hamburg University of Technology, Germany

**Keywords:** UHMWPE Additive, Oxidation, Small Punch Test, Accelerated Aging, Lanthanide, Stearate

## Introduction

The UHMWPE in the articulating surface of orthopedic endoprostheses fails under various mechanisms of wear and fatigue due to oxidation. This accounts for the majority of failures of these implants. Cross-linking of UHMWPE followed by high temperature annealing noticeably improves wear resistance and oxidative stability of these articulating surfaces, however decreasing fatigue resistance and ductility [1]. We have successfully tested europium (Eu), a representative element from the lanthanide group, as a stabilization agent to enhance oxidation hindrance while preserving mechanical integrity [2]. In this study, we hypothesized that the addition of Eu(II), would prevent oxidation of molded polyethylene components. Furthermore, based on its electron configuration, it would constitute a more active stabilizer than Eu(III). Eu(II) would readily accept one electron, and therefore actively scavenge radicals in addition to hindering oxidative reactions as it is believed Eu(III) does. Thus, this paper addresses the characterization of oxidation stabilization of Eu(II)-stearate doped UHMWPE and the effects on its mechanical properties. The latter are compared to a non-doped control, as well as a Eu(III)-stearate doped polyethylene after aging.

## Materials and Methods

UHMWPE powders were mixed with 750 ppm Eu(II)-stearate, fabricated from sodium stearate and europium nitrate. The powder was compression-molded into cuboids and oxidation was induced on the final samples by accelerated aging (ASTM-F2003-02). The samples were all manufactured from GUR1050 resin and gamma irradiated at 3.51 Mrad in the same way the control and the Eu(III)-stearate doped samples were.

Thin films were microtomed perpendicularly to the surface and tested by FTIR microspectroscopy (ASTM-F2102–06) for surface oxidation index.

The results were compared to those obtained with conventional UHMWPE as well as UHMWPE doped with Eu(III)-stearate, both aged in compliance with the aforementioned standard.

The mechanical properties were compared through load-deformation curves obtained from small punch testing (ASTM-F2183-02) aged and non-aged samples of all three conditions. Initial peak load, failure load, failure deformation, and work-to-failure (Fig.1) were evaluated for miniature disk samples (n=5). These properties were evaluated as relative conditions; in other words, as a ratio of aged to non-aged state to evaluate the proportion of each property that was retained after aging for each material condition.

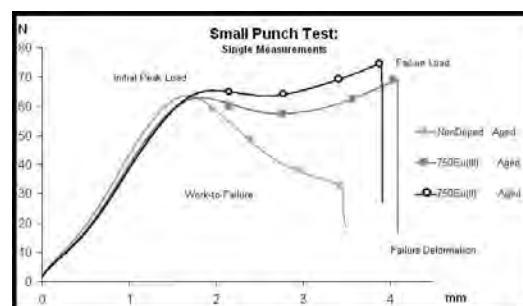Statistical significance analysis was performed using DOE and ANOVA.



Fig. 1. Load-Deformation curves obtained through small punch testing for aged Non-Doped UHMWPE and UHMWPE doped with Eu(II)-stearate and Eu(III)-stearate

## Results and Discussion

FTIR results indicate that oxidation levels after aging remained significantly lower for Eu(II)-stearate-doped samples than the non-doped control.

A reduction in the drop of mechanical properties after aging due to the stabilization was also demonstrated. Most notably, Eu(II)-stearate doped samples showed an 81% improvement in load to failure retention versus conventional UHMWPE (Fig.2). This enhancement of load bearing capacity has led to an improvement of work to failure of 63% versus conventional polyethylene (Fig. 3).

Eu(II)-stearate doped samples improved retention of deformation to failure by 51% with respect to conventional UHMWPE, 49% less than the improvement accomplished by Eu(III)-stearate (Fig.4). This less substantial enhancement of ductility and only slightly better enhancement of load bearing capacity by Eu(II) than Eu(III) have led to the improvement of work to failure 20% lower than the 83% improvement obtained with

Eu(III) [2]. P-values of the statistical analysis of the mechanical properties are shown in Table 1.

| | Eu(II) vs Conv | | | Eu(III) vs Conv | | | Eu(II) vs Eu(III) | | |
|---|---|---|---|---|---|---|---|---|---|
| | Lf | df | WtoF | Lf | df | WtoF | Lf | df | WtoF |
| Non-Ag | <0.001 | <0.001 | <0.001 | <0.001 | <0.001 | <0.001 | NS | <0.001 | <0.001 |
| Aged | <0.001 | NS | <0.001 | <0.001 | <0.001 | <0.001 | <0.05 | <0.05 | NS |

*Table 1. Statistical significance in failure load (Lf), failure deformation (df) and work to failure (WtoF) for non-aged and aged UHMWPE where NS = p>0.05*
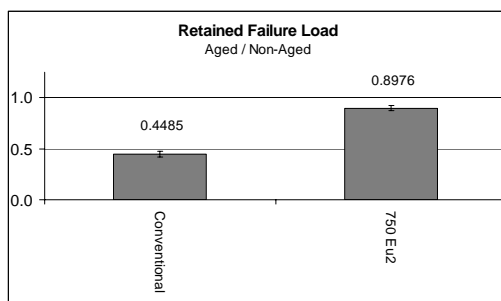


*Fig. 2. Failure load retained after aging for conventional and Eu(II)-stearate-doped UHMWPE. Error bar represents one standard error.*
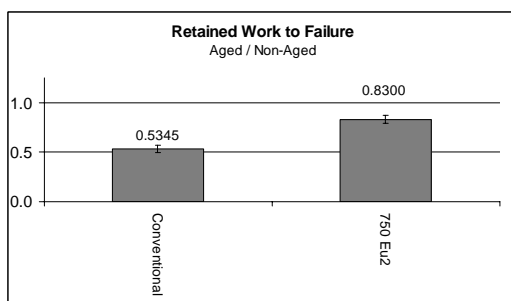


*Fig. 3. Work to failure retained after aging for conventional and Eu(II)-stearate-doped UHMWPE. Error bar represents one standard error.*
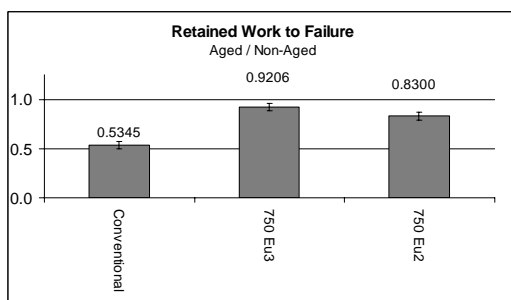


*Fig. 4. Failure deformation retained after aging for conventional, Eu(III)-stearate-doped, and Eu(II)-stearate-doped UHMWPE. Error bar represents one standard error.*

The results confirm our first hypothesis, showing that Eu(II)-stearate effectively improves oxidation resistance of UHMWPE after aging, consequently preserving mechanical performance in load bearing capacity, ductility, and energy absorption.

Our second hypothesis, however, was not confirmed. Eu(II)-stearate doped samples had slightly higher load-to-failure values than Eu(III)-stearate, but lower failure deformation. Thus, work-to-failure of Eu(II)-doped samples, although significantly improved when compared with conventional polyethylene, was not superior to Eu(III). Because the samples were doped with lanthanide-stearates fabricated with different purities and concentrations, further studies should be carried out to determine if the cause of this counterintuitive lower stabilization effect by Eu(II) is due to concentration, amount of total stearate, amount of europium-stearate or the europium valence.

In addition, effects of mixing and consolidation must also be investigated. The compression molding technique was not optimized for doped samples, which may have changed the state of Eu(II) to Eu(III) prior to aging.

**Conclusion**

Eu(II)-stearate was tested as an oxidation stabilization agent for UHMWPE and compared to Eu(III)-stearate. Doping with europium-stearate has shown once more to reduce oxidation and prevent the severe mechanical degradation that has been observed by this group and others in conventional polyethylene [3]. It was found that aging induced only a small decrease in the ductility and strength of the lanthanide-doped samples, suggesting that the europium stearate acted as an efficient oxidation stabilizer.

The actual mechanism has yet to be characterized. It is believed to respond to steric hindrance induced by the random allocation of europium-stearates on the free radicals resulting from high energy irradiation on polyethylene backbone chains. It is also believed to be related to the specific electron configuration of lanthanides, allowing access to additional electrons.

Further investigation is required to determine the optimum lanthanide concentration and appropriate production techniques to preserve pre-doping mechanical properties of UHMWPE while optimizing its oxidation resistance.

**References**

1. Kurtz, S. M. et al. Anisotropy and oxidative resistance of highly cross-linked UHMWPE after deformation processing by solid state ram extrusion. Biomaterials 27 (2006) 24-34

2. Gallardo, L.A. et al. Oxidative Stability of UHMWPE Doped with Europium-Stearate. 3rd Intl. Conference on MoBT. Abstract submitted for publication.

3. Edidin, A. A. et al. Degradation of mechanical behaviour in UHMWPE after natural and accelerated aging. Biomaterials 21 (2000) 1451-1460

# MECHANICAL AND OXIDATION BEHAVIOR OF SEQUENTIALLY CROSSLINKING ULTRA HIGH MOLECULAR WEIGHT POLYETHYLENE

R. Ríos[1]*, V.Martínez[1], M.J. Martínez-Morlanes[1], J. Cegoñino[1], J.A. Puértolas[1,2]

*[1]* *Instituto de Investigaciones en Ingeniería de Aragón. I3A-U. Zaragoza, 50018 Zaragoza, Spain (ricrios@unizar.es), [2] Instituto de Ciencia de Materiales de Aragón (CSIC-U. Zaragoza), Zaragoza, Spain.*

## Introduction

First generation of highly cross-linked polyethylenes (HXLPEs) have been used to the nowadays as the best candidates for bearing surfaces in total hip and knee replacements. These polyethylenes exhibit highly improved wear resistance owing to an elevated crosslink density obtained by gamma o electron beam irradiation. The oxidation stabilization in these materials to reduce the free radical arise during the irradiation is obtained by post-thermal irradiation processes like remelting or annealing. However, these thermal processes provide a reduction of the mechanical performance like toughness and fatigue resistance. Different strategies are currently applied to improve the first HXLPEs generation like the blended or doped polyethylene with vitamin E or the sequential irradiation and annealing process. However, some contradictory results appear in the literature concerning to the improvement in the mechanical properties obtained with this new sequential process [1-3].

The goal of this work consists of evaluating the sequentially crosslinked polyethylenes against of the single-dose crosslinking in GUR1050 from a mechanical and oxidation point of view.

## Materials and Methods

The raw UHMWPE material used in this study was GUR 1050 (G0) obtained from compression moulding sheets manufactured by (Orthoplastic Medical Ltd., Lancashire, UK). Different partial irradiation processes (gamma irradiation in air at 30 kGy, Aragogamma SA, Barcelona, Spain) followed by annealing (8 hours at 130º C) were carried out to obtain three different high crosslinked polyetylenes: 30-30-30A (G1), 30-30A-30A (G2) and 30A-30A-30A (G3).

Thermal characterization of G0, G1, G2 and G3 materials (n=3) was performed by Dynamic Scanning Calorimetry (DSC) (TA Instruments Q20) at a rate of 10 ºC/min from room temperature to 160 ºC, for obtaining the degree of crystallinity and the transition temperatures. Transmission Electron Microscopy (Jeol 100CX) was used to observe the microstructure of these polymers at 60000x magnification and to measure the lamellar thickness. Thermogravimetric analysis were done on thermobalance (TA Instrument Q5000) from

room temperature to 800 ºC in air at a heating rate of 10 ºC/min with samples

Mechanical properties were obtained from uniaxial tensile test per ASTM D638 in a Instron 5565 test machine at 23 ± 2 ºC for determine secant modulus, yield stress and fracture stress and strain. Toughness was calculated from the area under the strain-stress curve and from impact Izod test carried out on double-notched specimens following ASTM F648. The fatigue response was investigated by long-term stress-life experiments on dog bone specimens following ASTM E606 guidelines in a servohydraulic Instron 8032 machine. The load conditions were a sine waveform, frequency 1 Hz and R =0. The failure criterium was the yield strain. Finally, precraked standard compact tension specimens underwent near-threshold fatigue crack propagation test ASTM E647.

## Results and discussion

Figure 1 shows the DSC thermograms obtained in the dealt materials groups. Changes in melting temperature arose from 136.2±0.3 ºC in raw material to 141±0.6 ºC in crosslinked polymers, together the appearance of a previous small shoulder, at around 126 ºC, and all these results without significant variation in crystallinity content, ranged at 52-53 %.
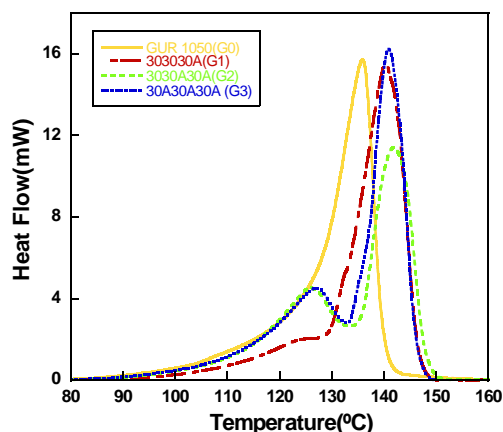


*Figure 1. Heating thermograms at 10 ºC/min*

However, microstructure changes appear concern the lamellar configuration. The micrographs of the irradiated polymers present a lower lamellar density with a lamellar thickness around 26-29 nm

versus the 15 nm observed in raw material, according to the Thomson-Gibbs relation.

Thermogravimetric decomposition curves showed in all the materials an oxidation process followed by an abrupt loss of weight corresponding to the thermal degradation. According to prior results in similar systems [4], the final temperature of the first region, denoted $T_1$, reflects the effect of the irradiation dose and the capability of the stabilization methods. The results point out that this temperature increases from 374.2±3.6 ℃ in the virgin sample to 383.4±3.9 ℃ with the presence of one annealing process, G1. The effect saturated when two annealing steps are presented in the final 90 kGy crosslinked polyethylenes, reaching T1 = 391.0±3.8 ℃.

The stress-strain curves of the uniaxial tensile test (Figure 2) showed similar shape with different mechanical parameters. Whereas the secant modulus is practically similar in three crosslinked polymers, small differences appears between the single-dose crosslinking, G1, and the other two crosslinked materials, that is the intermediate G2 material and the sequential cyclic irradiation-annealing, G3. These differences occur in the yield stress, fracture stress and strain fracture and also in the work to fracture, with better performance to the G1 group material.
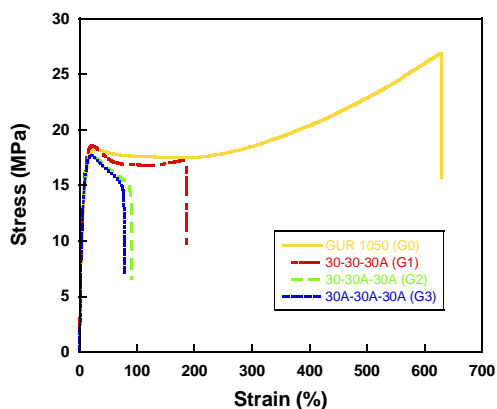


*Figure 2. Stress-strain curves in uniaxial tensile test*

The results of the impact Izod assessed the non significant difference in toughness behaviour between the three high crosslinked materials, with values around 47±3 $kJ/m^2$ and a loss of toughness respect to the virgin samples, 92±15 $kJ/m^2$, as expected. This last behaviour is in correlation with the idea that the main aspect governs the toughness is the crosslink density, which is non sensitive enough to the number of annealing steps.

Long-term fatigue test provided stress-life, S-N curves for all the four materials groups, which in a semilogarithmic scale gave parallel straight lines

for G1 and G2 material, with some deviation of this behaviour for G0 and G4. In any case, the fatigue resistance seem to decrease with the number of the annealing step carried out in the total process.

Finally, fatigue crack propagation curves, log (da/dN) vs log Δk, pointed out two different regions: the slow crack growth regime and the intermediated crack propagation described by the Paris equation. The raw material, G0, presents a Δk inception of 2.1±0.1 MPa $m^{1/2}$, which drops to values lower than 1.4 MPa $m^{1/2}$. According to the literature, this crack propagation should be influence by the lamellar thickness [5], better than the crystallinity content. The changes observed in our high crosslinked polyethylenes concerning to the lamellar thickness confirm also the previous statement.

**Conclusions**
The sequential irradiation and annealing process present a similar mechanical performance compared to the simple-dose crosslinked polyehylene for GUR1050. However, this new process seems to present a better oxidation resistance. From the mechanical and thermal results there are not practically differences between the processes 30-30A-30A and 30A-30A-30A.

**References**
[1] A. Wang et al. J. Phys D Appl. Phys. 39 (2006) 3213-3219
[2] A. Wang et al. The Journal of Arthoplasty. 23 (2008) 559-566
[3] M.L. Morrison et al. J. Biomed Mater Res B :Appl. Biomat Nov 2008
[4] FJ Medel et al. Poster N 448 55th ORS. Las Vegas 2009
[5]KS Simis et al. Biomaterials 27 (2006)1688

# RETRIEVAL ANALYSIS OF MATCHED CONVENTIONAL AND HIGHLY CROSS-LINKED ACETABULAR LINERS

David T. Schroder[1], Natalie H. Kelly*[2], Timothy M. Wright[2], Michael L. Parks[1]

[1]Adult Reconstruction and [2]Department of Biomechanics
Hospital for Special Surgery, 535 E. 70th St. New York, NY, 10021
*kellyn@hss.edu

## Introduction

Highly cross-linked ultra high molecular weight polyethylene (XLPE) has found popularity in use as a bearing material for total hip arthroplasty. Studies have found that XLPE, when compared to conventional ultra high molecular weight polyethylene (UHMWPE), is more resistant to wear clinically [1] and in hip simulator testing [2,3]. But cross-linking can decrease mechanical properties such as ultimate tensile strength, yield strength, and elongation to failure [4]. Reports of XLPE liner fracture in retrieved components has increased concern about these reduced mechanical properties [5,6]. We examined XLPE acetabular liners from a single manufacturer and design retrieved at our institution for evidence and type of wear damage. Matched pairs with a conventional UHMWPE liner with the identical design and manufacturer allowed us to compare the wear damage of these two materials while controlling for demographic and design variables. We hypothesized that XLPE acetabular liners would show evidence of wear damage, but that the damage would be less severe on XLPE liners than conventional UHMWPE liners.

## Materials and Methods

79 conventional UHMWPE liners (Trilogy, Zimmer) and 78 XLPE liners (Longevity, Zimmer) were available in our IRB-approved implant retrieval system. Twenty-two pairs were created by matching revision diagnosis, patient age at revision ($\pm$ 5 years), and length of implantation (LOI $\pm$ 2 years). When possible, patients were matched for body mass index (BMI) and head size. Damage was graded on three areas of the liner (articular surface, backside, and rim) in four quadrants per area. Eight damage modes were graded on a 0 to 3 scale [7] for a maximum damage score per area of 96. Rim impingement was graded based on depth of the lesion into the rim [8], and the amount of backside screw hole creep was assessed [9]. Cracks in the rim were visualized with a stereomicroscope using indirect illumination [10]. Implant alignment was measured from radiographs.

## Results

The average length of implantation in the entire cohort was 1.53 years (range 0.03 to 6.26 yrs.), the average age at revision was 66 years (range 17 to 87 yrs.), and the average BMI was 28 (range 19 to 43). The average wear grades were not significantly different between the UHMWPE and XLPE liners on any of the three areas. The average total wear score for the XLPE was 42 (range: 22 to 92) compared to 43 (range: 23 to 70) for the conventional liners (p=0.69). The average articular surface grade was 24 $\pm$ 6 for the XLPE and 26 $\pm$ 7 for the conventional (p=0.13), with burnishing less prevalent for XLPE. The backside wear grade was 12 $\pm$ 7 and 11 $\pm$ 6 for XLPE and conventional UHMWPE, respectively (p=0.86). The dominant wear modes were burnishing, pitting, and scratching. A previously described damage mechanism, "furrowing" [11], was seen on the articular surface of 12 of 22 XLPE liners (Fig. 1).



Figure 1: (A) Photomicrograph at 12X and (B) Scanning electron micrograph of furrowing on the articular surface of an XLPE liner.

Screw hole creep was present in 15 of the XLPE and 14 of the conventional UHMWPE. Rim impingement was present in 6 and in 17 of the XLPE and UHMWPE rims, respectively. Incipient rim cracks that had not led to fracture were identified in 4 of 22 XLPE liners (Fig. 2). Inclination angle at the time of revision was not significantly different (p=0.38).

*Figure 2: Photomicrograph taken at 15X magnification of an incipient crack within a rim notch.*

**Discussion**

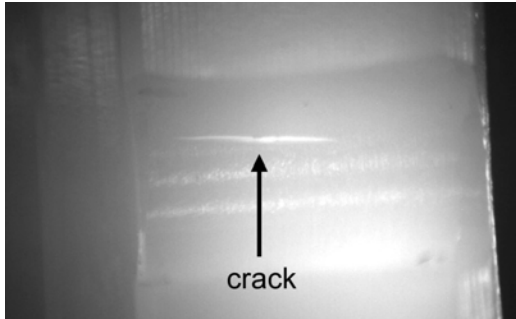Our hypothesis was supported in that the XLPE liners did show evidence of wear damage; however, no difference was found in the average wear scores between the two groups. XLPE liners had less burnishing on the articular surface, but other modes were as severe as in UHMWPE. The presence of "furrowing" supports a previous study [11], but the etiology of this mechanism remains unknown. Although impingement was found more frequently in the UHMWPE group, there were also more elevated liners in this group (19 vs. 4 in XLPE), which has been shown to increase the incidence of impingement [8]. We found cracks in just 18% of our XLPE implants, compared to a previous report of cracks in 66% of implants manufactured from the same material [10]. Whether such rim cracks would propagate into catastrophic liner failures with time remains unknown, but nonetheless they are a concern, since they are probably related to the inferior toughness of XLPE. We are limited by the short length of implantation and the fact that the damage score does not reflect release of debris or occurrence of osteolysis. XLPE shows a similar amount of in vivo damage as conventional UHMWPE. Further investigation is required to determine if polyethylene burden and incidence of osteolysis is decreased with XLPE.

**References**

[1] McCalden et al. (2009) *JBJS Am* 91:773. [2] Muratoglu OK et al. (2001) *J Arthroplasty* 16:24. [3] Estok DM 2nd et al. (2007) *J Arthroplasty* 22:581. [4] Pruitt LA (2005) *Biomaterials* 26:905. [5] Tower SS et al (2007) *JBJS Am* 89:2212. [6] Halley D et al. (2004) *JBJS Am* 86-A:827. [7] Hood RW et al. (1983) *J Biomed Mater Res* 17:829. [8] Shon WY et al. (2005) *J Arthroplasty* 20(4):427. [9] Kligman M et al. (2007) *J Arthroplasty* 22(2):258. [10] Furmanski et al. (2009) *Trans Orthop Res Soc* #2293. [11] Collier et al. (2003) *ASTM Intl* ASTM STP 1445:32.

# Surface cross-linked UHMWPE: The Holy Grail in Arthroplasty

Ebru Oral*[1,2], Bassem Ghali[1], Shannon Rowell[1] and Orhun Muratoglu[1,2]

[1] Massachusetts General Hospital [2] Department of Orthopaedic Surgery, Harvard Medical School
55 Fruit St. GRJ 1212B, Boston, MA 02114 *eoral@partners.org*

## Introduction

Radiation cross-linking is used to decrease wear in ultra high molecular weight polyethylene (UHMWPE) as a total joint arthroplasty bearing surface [1,2] but it also reduces its fatigue strength [1]. We propose to limit cross-linking to the surface of implants to improve the fatigue strength of wear- and oxidation-resistant cross-linked UHMWPEs (Fig 1) in order to improve their use in high stress applications and in young and active patients.
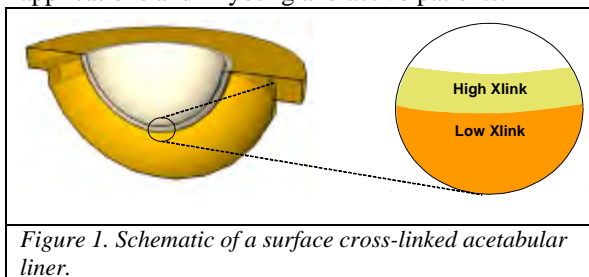


*Figure 1. Schematic of a surface cross-linked acetabular liner.*

Vitamin E, an antioxidant used to stabilize radiation cross-linked UHMWPE, hinders cross-linking in UHMWPE when present during irradiation [3]. We exploited this phenomenon to obtain a spatially controlled distribution of cross-linking in UHMWPE with high cross-link density on the surface for wear resistance and low cross link density in the bulk for fatigue resistance while maintaining oxidative stability.

We obtained surface cross-linked UHMWPE using layered molding of UHMWPE containing two different concentrations of vitamin E or extraction of the surface vitamin E from a UHMWPE containing a uniform concentration of vitamin E. Both of these methods were followed by radiation cross-linking. Using either method, we have obtained excellent wear resistance and very high fatigue strength.

## Materials and Methods

Layered Molding: Vitamin E-blended GUR1050 UHMWPE (62 mm dia., 39 mm length) with 0.05 wt% Vitamin E in one half and 0.5 wt% Vitamin E in the other half was e-beam irradiated to 150 kGy. Blocks with uniform 0.5 wt% and 0.05 wt% vitamin E were used as controls.

Surface Extraction: Compression molded, vitamin E-blended UHMWPE with 0.5 wt% vitamin E was machined into cylindrical pins (diameter 9 mm., length 13 mm). Pins were boiled under reflux in a 20% aqueous solution of Tween 20 in water for 40 hours. After extraction, the pins were e-beam irradiated to 150 kGy.

Cross-link density measurement: Cubes (3 mm) were cut from the low and high vitamin E regions (n=3) and the gradient region (n=6) of layer molded and irradiated UHMWPE. Specimens were swollen in 25 ml of hot xylene (130°C) for 2 hours, then blot-dried and weighed. The gravimetric swelling ratio was converted to cross link density as described previously [2].

Pin-on-disc (POD) wear testing: For layered molded samples, pins were machined such that the articulating surface was in the 0.05 wt% vitamin E-containing, highly crosslinked UHMWPE. For extracted and irradiated samples, the pins were directly tested after irradiation. We tested the pins against CoCr, under 2.6 MPa/pin, in undiluted bovine serum at 2 Hz for up to 2 million cycles (MC) [4]. Wear was determined gravimetrically every 0.5 MC. Wear rate was calculated as the linear regression of weight loss versus number of cycles from 0.5 MC to the end of the test.

Fatigue testing: Fatigue crack propagation tests were on A1 C(T) specimens per ASTM E 647 at 40°C in distilled water with a stress ratio of 0.1 at 5Hz. Cracks were measured optically every 20000 cycles. The stress intensity factor range at crack inception (? $K_i$) at $10^{-6}$ mm/cycle was calculated. Fatigue testing was performed on 0.05 wt% and 0.5 wt% vitamin E-blended and subsequently 150 kGy irradiated UHMWPEs.



*Figure 2. Schematic of unidirectional delamination testing with the gradient interface in UHMWPE 2mm below the surface*

Delamination testing: Cylindrical pucks (50 mm diameter, 12.7 mm thickness, n=2) were machined from irradiated layered molded blocks such that the articulating surface was located 2 mm into the highly cross-linked region (Fig 2). The pucks were accelerated aged at 80°C in air for 5 weeks, then were articulated against CoCr right-lateral uni-compartmental femoral components in undiluted preserved bovine serum at 2Hz for 5 MC. Photographs of the top surface were taken every 1 MC. One puck was melted in vacuum at 170°C.

**Results and Discussion**

The vitamin E concentration profiles were spatially controlled in both the layered molded blocks (Fig 3a) and surface extracted pins (Fig 3b). The gradient interface spanned approximately 3 mm in the layered molded blocks and about 1.6 mm in the surface extracted pins. We designed these concentration profiles such that there would be a highly cross-linked region in the UHMWPE, which would correspond to the articular surface of an implant and a low cross-linked region that would correspond to the bulk of the implant.
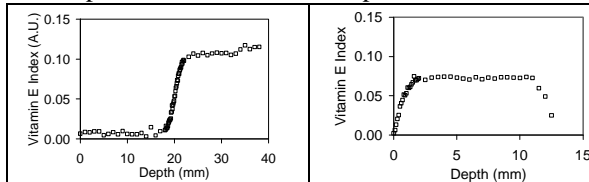


Figure 3.The vitamin E concentration profiles of (a) layered molded UHMWPE and (b) surface-extracted UHMWPE before radiation cross-linking.

We were able to determine the cross-link density of the 'surface' and 'bulk' layers as well as the interface cross-link density for the layered molded UHMWPE. The cross-link density of the highly cross-linked surface containing 0.05 wt% vitamin E during irradiation was $190\pm7$ mol/m$^3$, which was comparable to the cross-link density of 100-kGy irradiated and melted virgin UHMWPE; 198 mol/m$^3$ [2]. The interface had a cross-link density of $139\pm15$ mol/m$^3$ and the bulk had a cross-link density of $108\pm5$ mol/m$^3$, comparable to the cross-link density of unaged conventional UHMWPE; $93\pm3$ mol/m$^3$ [4].

| | Wear rate (mg/MC) | $? K_i$ (MPa m$^{1/2}$) |
|---|---|---|
| Layered molded | -1.7±0.1 | 0.93±0.03 |
| Extracted | -1.4±0.4 | |
| 100-kGy irradiated | -1.4±0.6 | 0.74±0.02 [1] |
| 100-kGy irradiated and melted | -1.1±0.7 | 0.56±0.02 [1] |

Table 1. Wear and fatigue properties of surface cross-linked UHMWPEs compared to irradiated and irradiated/melted UHMWPE.

Commensurate with the cross-link density, the wear of the surfaces of both the layered molded and the extracted and subsequently irradiated UHMWPEs were low and comparable to that of 100-kGy irradiated and melted virgin UHMWPE (Table 1).

It is our assumption that by limiting cross-linking to the surface of implant components, their mechanical properties will be governed by the bulk of the implant. The properties in the bulk are not affected by the cross-linking on the surface; the fatigue strength as determined by fatigue crack propagation resistance was much improved for the 0.5 wt% and 150 kGy irradiated UHMWPE compared to 100-kGy irradiated and irradiated/melted UHMWPEs (Table 2). One can imagine further improving the bulk properties by increasing the vitamin E concentration in the bulk. For example, the fatigue crack propagation resistance of 2 wt% vitamin E-blended and 100 kGy irradiated UHMWPE was $1.24\pm0.02$ MPa m$^{1/2}$, which was comparable to that of conventional UHMWPE; $1.29\pm0.04$ MPa m$^{1/2}$ [1].

One concern was the weakness of the gradient interface. It has been shown that conventional UHMWPE pucks, after aging for 5 weeks in air at 80°C, delaminate under unidirectional loading at less than 2 MC due to sub-surface oxidative embrittlement [4]. We observed no such delamination for the aged irradiated gradient pucks even after 5 MC (Fig 4b). This demonstrated (1) the presence of a cross-link gradient 2 mm below the surface did not cause subsurface weakness and (2) the vitamin E prevented oxidation. This was supported by the surface oxidation index of aged and delamination tested samples, which was 0.10. After melting, we observed no delamination and the creep/wear scar recovered to its original height, except for a shallow striated depression (Fig 4c).
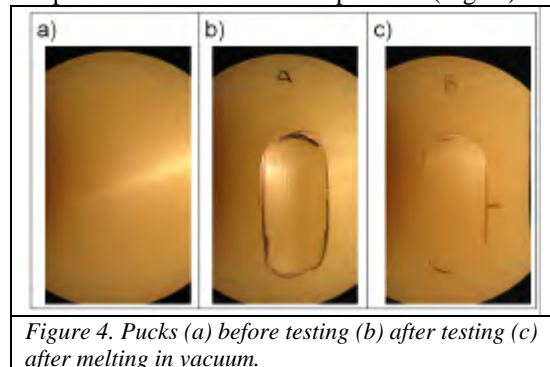


Figure 4. Pucks (a) before testing (b) after testing (c) after melting in vacuum.

One major benefit of this material is that the high vitamin E concentration in the bulk can be also used as a reservoir and redistributed to the surface of the components after cross-linking for additional resistance against oxidation.

**Conclusion**

We have limited cross-linking to the surface of UHMWPE implants by exploiting the free radical scavenging ability of vitamin E and spatially controlling its concentration profile during irradiation. By obtaining a surface cross-linked layer, the fatigue strength of the bulk was improved to levels comparable to that of unaged conventional UHMWPE. We believe that this new material has the potential of expanding the use of wear resistant UHMWPE to high stress applications and improving outcomes in joint arthroplasty.

**References**

[1] Oral et al. Biomaterials 2004. 25. pp 5515-5522; [2] Muratoglu et al. Biomaterials 1999. 20. pp 1463-1470; [3] Oral et al. Biomaterials 2008. 29: 3557-3560; [4] Oral et al. JBMR-B 2009 Available online [5] Christensen et al. Transactions of 52nd ORS 2006.

# CRACK INITIATION AND PROPAGATION AT NOTCHES IN CROSS-LINKED UHMWPE SUBJECTED TO SUSTAINED LOADING

Jevan Furmanski*, Clare M Rimnac

*Case Western Reserve University, Glennan 414, 10900 Euclid Avenue, Cleveland OH, 44106, USA*
*Jevan@case.edu*

## Introduction

In-vivo fracture of UHMWPE components is a failure mode that results in the surgical revision of some or all of the joint replacement system. Cross-linking substantially reduces the fracture and crack propagation resistance of UHMWPE, potentially elevating the risk of fracture in cross-linked implants. Recently published reports of the catastrophic fracture of a number of cross-linked acetabular liners with elevated rims demonstrates that fracture occurs clinically, albeit with an as-yet unknown rate of incidence [1,2]. Our group performed an inspection of clinically retrieved cross-linked liners, showing that small cracks had initiated in 5/8 intact components [3]. These cracks had a similar morphology and location to the initiation sites of the catastrophic fractures previously analyzed, indicating that initiated cracks could be relatively common.

Fatigue crack propagation in virgin UHMWPE has been shown to be insensitive to frequency, and dependent on waveform and mean stress precisely according static mode crack propagation [4,5]. Thus, we expect the processes driving crack propagation to be static mode, i.e., insensitive to load cycling.

This work describes the experimental results of crack initiation and propagation from acute notches in UHMWPE, which are compared to expectations from analytical predictions. Further, we outline a novel testing program and a failure criterion for crack initiation in UHMWPE.

## Analytical Model

Analytical models of crack propagation based on viscous crack tip phenomena have been in use for three decades. Viscoplastic deformation at the crack tip provides a physical mechanism for the static mode crack propagation observed in UHMWPE. We employ the model of Williams for a power-law creeping material to predict the conditions necessary for crack initiation under sustained loading of a notch [6]. This model enables predictions of the time to accumulate a critical J-integral at the crack tip for the initiation of a mobile crack.

$$C = \frac{1}{E_0}\left(\frac{t}{\tau_0}\right)^d \Rightarrow J = J_0\left(\frac{t}{\tau_0}\right)^d \Rightarrow \frac{t_i}{\tau_0} = \left(\frac{J_c}{J_0}\right)^{1/d} \quad (1)$$

In Equations 1, $C$ is the creep compliance, $E_0$ is the initial elastic modulus, $t$ is time, and $\tau_0$ and $d$ are fit parameters. $J_0$ is the initial J-integral at the notch root, and $J_c$ is the threshold value of $J$ for crack initiation. The initiation time, $\tau_0$, is therefore explicitly dependent on material creep resistance ($\tau_0$, $d$), fracture resistance ($J_c$) and the extrinsic loading and notch geometry ($J_0$). Controlling crack initiation in UHMWPE may be a robust approach for preventing catastrophic fracture in joint replacements. A minimum allowable initiation time could provide a transparent industrial target for crack initiation performance.

Equation 1 provides an explicit means for evaluating trade-offs in material behavior resulting from changes in processing or material treatments. Since the creep resistance typically increases with cross-linking, while the toughness decreases, the time to initiate a crack might be difficult to predict. Figure 1 shows a schematic of how the J-integral resulting from a ramp-to-constant load experiment for virgin and highly cross-linked UHMWPE can result in a substantial difference in the initiation time due to differences in material stiffness, creep resistance (increase of $J$ with time), and toughness.
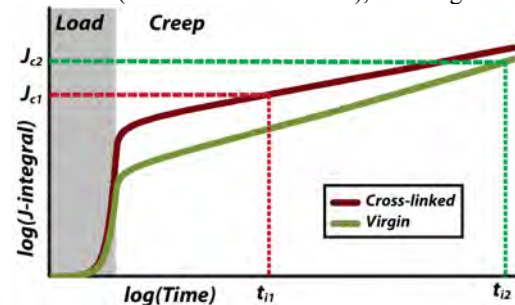


*Figure 1. J-integral increases with time under a constant applied load near a notch in two creeping formulations of UHMWPE. The initiation time is a function of the stiffness (initial J) creep resistance (rate of growth of J) and toughness ($J_0$). Modest variations in material behavior can substantially affect the initiation time. Data in figure derive from the predicted response of a notched specimen via FEA using a viscoelastic-viscoplastic constitutive model with material behavior obtained from quasi-static and dynamic experiments [7].*

## Materials and Methods

Crack propagation experiments utilized GUR 1020 resin, gamma irradiated with 50, 75, or 100 kGy dose, and subsequently remelted at 147 °C. Compact tension specimens were machined with side grooves and an initial crack length of 8.89 mm and a notch root radius of 0.13 mm. Samples were subjected to a constant load of 500 N on an Instron

8874 servohydraulic frame. The position of the apparent crack tip and the ligament width were recorded using a traveling microscope.

**Experimental Results and Discussion**
Crack propagation began almost immediately after the application of the load, indicating that the crack initiation was rapid. This could result from the applied J-integral exceeding the crack growth inception toughness, $J_c$. The applied elastic-plastic J-integral in the experiments was approximately 50 kJ/m$^2$. This exceeds some but not all values of $J_c$ reported in the literature for cross-linked UHMWPE. The findings of this study suggest that $J_c$ for these cross-linked UHMWPE formulations is below 50 kJ/m$^2$.

The crack velocity in each cross-linked formulation was approximately constant for the first 1 mm of growth, after which growth accelerated to fracture in 5000-25000 seconds. Further, the relative crack velocities in each formulation agree with the relative velocities observed in cyclic fatigue crack propagation tests on the same material batches [8]. Thus, steady load crack propagation experiments provide a means to compare the crack propagation behavior of UHMWPE formulations that is directly analogous to more complicated and costly fatigue crack propagation tests. Such tests could be conducted with weights instead of a load frame.
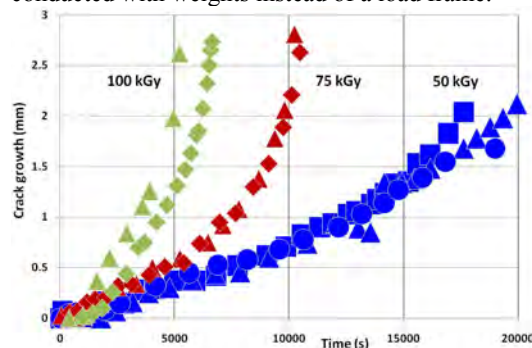


*Figure 2. Crack growth from an acute notch under a constant load in cross-linked GUR 1020 UHMWPE. Crack velocity is initially constant, and then accelerates to fracture.*

Though little can be concluded about crack initiation from the experiments, these propagation data are representative of the behavior of initiated cracks or flaws near notches in components. Initiated cracks have been observed in retrieved components that were in vivo for only a few days, and designing implants with tolerance to pre-existing defects near stress concentrations requires attention to crack propagation resistance.

It is notable that the crack velocity was initially constant. This implies that the J-integral is approximately constant for small crack extensions, which agrees with the Williams model for crack growth. Experimental estimates of $J$ for the deforming specimen also indicate that $J$ was approximately constant during the constant velocity phase.

Future work will address the initiation behavior under constant loading of notched specimens, along with the viscoplastic deformation at large strains. Such work would establish the applicability of the Williams fracture model to UHMWPE, and could be a powerful and simple tool for fatigue and fracture control in orthopaedic implants.

**Conclusion**
Clinical fracture of a variety of cross-linked UHMWPE acetabular liners has been seen in each case to initiate at stress concentrations in unsupported rims. Further, crack initiation may be substantially more common than inferred from the rarity of clinical fracture failure. While fatigue crack propagation resistance has been a useful indicator of relative fatigue performance, it may not accurately represent a material's resistance to crack initiation or notch fatigue resistance. Given the limited toughness of the material, the initiation time is likely to dominate the total life of a component, and so controlling crack initiation is an excellent companion approach to defect tolerant design. The analytical model of viscoplastic crack growth developed by Williams [6] provides a simple and direct method to assess the effect of altering material properties or implant design on the overall crack initiation performance of the component.

Constant load notched specimen experiments showed that the crack propagation behavior varied similarly with dose as in traditional cyclic fatigue crack propagation experiments. Constant load experiments could be an economical alternative to fatigue crack propagation experiments for UHMWPE formulation comparison purposes. We plan to extend this approach to examining crack initiation at acute notches in future experimental trials.

**References**
[1] Tower et al. JBJS 89A, 2007.
[2] Furmanski et al. *Ann. Meeting AAOS*, 2007.
[3] Furmanski et al. *Proc. 55th ORS*, 2008.
[4] Furmanski and Pruitt, *Polymer* 48, 2007.
[5] Furmanski et al. *ICMOBT*, 2007.
[6] Williams, *Fracture Mechanics of Polymers*. Ellis Horwood, 1984.
[7] Bergstrom et al. *Biomaterials* 23, 2002.
[8] Atwood et al. *ICMOBT*, 2007.

# EXPERIMENTAL AND THEORETICAL INVESTIGATION OF UHMWPE MECHANICAL BEHAVIOR

Frédéric Addiego*[1], David Ruch[1], Fatima Eddoumy[1], Olivier Buchheit[1], Christèle Vergne[1], Saïd Ahzi[2], Abdesselam Dahoun[3], Hamid Garmestani[4], Dongsheng Li[4]

[1] CRP Henri Tudor, Department of Advanced Materials and Structures, 66 Rue de Luxembourg, L-4221 Esch-sur-Alzette, Luxembourg
[2] Strasbourg-University, Institut de Mécanique des Fluides et des Solides, 2 Rue Boussingault, F-67000 Strasbourg, France
[3] Nancy-University, Institut Jean Lamour, Ecole des Mines de Nancy, Parc de Saurupt, F-54042 Nancy, France
[4] Georgia Institute of Technology, Laboratory of Micromechanics of Material, School of Materials Science and Engineering, 771 Ferst Drive, N.W., Atlanta, G.A. 30332-0245, USA

* Corresponding author, E-mail: frederic.addiego@tudor.lu

## Abstract
Tensile response of UHMWPE is finely studied at both macroscopic and microscopic scales to identify and quantify its deformation mechanisms. A physical-based model derived from these mechanisms has been applied with success to predict the tensile curve. The contribution of this modeling on wear prediction is also discussed.

## Introduction
UHMWPE is employed in medical industry as prosthesis, in sport industry as sliding surface for skis, or in machine construction as chain/belts guides. To optimize the shape of these components, designers employ finite element methods (FEM) in such a way that the tested shape reaches the targeted mechanical properties under a given loading. This process is directly influenced by the constitutive equations utilized in the simulation that are derived from phenomenological or physical approaches. To date, mechanical behavior of UHMWPE is only modeled by phenomenological models [1,2]. In this work, the first objective is to simulate tensile behavior of UHMWPE using physically-based equations. For this, Ahzi et al. model [3] has been selected. The applicability of the present model will be verified at macroscopic and microscopic scales to check if the predicted stress-strain curve and deformation mechanisms are in good accordance with the experimental ones. Macroscopic behavior is assessed by the means of a universal testing machine equipped with a video-controlled extensometer, while microscopic one is quantified using nanoscratch, nanoindentation, x-ray diffraction, differential scanning calorimeter, and scanning electron microscope. Furthermore, it has been shown that wear of UHMWPE, evaluated with a pin-on-disk tribometer under dry condition, is linked to deformation state of the material obtained after a solid-state deformation treatment [4]. Since the present modeling could predict a deformation state, the second objective of this work is to investigate the relevance of using Ahzi et al. equations to predict wear behavior under dry condition.

## Materials and Methods
Investigations are conducted on a UHMWPE provided by Ticona (Belgium) under the reference GUR 1020. The powder is compression-molded at 240°C, under 33 bars and during 30 minutes, with a hydraulic press Carver. Then, UHMWPE is annealed under vacuum at 130°C during 24h. Mechanical tests are performed with a universal testing machine MTS 810 equipped with an accurate optical extensometer. This equipment, called VidéoTraction, provides the true mechanical behavior of a representative volume element located in the center of tensile specimen. One important feature of this technique is that the development of neck is finely taken into account in the mechanical behavior. As for microstructural study, crystalline aspects are evaluated by differential scanning calorimetry (DSC) using a DSC 204 F1 equipment from Netzsch, and by X-ray diffraction (XRD) using a Philips X'Pert PW3040 MRD system equipped with a pole figure goniometer and a Panalytical X'Pert Pro MPD equipped with the transmission mode (WAXS and SAXS). Furthermore, an environmental scanning electron microscope (ESEM) is employed to investigate the morphology of UHMWPE. Last, a nanoindenter, reference XP from MTS, and a nanoscratch tester, from CSM Instruments, are utilized to characterize elastic properties at microscopic scale.

## Results and discussion
After consolidation, the material is characterized by an index of crystallinity of 52 % from DSC measurements and 58 % from XRD measurement. A melting temperature of 139.7°C is noted, which corresponds to a lamellar thickness of 43 nm (using Gibbs-Thomson equation). At large scale, ESEM micrographs have revealed a homogeneous fusion of the initial powder particles, and at low scale a

random lamellar structure is noted. This morphology results from a slow and incomplete crystallization that is induced by a high entanglement density of the macromolecules.

The tensile behavior of UHMWPE deformed at temperature ranging from 30 to 90°C and at the constant true axial strain rate $1.10^{-3}$ $s^{-1}$ is represented in the Fig. 1. The resulting curves are representative of semi-crystalline polymers tensile behavior. For various states of deformation (axial strains $\varepsilon_{33}$ = 0, 0.5 and 1.2), microstructural investigations have been conducted using XRD and ESEM. As expected, pole figures and WAXS/SAXS results show that amorphous chains, crystalline chains and crystallites progressively orient towards tensile direction. As the index of crystallinity, measured by a spatial weighted averaging, it slightly decreases with the deformation. On ESEM micrographs, both an orientation and a fragmentation of lamellae are noted with increasing deformation state. Also, no cavitation phenomena are observed. All these mechanisms are generally observed in such a material [5,6].
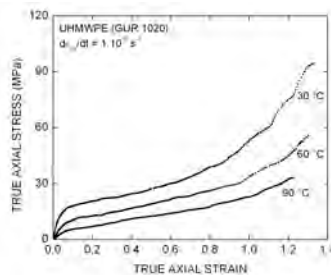


*Fig 1: True stress – true strain curves of UHMWPE subjected to tensile test at $1.10^{-3}$ $s^{-1}$ and 3 temperatures*

Ahzi et al. model [3] is able to predict tensile curve of a semi-crystalline polymer from the combination of deformation mechanisms of amorphous phase and crystalline phase. In particular, basic structural unit of semi-crystalline polymers is introduced as a two-phase composite inclusion consisting of a single, flat lamella and its adjacent amorphous layer. This modeling is based on the following points. First, elasticity is neglected since at large strains, elasticity neither contributes significantly to overall deformation nor has much effect on the texture development. Second, crystalline lamella is considered to deform following the crystallographic slip systems, each slip system being described by a power law to relate shear strain to its resolved shear stress, its critical resolved shear stress (CRSS), a reference shear rate, and a rate sensitivity coefficient. Last, amorphous chains are modeled as a rubber elastic network, orientation hardening being modeled via different theories (the three-chain model and the eight-chain model). It is important to note that Ahzi et al. model can predict pole figures of crystalline planes. Thus, at microscopic scale, we have verified that predicted

and experimental pole figures were in good agreement, as shown in the Fig. 2. Subsequently, at macroscopic scale, we have verified that predicted and experimental stress – strain curves were in good accordance.
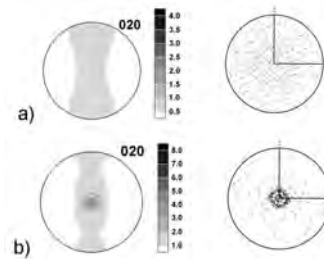


*Fig. 2: Experimental (left) and predicted (right) pole figures of UHMWPE at the strain state 0 (a) 1.2 (b) (tensile direction is horizontal)*

It is well known that under dry condition, wear of UHMWPE is linked to elastic modulus and fracture toughness. These two parameters can be modified by a solid-state deformation process. Nanoscratch and nanoindentation experiments, well suited to study (sub)surface mechanical properties, have shown differences between oriented and unoriented products. These differences could be linked to the evolution of the microstructure. As a result, wear can be linked to deformation state, and hence to amorphous and crystalline phases states. Since Ahzi et al. model can predict such parameters, we plan to study and model wear resistance of UHMWPE vs. deformation state using these equations.

**Conclusion**
Ahzi et al. physically-based model has been applied to predict tensile behavior of UHMWPE, showing a good correlation between experimental and predicted behaviors at both macroscopic and microscopic scales. This model will be related to wear properties of the material by studying the effect of solid-state deformation on wear. Interaction between solid-state deformation and crosslinking will be also investigated.

**References**
[1] A. Avanzini, Materials and Design, 29, (2008), 330-343
[2] J.S. Bergström, C.M. Rimnac, S.M. Kurtz, Biomaterials, 25, (2004), 2171-2178
[3] S. Ahzi, D.M. Parks, A.S. Argon, Computer modelling and simulation of manufacturing processes, MD - 20, 287
[4] H. Marrs, D.C. Barton, C. Doyle, R.A. Jones, E.L.V. Lewis, I.M. Ward, J. Fischer, Journal of Materials Science: Materials in Medicine, 12, (2001), 621-628
[5] F. Addiego, A. Dahoun, C. G'Sell, J.M. Hiver, Polymer, 47, (2006), 4387-4399
[6] M.F. Butler, A.M. Donald, A.J. Ryan, Polymer, 39, (1998), 39-52

# Reinforced ultra high molecular weight composite by carbon nanotube and gamma irradiation

*M.J.Martínez-Morlanes[1], P. Castell[2], V. Martínez[1], A. Benito[2], W. Maser[2], M.T. Martínez[2], J.A. Puértolas[1,3]*

*1Dept. Materials Science and Technology. I3A- University of Zaragoza. Zaragoza. Spain (mjm@unizar.es)*
*2Dept. of Carbon Nanostructures and Nanotechnology. Instituto de Carboquímica-CSIC. Zaragoza. Spain*
*3Instituto de Ciencia de Materiales de Aragón. Universidad de Zaragoza-CSIC. Spain.*

## Introduction

Ultra high molecular weight polyethylene (UHMWPE) is a polymer with good mechanical and tribological performance used in industrial applications. UHMWPE has also been the choice of material for bio-implants, like total joint replacement. This material has the required properties for such applications: biocompatibility, high wear resistance, low friction coefficient and suitable stiffness, toughness and fatigue resistance[1].

Various techniques have been used to increase the mechanical performances of UHMWPE. These include self-reinforcement, reinforcement with carbon fibers, reinforcement with nanoparticles, etc.

The initial biocompatibility of the carbon nanotubes (CNT´s) and their exceptional properties allows considering the reinforcement with nanotubes as a good option. From an orthopaedic point of view, the improvement of the mechanical and tribological properties of UHMWPE could extend the lifespan of the prostheses and reduce the overall thickness of some polyethylene components with a better function. On the other hand, gamma irradiation is a technique used by the orthopaedic manufacturers for introducing a crosslink among the polymer chain, by means of the free radical arisen during the irradiation process. Our hypothesis in this work is that these radicals might react with the nanotubes present in the polymer matrix increasing the transfer of properties from the nanotubes to the polymer matrix. Using our approach we keep the benefit of the gamma irradiation concerning to the improvement of the wear resistance associated to the crosslinking of the matrix, together with a better interaction between the CNT´s and the UHMWPE. This better interaction should result in an improved load transmission with the subsequent increase of the resulting mechanical properties. The assesment of this hypothesis is the content of this study.

## Materials and Methods

The UHMWPE/CNTs composites were obtained by ball milling. UHMWPE powder (Goodfellow) was mixed with 0.5, 1, 3 and 5 wt % of multiwall nanotubes (MWNTs, NC7000 from Nanocyl) pre-dispersed in ethanol to obtain homogeneous dispersions of the CNTs in the polymer matrix (ethanol was used in order to break the bundles of the CNTs). Different amounts of CNTs were pre-dispersed in (10 ml approximately) of ethanol using and ultrasonic tip (Amplitude 50%) during 1 h. Once the CNTs were completely dispersed in ethanol UHMWPE was incorporated and the mixture was homogenized in a ball mill during 2 h at 400 rpm. The obtained powders were dried under vacuum before being thermo-compressed. Specimens for mechanical analysis were obtained by thermo-compression (Perkin Elmer) during 15 minutes at 175ºC under a pressure of 10 MPa followed by a controlled cooling in air down to 70ºC under the same pressure.

The composites were denoted like PE (raw material), PE-CNT (blending without dispersant), and PE-CNT-ET (ethanol like dispersant). Several PE and PE-CNT specimens (n=3) were gamma irradiated at 90 KGy doses and denoted as PEI and (PE-CNT)I, respectively.

The melting temperatures, melting enthalpy, crystallinity and the glass transition temperatures of the obtained composites were obtained by DSC. Uniaxial tensile test were carried out at 5 mm/min for obtaining the mechanical parameters. Analysis of the fracture was also conducted by SEM and TEM.

## Results and discussion

Table 1 shows the crystallinity and the melt temperature of the obtained composites.

The results obtained by DSC, showed small differences in the melting temperature within specimens and a decrease in the percentage crystallinity of UHMWPE due to addition of MWNTs. These results are similar to the results obtained in the Bakshi study [2].This fact is in accordance with the idea that the CNTs may act as obstacles and hinder the mobility of the chains leading to lower amount of crystallinity.

| Material Group | Tf(ºC) | Hf(J/g) | % Cristallinity |
|---|---|---|---|
| **PE** | 135 ± 0 | 157 ± 3 | 54 ± 1 |
| **PE-CNT(1%)** | 135 ± 1 | 154 ± 1 | 53 ± 0 |
| **PE-CNT(3%)** | 135 ± 1 | 139 ± 1 | 48 ± 0 |
| **PE-CNT(5%)** | 134 ± 1 | 132 ± 4 | 45 ± 1 |

*Table 1. Thermal parameters for the raw UHMWPE and CNTs/UHMWPE composite with different CNTs loadings*

The samples obtained showed a homogeneous distribution of the CNTs in the matrix as determined by SEM and TEM even at the highest CNT loading.
Studies are in progress to determine the formation of covalent bonds between the CNTs and the UHMWPE via the generated radicals.

Figure 1 shows the stress-strain curves obtained for virgin and CNTs/UHMWPE composites with different CNTs concentrations.
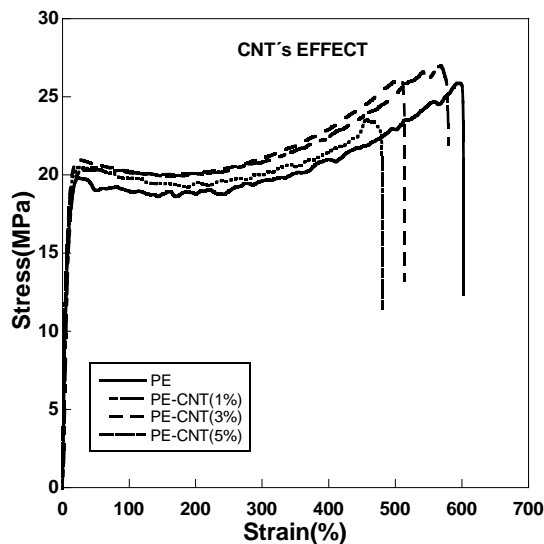


*Figure1.Stress-strain curves for virgin and CNTs/UHMWPE composites with different CNTs concentrations.*

The incorporation of the MWNTs showed a 62% increase in Young´s modulus and yield stress of the UHMWPE as expected, but reduced the fracture strain of the material. The reinforced specimens are less stiff than the virgin material due probably to small consolidation defects arisen during the thermo-compression process.

The irradiation effects is reflected in the stress-strain curves obtained for virgin and irradiated CNTs/UHMWPE composites (Figure 2).
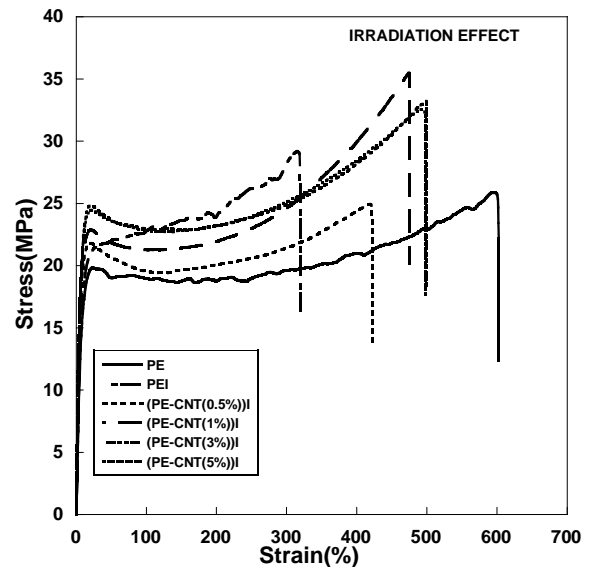


*Figure 2. Stress-strain curves for virgin and irradiated CNTs/UHMWPE composites with different CNTs concentrations.*

The tensile tests showed a 64% increase in Young´s modulus in the irradiated specimens due to addition of 1% of MWNT. The irradiated nanocomposites showed an increase in the yield stress, associated to the crosslinking induced by the gamma irradiation, and also an increase in the fracture strain value of these specimens because of the presence of nanotubes.
On the other hand, the reinforced specimens were less stiff probably due to some small consolidation defects.

**Conclusions**
Nanocomposites of UHMWPE containing different loadings of MWNT (0.5-5%) were obtained by a ball milling process. The presence of the CNTs increased the Young modulus and the yield stress of the resulting nanocomposites. The gamma irradiation of the composites resulted in an increase in the yield stress due crosslinking and an increase of the fracture strain due to the presence of the CNTs.

**References**
[1] E. Gómez-Barrena, J.A. Puértolas, L. Munuera, Y.T. Konttinne. Acta Ortopaedica 79 (2008) 832
[2]S.R.Bakshi,J.E.Tercero,A.Agarwal. Composites: Part A 38 (2007) 2493-2499

**Acknowledgements**

# FATIGUE AND FRACTURE BEHAVIOR OF CROSSLINKED UHMWPE: IMPLICATIONS FOR IMPLANT DESIGN

Lisa A. Pruitt,* Sara Atwood, and Jevan Furmanski^

[1] 5134 Etcheverry Hall, UC Berkeley, Berkeley CA 94720, USA; lpruitt@me.berkeley.edu*
^Case Western University, Cleveland OH

## Introduction

UHMWPE remains the standard bearing material used in total joint replacement. Cross-linked UHMWPE resins are now prevalent in total hip arthroplasty. These crosslinked resins provide improved wear-resistance but at the expense of fatigue and fracture properties [1-3]. For this reason there has been concern about using highly crosslinked UHMWPE as a counterbearing material in total knee replacements where contact stresses are known to be high. Degradation of mechanical properties is also of clinical concern in total hip replacement designs. Components comprising crosslinked UHMWPE are more susceptible to fracture due to design related stress concentrating features such as locking mechanisms or elevated rims and clinical factors such as impingement.

In a recent study, four fractured crosslinked UHMWPE acetabular liners from different manufacturers were evaluated for the source and mechanism of failure [4]. This study revealed that all fractures initiated at stress concentrations in an unsupported region of the elevated rim (Figure 1). Finite element analyses demonstrated that the predicted magnitude and orientation of maximum principal stress due to mechanical loading of the elevated rim was sufficient to propagate initiated fatigue cracks in each case and also predicted that cracks may arrest after some amount of growth due to a steep stress gradient near the initiation site.



*Figure 1. Fractures in four crosslinked UHMWPE acetabular cups that all have elevated rim designs [4].*

The fatigue crack propagation behavior of UHMWPE depends strongly on processing methods and crosslink dose [5]. Figure 2 shows that the stress intensity range necessary to propagate cracks is reduced as the radiation (crosslink) dose is increased.
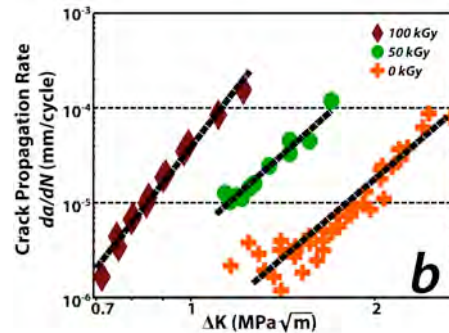


*Figure 2. Fatigue crack propagation in UHMWPE as a function of radiation dose[5].*

Recent work has shown that the process of fatigue crack growth is dominated by static mechanisms; the polymer is insensitive to frequency and waveform but is highly sensitive to the peak stress intensity of the loading cycle [6]. Furmanksi [7] has recently utilized a power-law creeping material model to predict the conditions necessary for crack initiation under sustained loading and a critical Jintegral at the crack tip for the initiation of a propagating flaw (Figure 3).
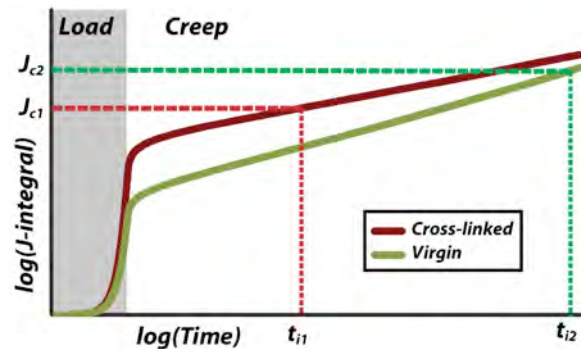


*Figure 3. Schematic depicting the initiation time ($t_i$) for two UHMWPE formulations exhibiting distinct fracture toughness ($J_c$), creep resistance and stiffness [7].*

This work addresses the fatigue crack propagation behavior for a number of clinically relevant forms of crosslinked UHMWPE and discusses factors that can contribute to fracture in orthopedic implants.

## Materials and Methods

The fatigue crack propagation behavior of nine distinct formulations of UHMWPE and two untreated controls were evaluated [5]. Tests were performed using a stress ratio of 0.1 and a test frequency of 5 Hz. The materials used were subjected to gamma irradiation in one or multiple doses (0 to 10 Mrad) followed by heat treatments either above or below the melting temperature (130C or 147 C). All were either compression molded GUR 1020 or ram extruded GUR 1050. The crystallinity was assessed using differential scanning calorimetry. Microstructures were studied with SEM. Artificial aging of the specimens was performed in a previously validated environment, placing samples in a pressure vessel with 3 atm $O_2$ at 63° C for 28 days [5]. Oxidation was measured by FTIR absorbance spectroscopy. Microscope oxidation measurements were made on 200 micron-thick cross-sections of each sample at 200 micron intervals. Oxidation of the thin sections was defined as the measured ketone (1715 cm-1) peak height normalized to the 1368 cm-1 peak height.

## Results and discussion

Fatigue crack propagation tests indicate that annealed materials have better crack propagation resistance than remelted materials (Figure 4). However, artificial aging reveals that annealed materials have a higher oxidation index than either virgin or remelted materials after aging. Microstructural analysis reveals the least crystallinity and lamellar size in the remelted materials. The annealed materials show a higher crystallinity than virgin UHMWPE with a similar lamellar size. Crosslinking via irradiation in combination with annealing, either singly or sequentially, appears to leave the material susceptible to oxidation during accelerated aging. The long term effects of this oxidation remain unknown. However, previous work [8] has shown that highly oxidized materials owing to artificial aging have a decreased resistance to FCP and will tend to shift FCP curves to the left (as noted by the arrow). However, increasing crystallinity benefits FCP and tends to shift FCP curves to the right. As annealing preserves the crystallinity better than the remelt process it may aid in balancing the mechanical integrity for the aged conditions.

## Conclusion

Cross-linked UHMWPE remains an excellent bearing material for total joint replacements but designs employing this material should mitigate stress concentrations or other design features that increase the risk of fracture. Moreover, the ability to fully tailor the material properties through processing and thermal treatments requires further exploration.



*Figure 4. Fatigue crack propagation for nine clinically relevant formulations of UHMWPE.*

## References

[1] Pruitt, *Biomaterials* (2005)
[2] Rimnac and Pruitt, AAOS (2008)
[3] Gencur, Rimnac and Kurtz, *Biomaterials* (2003)
[4] Furmanski et al. *Biomaterials, in press* (2009)
[5] Baker, Bellare, Pruitt, *JBMR* (2003)
[6] Furmanski and Pruitt, *Polymer* (2005)
[7] Furmanski, Rimnac and Pruitt, DYF (2009)
[8] Baker, Hastings and Pruitt, *Polymer* (2000)

# INFLUENCE OF PROTEIN AND PHOSPHOLIPID ON WEAR PROPERTY OF UHMWPE

Yoshinori Sawae*[1], Akio Yamamoto[2], Takayuki Saruwatari[3], Seido Yarimitsu[2] and Teruo Murakami[1]

[1] *Faculty of Engineering, Kyushu University, 744 Motooka, Nishi-ku, Fukuoka 819-0395, sawa@mech.kyushu-u.ac.jp*
[2] *Graduate School of Engineering, Kyushu University*
[3] *Graduate School of Systems Life Sciences, Kyushu University*

## Introduction

Articulating surfaces of joint prostheses are lubricated with periprosthetic fluid, a kind of body fluid secreted into a reconstructed joint capsule after the total joint arthroplasty. The periprosthetic fluid has similar composition to the original synovial fluid and it contains many kinds of biological macro molecules, such as proteins and lipids etc [1]. These molecules can be entrained into a contact zone during articulation and possibly affect the wear behaviour of the polyethylene surface and the formation process of wear particles. Chemical interactions between the periprosthetic fluid and implanted UHMWPE have been investigated by several researchers through the FT-IR analysis of retrieved polyethylene components [2,3]. Their results have indicated two important incidents in the synovial environment, the protein adsorption on the polyethylene surface and the lipid diffusion into the bulk of UHMWPE. Costa et al. [3] also suggested the possible effects of these incidents on the *in vivo* wear of UHMWPE. In fact, effects of protein molecules on the wear behaviour of UHMWPE have been indicated by several research groups in their laboratory experiments [4]. However, the role of lipid constituents in the *in vivo* wear mechanism of UHMWPE has not been clarified enough yet.

In this study, the influence of protein and phospholipid molecules on the wear property of UHMWPE and characteristics of released polyethylene wear particles were examined experimentally in the multidirectional sliding pin-on-plate wear test.

## Materials and Methods

A sliding motion arising between a pin and plate specimen in the custom-made multidirectional sliding pin-on-plate wear tester used in this study is shown in Fig.1 [5]. The basic principle of the multidirectional sliding in this wear tester is identical to that of the CTPOD device developed by Saikko [6]. The pin specimen was attached to a loading bar while the plate specimen is moved circularly by crank mechanism. Consequently, the fixed pin specimen articulates upon the plate specimen surface along a circular path with a diameter of 30mm and the direction of the sliding velocity vector changes continuously relative to the UHMWPE pin surface.

Cylindrical polyethylene pin specimens with a diameter of 6mm and a length of 15 mm were machined from GUR415 bar stock and medical grade cast Co-Cr-Mo alloy (ASTM-F75) was used as plate specimens. Phosphate buffered saline (PBS) solutions containing protein and phospholipid were prepared and used as test lubricants in the wear test. Bovine serum γ-globulin was chosen as a protein constituent of lubricants to represent the protein molecules contained in the joint fluid. On the other hand, Synthetic phospholipid (L-α-dipalmitoyl phosphatidylcholine (DPPC)) was used as an alternative of natural lipid constituents of the periprosthetic fluid.

The sliding speed was 20 mm/s and the mean contact pressure was varied from 1.0 MPa to 7.0 MPa. Each wear test was run for the sliding distance of 10 km. Every 5 km sliding, weight of UHMWPE pin specimens were measured by an electric balance and the specific wear rate was calculated from the weight change. After the wear test, polyethylene wear particles were isolated from the test lubricant and observed by SEM. Captured SEM images were subsequently analyzed to evaluate morphological characteristics of polyethylene wear particles.
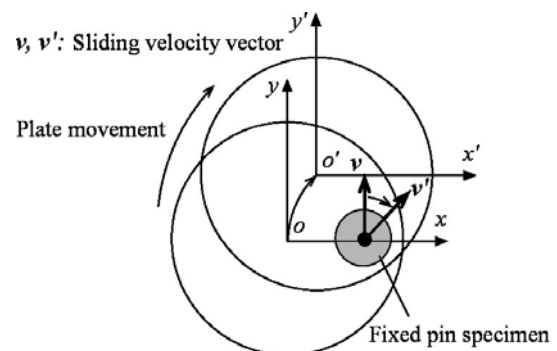


*Fig.1 Schematics drawing of sliding motion in the multidirectional sliding pin-on-plate wear tester*

## Results and discussion

The phospholipid concentration of test lubricants for the first series of experiments was fixed to 0.02wt% and the protein concentration was varied

from 0.1 to 2.0wt%. All tests were conducted under the contact pressure of 7.0MPa. The specific wear rates of UHMWPE were plotted against the protein concentration of test lubricants in Fig.2. The protein concentration of ambient solution had a significant effect on the wear property of UHMWPE in our wear test, and the wear rate increased with increasing the protein concentration, as reported previously by Wang et al. [4].
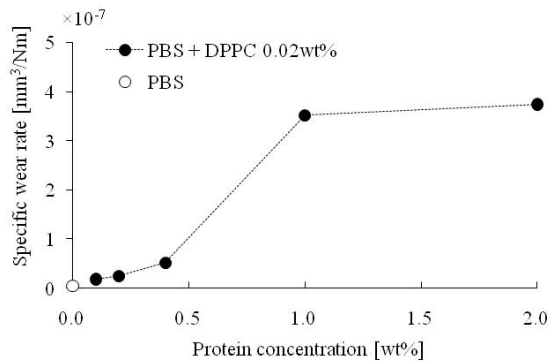


*Fig.2 Specific wear rate of UHMWPE plotted against protein concentration of test lubricants, which contained 0.02wt% phospholipid and various amounts of protein. Contact pressure = 7.0MPa. n =3, mark indicates average value.*

In the second series of experiments, the protein concentration of test lubricants was adjusted to 2.0wt% and influences of the phospholipid concentration were examined. The wear tests were conducted under three different contact pressures and the effect of the contact pressure on test results was also confirmed (Fig.3). UHMWPE wear rates in three lubricants with different lipid concentrations were compared in Fig.3. The polyethylene wear rate increased with decreasing the contact pressure and became comparable to the clinical value of polyethylene wear rate estimated from retrieved UHMWPE cups by Hall et al. [7] under the contact pressure of 1.0MPa. Despite levels of the contact pressure, UHMWPE wear rate was reduced by adding 0.005wt% L-α-DPPC to test lubricants. Small amount of phospholipid molecules might form a kind of boundary lubrication film on solid surfaces and reduce wear of UHMWPE. However, the boundary lubrication effect of phospholipid had diminished by increasing the lipid concentration from 0.005 wt% to 0.02 wt% and the wear rate of UHMWPE clearly increased.

Morphological characteristics of polyethylene wear particles were compared in Fig.4. The size and shape of wear particles were also affected by the lipid concentration of the test lubricant and polyethylene wear particles became smaller and more spherical with increasing lipid concentration to 0.02wt%. Greenbaum et al. experimentally demonstrated that UHMWPE could be plasticized by the lipid adsorption [8]. Therefore, the increased amount of phospholipid might induce the

plasticization in the polyethylene surface and alter the resistance to the adhesive and abrasive wear. Subsequently, the phospholipid concentration had influence on the wear process of UHMWPE.
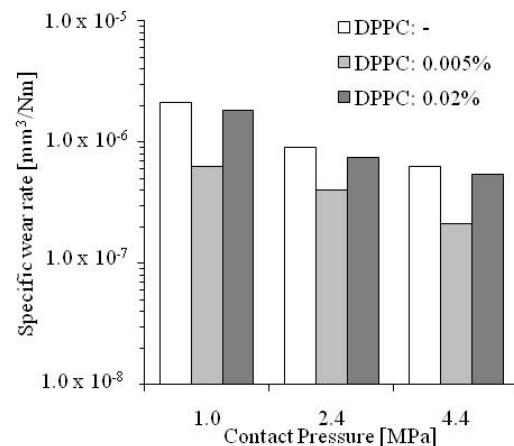


*Fig.3 Comparison of UHMWPE wear rate in test lubricants containing 2.0wt% γ-globulin and various amounts of phospholipid.*
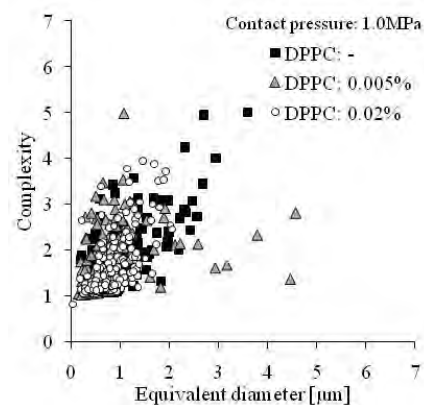


*Fig.4 Comparison of morphological characteristics of UHMWPE wear particles. Values of vertical axis represent a shape complexity of wear particles and vertical axis indicates a size of particles.*

## Conclusion
Our test results indicated that both protein and phospholipid had significant effects on the wear process of UHMWPE in the multidirectional sliding wear test.

## References
[1] J. DesJardins et al., Proc. IMechE, 220 Part H, 2006, 609-623. [2] S.P. James et al., Biomaterials, 14, 1993, 643-647. [3] L. Costa et al., Biomaterials, 22, 2001, 307-315. [4] A. Wang et al., Tribology International, 31, 1998, 17-33. [5] Y. Sawae et al., Tribology International, 41, 2008, 648-656. [6] V. Saikko, J Biomed Mater Res, 41, 1998, 58–64. [7] R.M. Hall et al., Proc. IMechE. 210 Part H, 1996, 197-207. [8] E.S. Greenbaum et al., Biomaterials, 25, 2004, 4479-4484.

# EFFECTS OF SERUM AND LOAD CONDITIONS ON THE FRICTIONAL PROPERTY OF VITAMIN E-BLENDED UHMWPE

Yasushi Okubo[1], Daisuke Hamada[1], Koji Yamamoto[1], Shin-ichiro Mori[1],
Kunihiko Fujiwara[2], Ken Ikeuchi[3] and Naohide Tomita*[1]

[1]*Graduate School of Engineering, Kyoto University,
Yoshida-Honmachi, Sakyo-ku, Kyoto 606-8501, Japan
E mail: ntomita@iic.kyoto-u.ac.jp*
[2]*Nakashima Medical corporation*
[3]*Department of Clinical Engineering, Suzuka University of Medical Science*

## 1. Introduction

Vitamin E (*dl*-α-Tocopherol) -containing ultra-high molecular weight polyethylene (UHMWPE) has been reported to prevent crack initiation at subsurface grain boundaries of UHMWPE [1]. In addition, we have also reported that the wear volume of vitamin E-containing UHMWPE tested with a knee joint simulator was approximately 30% lower than that of virgin UHMWPE at 5 million cycles [2]. However, the wear resistance mechanism of vitamin E-containing UHMWPE has not been clarified yet. The present study examines the effects of the addition of vitamin E on the frictional properties of UHMWPE in the case of several different lubricants and loads using pin-on-disk apparatus as a fundamental approach.

## 2. Materials and Methods
### 2.1. Preparation of sliding specimens

UHMWPE resin powder (GUR1050, Ticona, USA) was blended with vitamin E (0.3% w/w, *dl*-α-Tocopherol, Eisai, Japan) using a screw cone mixer. The vitamin E-containing UHMWPE board was manufactured using direct compression molding at 220°C under 25 MPa for 30 min. The virgin UHMWPE board, which was used as the control material in this study, was manufactured in the same way without the addition of vitamin E. Conical pin specimens with a diameter of 1 mm and a flat sliding surface (Ra < 0.1 μm) were machined from the UHMWPE boards and were subjected to ultrasonic immersion cleaning in isopropyl alcohol (50% v/v) for 15 minutes. Disk specimens with a highly polished flat sliding surface (Ra < 0.01 μm) were machined from a Co-28Cr-6Mo alloy ingot and were subjected to ultrasonic immersion cleaning in acetone (99.5% v/v) for 15 minutes.

### 2.2. Preparation of lubricants

Bovine calf serum (SAFC Biosciences, USA) and ultrapure water (Arium611VF, Sartorius, Germany) were used as lubricants. Three classifications of serum lubricant were used in this study: fresh serum, post-friction (PF) serum and diluted-PF (DPF) serum. The preparation of PF-serum lubricant was carried out using a pin-on-disk apparatus. The load was applied to the UHMWPE pin, and the contact stress on the sliding surface was set to 30 MPa. The Co-28Cr-6Mo alloy disk was fixed within the lubricant bath on the X-stage, and was set into linear reciprocating sliding motion for 2,000 cycles with an amplitude of 1 mm and a frequency of 1 Hz. The lubricant bath was filled with 5 ml of fresh serum, which was kept at a temperature of 37°C. After the sliding cycles, the lubricant was retrieved from the bath. To prepare the DPF-serum lubricant, the PF serum was diluted to contain the same amount of serum proteins as the fresh serum lubricant by the addition of pure water.

### 2.3. Measurement of dynamic friction force

Friction tests were carried out using a pin-on-disk test apparatus as shown in Fig. 1. All tests were conducted at room temperature inside a clean bench. The pin specimen was mounted vertically at the tip of the leaf spring. The load was applied to the pin specimen, and was set to 2.4 N or 24 N. The nominal contact stress was 3 MPa or 30 MPa, respectively. The disk specimen was fixed within the lubricant bath on the X-stage and was set into linear reciprocating sliding motion for 2,000 cycles with an amplitude of 1 mm and a frequency of 1 Hz. The lubricant bath was filled with 5 ml of lubricant, which was kept at a temperature of 37°C. The friction force was calculated from the displacement of the leaf spring during the sliding motion.
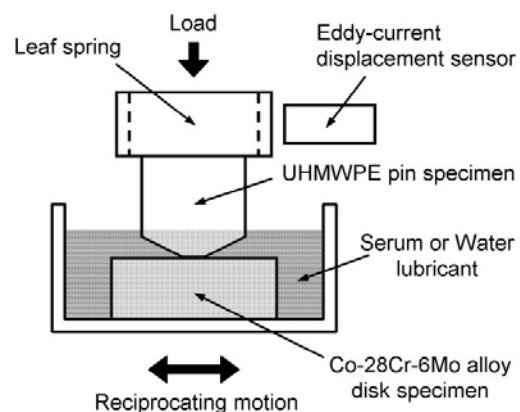


*Fig. 1 Block diagram of the apparatus for friction tests.*

## 3. Results and discussion

Vitamin E-containing UHMWPE showed a significantly higher friction force than virgin UHMWPE at 30 MPa loading in fresh serum lubricant (Fig. 2b), while there were little differences in ultrapure water (Fig. 2a). However, in the use of PF and DPF serum, the frictional properties between virgin and vitamin E-containing UHMWPE tended to exhibit a same behavior during the tests (Fig. 2c, d). Considering the fact that amount of serum proteins in the fresh serum and in DPF serum lubricants were same, these results suggest that the frictional properties are affected not only by the change in material properties of UHMWPE by the addition of vitamin E, but by the conformation of serum proteins.

It has been suggested that denatured proteins are likely to be preferentially adsorbed onto hydrophobic surfaces and other denatured proteins due to strong hydrophobic interactions, and friction and wear are affected by the adsorption of these denatured proteins [3]. In our results in the use of PF and DPF serum, the friction force is not much different regardless of vitamin E. Therefore, it may be explained that the effect of hydrophobic interaction of denatured proteins is much more predominant factor than the effect of vitamin E on the frictional property of UHMWPE.

However, the vitamin E-containing UHMWPE showed a significantly higher friction force than virgin UHMWPE in fresh serum lubricant. In addition, it has been reported that vitamin E-containing UHMWPE adsorbed slightly less human plasma proteins, especially immunoglobulin G (IgG), than virgin UHMWPE [4]. On the basis of these results, it is though that the adsorption of native conformation proteins onto the surfaces of UHMWPE was inhibited by some effects of vitamin E, thus the friction force of vitamin E-containing UHMWPE might have had a significant difference in fresh serum lubricant compared to virgin ones.

Regarding the load dependence on the frictional property, vitamin E-containing UHMWPE tends to exhibit a lower dynamic friction force relative to virgin UHMWPE within the first few hundred cycles in the case of all serum lubricants at 30 MPa loading, while there were little differences at 3 MPa loading (Fig. 2e). These results may suggest some transitional phenomenon such as weeping of vitamin E and so on at early stage of sliding.

## 4. Conclusion

Our results suggest that the adsorption of native conformation proteins onto the UHMWPE surface was inhibited by some effects of vitamin E.

**References** [1].Tomita N, et al. J Biomed Mater Res 1999;48:474. [2].Teramura S, et al. J Orthop Res 2008;26;460. [3].Heuberger MP, et al. Biomaterials 2005;26:1165. [4].Reno F, et al. Biomaterials 2006;27:3039.



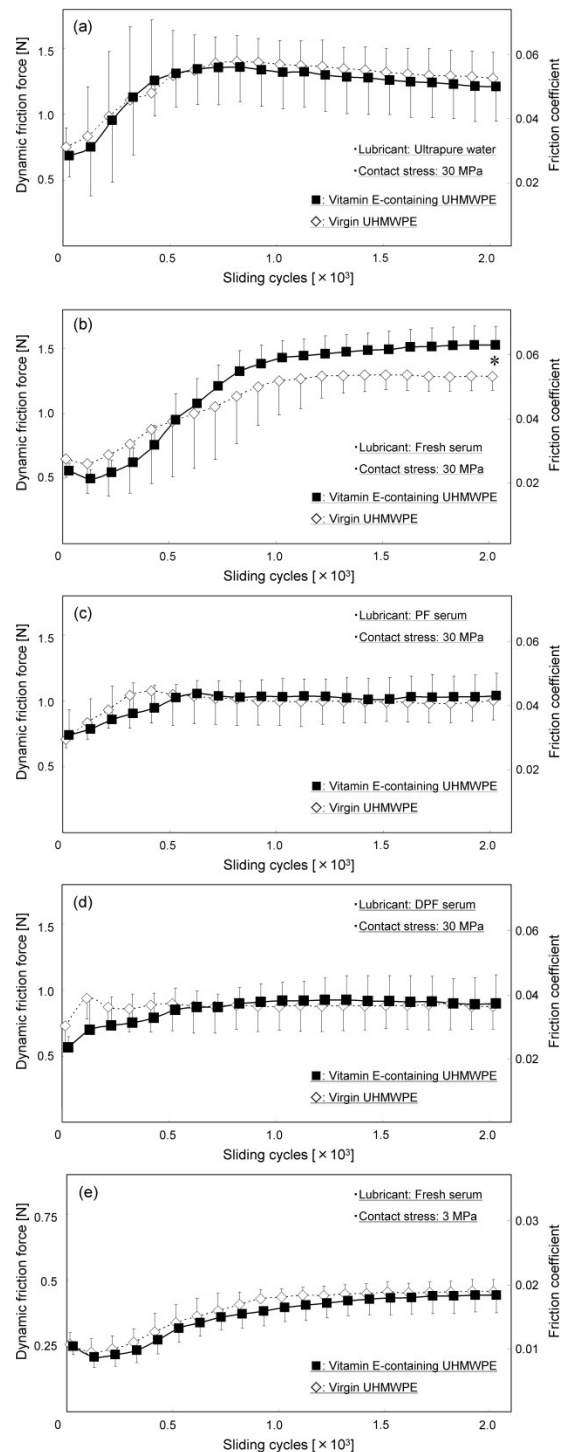*Fig. 2  Transitions of the dynamic friction force of vitamin E-containing UHMWPE and virgin UHMWPE for several lubricants and contact stresses. (a) Ultrapure water at 30 MPa loading, (b) Fresh serum at 30 MPa, (c) PF serum at 30 MPa, (d) DPF serum at 30 MPa, (e) Fresh serum at 3 MPa.  Data represent mean $\pm$ SD. Asterisk indicates a statistically significant difference (*; $P < 0.01$, n = 6, by Student's t-test).*

# TRANSFER FILM FORMATION OF VITAMIN E-BLENDED UHMWPE ON CO-28CR-6MO ALLOY SURFACE

Shin-ichiro Mori [1], Yasushi Okubo[1], Koji Yamamoto[1], Daisuke Hamada[1],
Kunihiko Fujiwara[2], Ken Ikeuchi[3] and Naohide Tomita*[1]

[1]Graduate School of Engineering, Kyoto University,
Yoshida-Honmachi, Sakyo-ku, Kyoto 606-8501, Japan
E mail: ntomita@iic.kyoto-u.ac.jp
[2]Nakashima Medical corporation
[3]Department of Clinical Engineering, Suzuka University of Medical Science

## 1. Introduction

Vitamin E (dl-α-Tocopherol) -containing ultra-high molecular weight polyethylene (UHMWPE) has been reported to prevent crack initiation at subsurface grain boundaries of UHMWPE [1]. In addition, we have also reported that the wear volume of vitamin E-containing UHMWPE tested with a knee joint simulator was approximately 30% lower than that of virgin UHMWPE at 5 million cycles [2]. However, the wear resistance mechanism of vitamin E-containing UHMWPE has not been clarified yet. The present study examines the effects of the addition of vitamin E on the formation of UHMWPE transfer film at the Co-28Cr-6Mo alloy surface, as well as the pull-away force between UHMWPE and the Co-28Cr-6Mo alloy as a fundamental approach to clarifying the mechanism of resistance to wear of vitamin E-containing UHMWPE.

## 2. Materials and Methods
### 2-1. Preparation of specimens

UHMWPE resin powder (GUR1050, Ticona, USA) was mixed with vitamin E (0.3% w/w, dl-α-Tocopherol, Eisai, Japan) using a screw cone mixer. The vitamin E-containing UHMWPE board was manufactured using direct compression molding at 220°C under 25 MPa for 30 min. The virgin UHMWPE board, which was used as the control material in this study, was manufactured in the same way without the addition of vitamin E. Conical pin specimens with a diameter of 1 mm and a flat sliding surface (Ra < 0.1 μm) were machined from the UHMWPE boards and were subjected to ultrasonic immersion cleaning in isopropyl alcohol (50% v/v) for 15 minutes. Disk specimens with a highly polished flat sliding surface (Ra < 0.01 μm) were machined from a Co-28Cr-6Mo alloy ingot and were subjected to ultrasonic immersion cleaning in acetone (99.5% v/v) for 15 minutes.

### 2-2. Pin-on-disk transfer test

The UHMWPE transfer tests were carried out using a pin-on-disk test apparatus. For the purpose of avoiding contamination with air dust particles, all tests were conducted inside a clean bench. The load was applied to the UHMWPE pin specimen, and was set to 8 N, 16 N or 24 N. The nominal contact stress was 10 MPa, 20 MPa or 30 MPa, respectively. The Co-28Cr-6Mo alloy disk was fixed within the lubricant bath on the X-stage, and was set into linear reciprocating sliding motion for 5,000 cycles with an amplitude of 1 mm and a frequency of 1 Hz. The lubricant bath was filled with 5 ml of ultrapure water (Arium611VF, Sartorius, Germany), which was kept at a temperature of 37°C.

### 2-3. Quantification of the transfer film

The quantification of the UHMWPE transfer film formed on the disk specimen surface was performed as shown in Fig. 1. The tested disk specimen was observed under a digital microscope at 300-fold magnification, and was photographed as an 8-bit grayscale image. The central part of the sliding region ($0.5 \times 0.5$ mm$^2$ at a resolution of $500 \times 500$ pixels) was acquired, and all pixels were classified in accordance to their brightness value. The histogram took the form of a bell-shaped curve with a more gradual slope in the low brightness regions in comparison to the high brightness ones. This slightly more gradual slope was assumed to be the result of the adhesive substance produced by the reciprocating slide of the specimens, thus defined as the apparent transfer film.
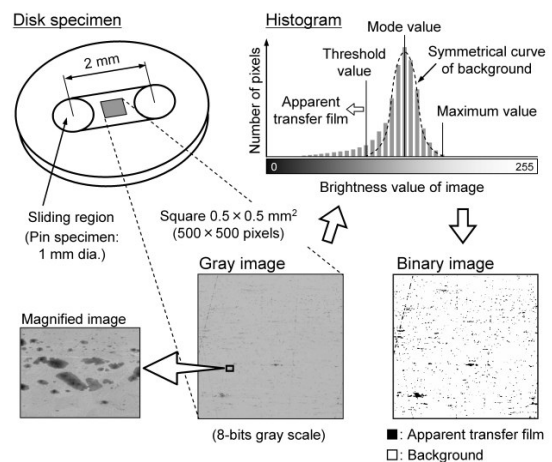


Fig. 1 Quantification procedure for the UHMWPE transfer film formed on the Co-28Cr-6Mo alloy surface.

The apparent transfer film region and the background region were digitalized using the threshold value of brightness. The threshold value in the brightness histogram was determined by subtracting the difference of the mode value and the maximum value from the mode value. The quantification of the UHMWPE transfer film was defined as the ratio of the apparent transfer film region to the acquired whole image.

**2.4. Measurement of the pull-away force**

The measurement of the pull-away force between UHMWPE and Co-28Cr-6Mo alloy was carried out using the vertical force measuring apparatus as shown in Fig. 2. The pin specimens were vertically pressed against disk specimen in a water droplet, and the pressing load was gradually increased until the contact stress reached 30 MPa. Thereafter, the pressing load was gradually decreased until the pin holder was separated from the base plate of the apparatus. The disk specimen was continuously pulled away at a velocity of 2.5 μm/s until the pin and disk specimens were separated. At the moment of separation, the peak force was detected, and the deadweight of the pin specimen with the holder was measured at another moment. The pull-away force is determined as the difference of the peak force and the deadweight.

**3. Results and discussion**

The formation of a UHMWPE transfer film on the surface of the Co-28Cr-6Mo alloy was reduced by the addition of vitamin E to UHMWPE as shown in Fig. 3. The pull-away force between UHMWPE and the Co-28Cr-6Mo alloy was also reduced by the addition of vitamin E as shown in Fig. 4. The formation of the transfer film is affected not only by the mechanical properties of the materials, but also by surface interactions. Our previous study showed that the elastic modulus, elongation at break, and tensile strength of non-oxidized vitamin E-containing UHMWPE are almost same as those of virgin UHMWPE [3]. If some kind of attractive force between UHMWPE and the surface of the Co-28Cr-6Mo alloy is changed by the addition of vitamin E, following two possibilities can be considered. One possibility is that the oxidation of UHMWPE caused by the combination of free radicals with oxygen may produce peroxides and hydroxyl groups in UHMWPE. Another possibility is that vitamin E seeped onto the surface of the UHMWPE as a result of the applied loading.

**4. Conclusion**

Our results suggest that the addition of vitamin E reduces the attraction between UHMWPE and the surface of the Co-28Cr-6Mo alloy.

**References** [1].Tomita N, et al. J Biomed Mater Res 1999;48:474. [2].Teramura S, et al. J Orthop Res 2008;26;460. [3].Sakuramoto, et al. Trans Jpn Soc Mech Eng A 2001;67:1702.



Fig. 2 A schematic drawing of the apparatus and the procedure for measuring the pull-away force between UHMWPE and the Co-28Cr-6Mo alloy.



Fig. 3 Apparent region ratio of the UHMWPE transfer film formed on the Co-28Cr-6Mo alloy surface at different contact stress values. Data represent mean ± SD. Asterisks indicate a statistically significant difference (*; $P < 0.05$, **; $P < 0.01$, n = 6, by two-way ANOVA).



Fig. 4 Pull-away force between UHMWPE and the Co-28Cr-6Mo alloy. Data represent mean ± SD. Asterisk indicates a statistically significant difference (*; $P < 0.05$, n = 8, by student's t-test).

# DISCOVERY OF UHMWPE WEAR NANOPARTICLES GENERATED *IN VIVO*: WERE THE PREVIOUS ANALYSES OF WEAR DEBRIS WRONG?

Miroslav Slouf*[1], Monika Lapcikova[1], David Pokorny[2], and Gustav Entlicher[3]

[1] *Institute of Macromolecular Chemistry of the AS CR, v.v.i., Heyrovskeho namesti 2, 16206 Praha 6, Czech Republic; slouf@imc.cas.cz*
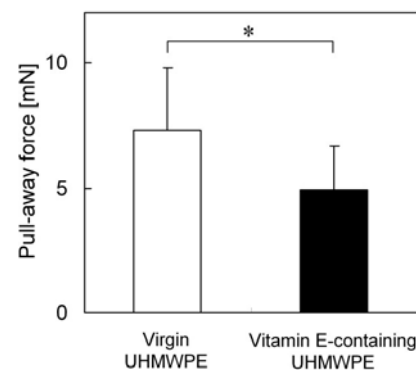[2] *Orthopedics Clinic, Hospital Motol, V Uvalu 84, 156 06 Prague 5, Czech Republic*
[3] *Faculty of Sciences, Charles University, Hlavova 8, 128 40 Prague 2, Czech Republic*

## Abstract

Recent discovery of *in vivo* UHMWPE wear nanoparticles questioned validity and accuracy of previous wear debris isolation and quantification procedures. Nevertheless, our results suggest that in most cases the number of the UHMWPE wear microparticles is much higher than the number of nanoparticles. Moreover, a good correlation between the volume of wear microparticles and extent of osteolysis in various zones around total joint replacements was found. This implied that the UHMWPE wear microparticles, rather than the nanoparticles, are responsible for most failures of total joint replacements.

## Introduction

UHMWPE wear particles have been recognized as one of the major causes of TJR failures [1]. It was shown that the most biologically active and thus the most dangerous wear particles have sizes below 10 μm [2]. A few years ago *in vitro* experiments on wear testing machines proved that a significant fraction of wear particles can be smaller than 0.2 μm [3, 4]. Recent studies, both in our laboratory [5] and elsewhere [6], showed that nanometer-sized wear particles are also generated *in vivo*.

The discovery of *in vivo* UHMWPE wear nanoparticles somewhat changed the situation in the field of wear debris quantification. In this contribution, we focus on two questions, which are closely connected with the polyethylene wear nanoparticles: (i) Why the wear nanoparticles were not observed in previous studies? (ii) Do the wear nanoparticles play an important role in total joint replacement failures?

## Materials and Methods

*In vivo* UHMWPE wear particles were isolated from periprosthetic tissues, which came from revisions of total joint replacements (TJR) of more than 100 patients. The isolation was based on our method that combines $HNO_3$ digestion with several purification steps and yields pure UHMWPE particles with sizes below 10 μm [7]. Purity of the isolated particles was confirmed by field-emission gun scanning electron microscopy (FESEM) with X-ray microanalysis (EDX) and infrared spectroscopy (IR, refs. [5,7]). Size distribution of the isolated particles was obtained by image analysis of

FESEM micrographs [5]. Correlation between extent of osteolysis and volume of wear particles in specific zones around TJRs was investigated at both qualitative [8] and quantitative level [9].



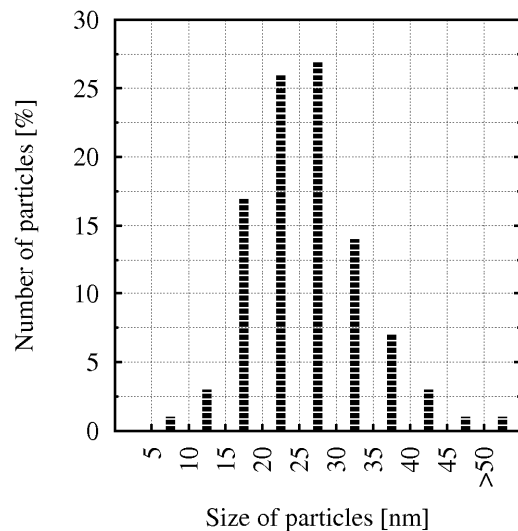Figure.1. FESEM micrograph showing in vivo UHMWPE wear nanoparticles on PC membrane filter.



Figure 2. Size distribution of in vivo UHMWPE wear nanoparticles from Fig. 1.

## Results and discussion

More than 100 samples of periprosthetic tissues, obtained from revisions of TJR, were analyzed. In two patients, the UHMWPE wear debris contained mostly nanoparticles with average size <50nm as proved by image analysis of FESEM micrographs

(Figs. 1,2; ref. [5]). The other samples contained mostly microparticles, although detailed analysis of high magnification FESEM micrographs proved that also small amounts of wear nanoparticles were present (Fig. 3).
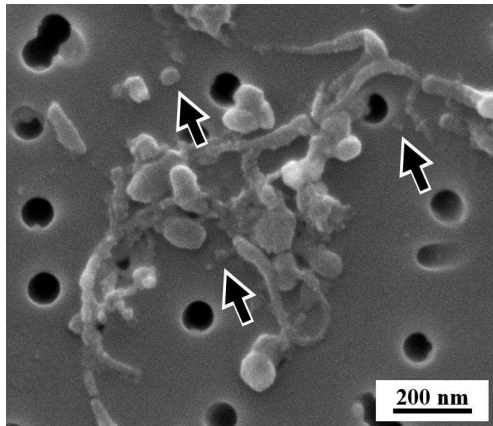


*Figure 3. FESEM micrograph showing PC membrane filters with isolated UHMWPE wear microparticles and nanoparticles, which are denoted by arrows.*

Therefore, our results suggested that in most of the specimens microparticles predominate. Moreover, the samples containing mostly microparticles were further analyzed by IRc method, which yields total volume of UHMWPE wear debris with sizes <10μm [8, 9]. A correlation between extent of osteolysis in various zones around TJR and volume of wear particles in these zones was found. This indicated that the common wear microparticles were the main reason of TJR failures.

It seems that UHMWPE wear nanoparticles were not detected in previous studies as their observation required rather unusual combination of FESEM microscopy, very high magnifications and intensive sonication just before the filtration of the suspension of isolated particles [5]. In previous investigations, the researchers used a standard scanning electron microscopes (SEM), lower magnifications and different sonication conditions. Standard SEM usually prevents observation of wear particles at the highest magnification due to beam damage of the specimen. Lower magnifications are not sufficient to distinguish individual wear nanoparticles, which tend to agglomerate. Insufficient sonication further supports formation of nanoparticle agglomerates, which might be confused with single microparticles.

## Conclusion

1. More than 100 periprosthetic tissues containing UHMWPE wear particles were analyzed. Wear nanoparticles smaller than 50 nm predominated in 2 samples. However, in all other samples the microparticles with sizes >50 nm prevailed [5].

2. Samples containing mostly microparticles were further analyzed and the correlation between total volume of UHMWPE wear microparticles and osteolysis in various zones around TJR was found [8, 9]. This suggested that wear microparticles, rather than wear nanoparticles, caused TJR failures.

## References

[1] T. M. Wright, S. B. Goodman SB (Eds.), Implant Wear in Total Joint Replacement, American Academy of Orthopaedic Surgeons, IL, USA, 2001, pp. 3–12.

[2] J. B. Matthews, A. A. Besong, T. R. Green, M. H. Stone, B. M. Wroblewski, J. Fisher, E. Ingham, Evaluation of the response of primary human peripheral blood mononuclear phagocytes to challenge with in vitro generated clinically relevant UHMWPE particles of known size and dose, *J. Biomed. Mater. Res.* 52 (2000) 296–307.

[3] M. Scott, K. Widding, S. Jani, Do current wear particle isolation procedures underestimate the number of particles generated by prosthetic bearing components? *Wear* 251 (2001) 1213–1217.

[4] A. L. Galvin, J. L. Tipper, E. Ingham, J. Fischer, Nanometre size wear debris generated from crosslinked and non-crosslinked ultra high molecular weight polyethylene in artificial joints. *Wear* 259 (2005) 977–983.

[5] M. Lapcikova, M. Slouf, J. Dybal, E. Zolotarevova, G. Entlicher, D. Pokorny, J. Gallo, A. Sosna (2009). Nanometer size wear debris generated from ultra high molecular weight polyethylene in vivo. *Wear*, 266 (2009) 349-355.

[6] L. Richards, C. Brown, M. H. Stone, J. Fisher, E. Ingham, J. L. Tipper. Identification of nanometre-sized ultra-high molecular weight polyethylene wear particles in samples retrieved in vivo. *J. Bone Joint Surg. (Br)* 90B (2008) 1106-13.

[7] M. Slouf, S. Eklova, J. Kumstatova, S. Berger, H. Synkova, A. Sosna, D. Pokorny, M. Spundova, G. Entlicher. Isolation, Characterization and Quantification of Polyethylene Wear Debris from Periprosthetic Tissues around Total Joint Replacements. *Wear* 262 (2007) 1171-1181.

[8] M. Slouf, D. Pokorny, G. Entlicher, J. Dybal, H. Synkova, M. Lapcikova, Z. Fejfarkova, M. Spundova, F. Vesely and A. Sosna. Quantification of UHMWPE wear debris in periprosthetic tissues of hip arthroplasty: description of a new method based on IR and comparison with radiographic appearance. *Wear*, 265 (2008) 674-684.

[9] D. Pokorny, M. Slouf, J. Belacek, F. Vesely, P. Fulin, D. Jahoda, I. Landor, S. Popelka, E. Zolotarevova, A. Sosna. Distribuce otěrových částic UHMWPE v periprotetických tkáních u TEP kyčelního kloubu. *Acta Chir. ortop. Traumat. čech.*, submitted.

# Nanometer-sized UHMWPE Particle Effect on Osteoblasts

Musib, MK[1,2]; Marshall AD*[1]; Oxley J [3], Sylvia VL[1]; Agrawal CM[2]; Dean DD[1]
[1]University of Texas Health Science Center at San Antonio, San Antonio, TX; [2]University of Texas at San Antonio, San Antonio, TX; [3]Southwest Research Institute, San Antonio, TX
Corr. Author: Amanda Marshall, MD marshalla2@uthscsa.edu 7703 Floyd Curl Drive #7774, San Antonio, TX 78229

## INTRODUCTION:

Ultra-high molecular weight polyethylene (UHMWPE) is widely used to fabricate components of orthopaedic implants. Despite good mechanical properties, it produces wear debris particles that have been implicated in implant loosening. Cell response to submicron size UHMWPE particles has been well documented[1,2], while reports of response to particles smaller in size (<0.2µm) are virtually absent. In the present study, UHMWPE resin was fractionated into 3 size ranges and added to cultures of human osteoblasts (MG63). At harvest, the effect of particle treatment on cell viability and membrane integrity was assessed.

## METHODS:

**Fractionation of UHMWPE particles.** UHMWPE (GUR 1050) particles were suspended in water, pH 5.5, containing 500ppm Pluronic. The suspension was vortexed for 15mins, sonicated for 2hrs and then stored at 4ºC for 7 days. Earlier studies in our lab demonstrated that this solvent minimizes particle aggregation and facilitates fractionation. After 7 days, the suspension was filtered through a 10µm pore size filter to remove large resin particles. The suspension was then fractionated into 3 size ranges (1.0-10.0µm, 0.2-1.0µm and 0.01-0.2µm) by filtration through filters of varying pore size. Representative images were obtained using a Zeiss EVO50 SEM and analyzed according to ASTM F-1877 using software which determines equivalent circle diameter (ECD) and various shape descriptors[3,4].

**Effect of particle size on MG63 cell viability and membrane integrity.** MG63 cells (ATCC) were cultured in DMEM containing 10% FBS. Cells were seeded into 24 well plates and allowed to attach. After 12hrs, media were changed and fresh media containing $10^5$ to $10^7$ particles/well for each of the 3 size ranges added. Control cultures only received fresh media. Treatment continued for 4 to 120hrs. At harvest, the number of viable cells was measured using the CellTiter-Blue Assay (Promega), while release of LDH (a marker of membrane integrity and cytotoxicity) was measured using a CytoTox-ONE kit (Promega).

**Statistical Interpretation of Data:** ANOVA was used to analyze the data; post-hoc testing was performed using Student's t-test with Bonferonni correction. P values $\leq$ 0.05 were considered significant.

**RESULTS:** All particle suspensions were endotoxin-free. Equivalent circle diameter (ECD) for each of the 3 preparations is shown in Table 1. Minimum and maximum particle size in each fraction was predictable based on the pore size of the filter (Table 1). Up to 24hrs, particles had a dose-dependent stimulatory effect on the number of viable cells; the magnitude of the effect was greatest with the nanoparticle fraction. After 24hrs, particles dose-dependently inhibited cell viability and the effect was greatest for the nanoparticle fraction. Particle treatment also had a dose-, size-, and time-dependent effect on LDH release (Figure 1). As seen for cell viability, the nanoparticle fraction produced the greatest release of LDH. Unlike viability, the most pronounced effect of particles on LDH release was seen after 120hrs of treatment.

| Particle Fraction | Mean (µm) | S.E.M. | Min. | Max. |
|---|---|---|---|---|
| 10.0µm filtrate (collect on 1µm) | 2.240*# | 0.084 | 0.220 | 7.650 |
| 1.0µm filtrate (collect on 0.2µm) | 0.513* | 0.012 | 0.017 | 0.909 |
| 0.2µm filtrate (collect on 0.01µm) | 0.056 | 0.002 | 0.015 | 0.190 |

**Table 1: Mean ECD (µm) of Fractionated Particle Suspensions**
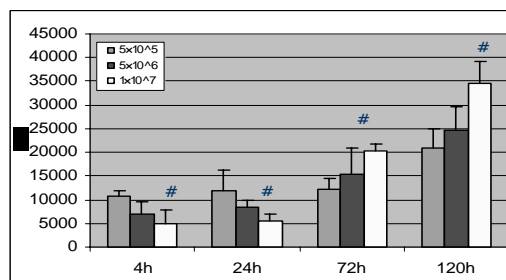A total of 300 particles in each fraction were analyzed. *P<0.05, vs 0.2µm filtrate; #P<0.05, vs. 1.0µm filtrate.



**Figure 1.** Effect of UHMWPE nanoparticles on LDH release [above control] by MG63 cells. (#P<0.05, vs treatment with $10^5$ particles).

**CONCLUSIONS:** A method for fractionating UHMWPE particles has been developed. Fractionated particles were found to have size-, dose-, and time-dependent effects on osteoblast cell viability and membrane integrity. With 24hrs of treatment, nano-size particles demonstrated a 1.3 to 2.5-fold stimulatory effect on the number of viable cells compared to submicron- and micron-size particles. Cell viability decreased with longer treatment times. Similarly, LDH release was dose-dependently increased, suggesting a cytotoxic effect of the nanoparticles. These results suggest that nano-sized particles may elicit more adverse affects on osteoblasts than previously reported for submicron-sized particles.

## REFERENCES
[1]Dean DD, et al., *J Orthop Res* 17:9-17, 1999.
[2]Dean DD, et al., *J Bone Joint Surg* 81A:452-461, 1999.
[3]Landry M, et al., *J Biomed Mat Res* 48:61-69, 1999.
[4]McMullin BT, et al., *Biomaterials* 27:752-757, 2006.

# HIGH-DENSITY BRUSH-LIKE STRUCTURE MIMICKING CARTILAGE GIVES HIGH DURABILITY TO CROSS-LINKED POLYETHYLENE

Masayuki Kyomoto*[1,2,3], Toru Moro[3], Fumiaki Miyaji[1], Hiroshi Kawaguchi[4],
Yoshio Takatori[3], Kozo Nakamura[4], Kazuhiko Ishihara[2]

[1]*Research Department, Japan Medical Materials Corporation,*
*3-3-31 Miyahara, Yodogawa-ku, Osaka 532-0003, Japan, E-mail: kyomotom@jmmc.jp*
[2]*Department of Materials Engineering, School of Engineering,* [3]*Division of Science for Joint Reconstruction,*
*School of Medicine, and* [4]*Department of Orthopaedic Surgery, Faculty of Medicine, The University of Tokyo*

## Introduction

Osteolysis caused by wear particles from polyethylene (PE) in the artificial hip joints is a serious issue. We have used surface-initiated graft polymerization with poly(2-methacryloyloxyethyl phosphorylcholine) (PMPC) on the cross-linked PE (CLPE) surface by ultraviolet (UV)-irradiation, in order to reduce friction and wear at the orthopaedic bearing surface. In the present study, the change in properties of the PMPC layer with UV-irradiation times was examined, and the wear-resistant properties of the PMPC-grafted CLPE were discussed in terms of the high-density brush-like structure mimicking cartilage of the PMPC layer.

## Materials and Methods

The CLPE (GUR1020 resin, 50 kGy gamma-ray irradiation, and 120°C annealing) specimens coated with benzophenone as photo-initiator were immersed in the 0.5 mol/L aqueous MPC solution. The graft polymerization on the CLPE surface was carried out with UV-irradiation of 5 mW/cm$^2$ for 23–180 min at 60°C. The functional groups vibration of the PMPC-grafted CLPE surface was examined by Fourier-transform infrared (FT-IR) spectroscopy. The relative amount of grafted PMPC unit on the CLPE surface was evaluated by quantification of the phosphate (P–O) group which was contained in the structure of MPC unit, as the P–O group index = (P–O peak intensity) / (-CH$_2$- peak intensity).

The PMPC-grafted CLPE cups and Co-Cr-Mo alloy femoral ball were used for the hip joint simulator wear test. The 5 x 10$^6$ cycles wear test was performed using a 12-stations MTS hip joint simulator. A mixture of 25% bovine serum was used as lubricant. For the isolation of wear particles, the lubricant after wear test was incubated with 5 mol/L NaOH solution in order to digest adhesive proteins that were degraded and precipitated. The digested solution was then sequentially filtered, and the membrane used for filtration was observed by scanning electron microscopy (SEM).

## Results and discussion

The P–O group index increased with an increase in the UV-irradiation time. In hip joint simulator test, the gravimetric wear was substantially lower in PMPC-grafted CLPE cups than in the untreated CLPE cups. The wear of the PMPC-grafted CLPE cups with 23 min UV-irradiation started to increase after 2.5 x 10$^6$ cycles (Fig. 1). The wear particles of the untreated CLPE and PMPC-grafted CLPE cups were submicrometer-sized granules.

The number of wear particles of the PMPC-grafted CLPE cups was significantly less than that of the untreated CLPE (Fig. 2).

The cartilage surface is assumed to have a brush-like structure: a part of the proteoglycan aggregate brush is bonded with the collagen network on the cartilage surface. The surface-initiated graft polymerization of this study has been utilized to synthesize high-density polymer brushes. Therefore, the bearing surface with PMPC-graft layer is assumed to have a brush-like structure similar to that of cartilage. It is assumed that a high density of the introduced PMPC is involved in the long-term retention of the benefits of PMPC in the artificial joint. In order to obtain a high density PMPC layer, the UV-irradiation time must be controlled.



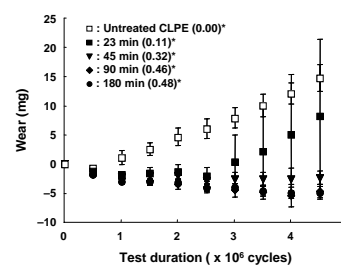Fig. 1. Wear of the PMPC-grafted CLPE cups with various UV-irradiation times in the hip joint simulator test. *P–O group indexes are in parentheses.
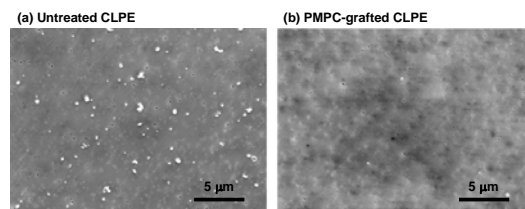


Fig. 2. SEM images of wear particles of the PMPC-grafted CLPE during the hip joint simulator test.

## Conclusion

The high-density brush-like structure mimicking cartilage of the PMPC-grafted CLPE could give a high durability as an orthopedic bearing.

# ENDOSOMAL DAMAGE AND TLR2 MEDIATED INFLAMMASOME ACTIVATION BY UHMWPE  PARTICLES IN THE GENERATION OF ASEPTIC OSTEOLYSIS

Radhashree Maitra[*1], Cristina C. Clement[1],  Brian Scharf[l],   Giovanna M,  Crisi [2] ,Sriram Chitta[3]  Daniel Paget [4],  P. Edward Purdue[4], Neil Cobelli[5], Laura Santambrogio[1].

[1]Department of Pathology, Albert Einstein College of Medicine, Bronx, NY-10461[2]Department of Pathology, Baystate Medical Center, Springfield, MA, 01199, USA [3] Department of Pathology, University of Massachusetts Medical School, Worcester, MA, 01655  . [4] Osteolysis Research Laboratory, Hospital for Special Surgery, New York, NY10021. [5] Division of Orthopedic Surgery, Montefiore Medical Center, New York, NY,10461, USA. **Corresponding Author**: Radhashree Maitra, Department of Pathology, Albert Einstein College of Medicine, 1300 Morris Park Avenue, Bronx, New York 10461. Ph 718-430-3468; Fax 718 430 8541; E-mail: rmaitra@aecom.yu.edu
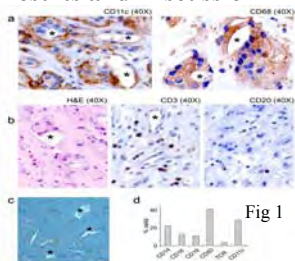
## INTRODUCTION

Ultra high molecular weight polyethylene is widely used as a bearing surface in prosthetic arthroplasty. Over time the generation of implant-derived wear particles can initiate an inflammatory reaction characterized by periprosthetic inflammation and ultimately bone resorption at the prosthetic bone interface. Herein we present evidence that the different sized particles as well as the different length alkane polymers generated by implant wear leads to a two component inflammatory response. Polymeric alkane structures, with side chain oxidations, directly bind and activate the TLR-1/2 signaling pathway.  Whereas micron and nanometer sized particulate debris are extensively phagocyted and induce enlargement, fusion and disruption of endosomal compartments. The resulting lysosomal damage and subsequent enzymatic leakage induces the NALP3 inflammasome activation as determined by cathepsins S and B cytosolic release, Caspase 1 activation and IL-1β, and IL-18, processing.  These two processes synergistically results in the initiation of a strong inflammatory response with consequent cellular necrosis and extracellular matrix degradation.

## Materials and Methods

**Imunohistochemistry:** Periprosthetic tissue was formalin-fixed, paraffin embedded. Polarized light microscopy was utilized to identified birefringent UHMWPE particles. Expression of various cell surface markers was determined by labeling  for 30 min on ice with saturating amounts of primary mAb in staining buffer  (PBS/0.1 % BSA/ 0.01% NaN3).  FACSCalibur flow cytometer and cellquest software program were utilized for the acquisition of the histogram and mean fluorescence was calcutaed by Flo Jo 7.2. **Microscopy: TEM:** Tissue samples and cultured Monocytes, DC, MØ  were fixed with a mixture of 2% para-formaldehyde and 2.5 % glutaraldehyde in cacodylate buffer 0.1 M, pH 7.4 at 4°C Fixed cells were infiltrated in sequentially increasing concentrations of LX112-Araldite to 100%, embedded in BEEM capsules. **SEM:** The samples were mounted on a stub but not sputter coated  and viewed at 300X magnification. **Confocal**: Primary dendritic cells were grown on culture slides with GMCSF for 6 days with and without UHMWPE. The cells were treated either with LysoTracker Green DND-26 (excitation/emission 504/511 nm) at 75 nM concentration for 30 mins individually or in combination with cathepsin specific activity probe, GB123 (excitation/emission 646/666 nm)  washed, counterstained with DAPI (excitation/emission 358/461 nm) and fixed in 4% paraformaldehyde. **β-hexosaminidase Assay:** ß-hexosaminidase release from human monocyte derived DC was determined by addition of 100ul of incubation buffer from UHMWPE treated or untreated cells to 100ul of reaction mixture (5ml 0.4M Sodium acetate pH 4.4, 5ml of 8mM 4-methylumbelliferyl-N-acetyl-B-D glucopyranoside in water, 0.250ml Triton X-100, 9.750 ml water) in a 96 well plate incubated at $37^0$C for 30 minutes in an hybridization oven. The reaction was stopped by addition of 75ul of 2M $Na_2CO_3$, and the fluorescence measured in a spectrofluorimeter  at excitation 350nm/emission 450nm: **Western Blot Analysis**: Jaws cells untreated and treated 24 hours with UHMWPE in presence and ere cultured. Western analysis of the total cell lysate was then probed with antibodies specific to Cathepsin B, Caspase 1 p10 fragment,  IL-1β,  Il-18 proteins to evaluate the inflammasome activation. Cell lysates from human monocytes cultured with or without particles for 6 hours in the presence or absence of TLR stimulation were likewise immunoblotted to detect expression of Pro-IL1β.**Gene Chip Assay:**Five micrograms of total RNA were hybridized on the Human Toll-like Receptor Oligo. Data are reported as average hybridization numbers for each gene subtracted for background. **Luciferase assay:** The HEK 293/ TLR 1/2 clones were  transfected with the NF-Kβ  cis- reporter enhancer with an independent GFP plasmid  using Fugene 6. 48hrs post transfection the cells were treated with UHMWPE, as well as a positive control. The luciferase  readout was measured at different time points using the standard Luciferase reporter assay kit.**In vitro processing of Collagen I by cathepsins:** Collagen I processing was performed in vitro using human recombinant cathepsins (B, D, L and S) In order to identify fragments generated only from cathepsin processing of collagen-I, all enzymatic reactions were performed in parallel using selective inhibitors of cathepsins, such as calpain inhibitor II (ALLM) and Pepstatin A. **ELISA:**The cytokine assay was performed with the control and PE treated (48hrs) dendritic cells using the Bio-rad human 17-plex reagent kit.

## Results and Discussion


Fig 1

**Myelomonocytic infiltration and giant cell formation around micrometer size UHMWPE wear debris** Immunohistochemistry analysis was performed on periprosthetic tissue obtained at the time of implantfailure revision surgery. Peri-articular tissue was stained with antibodies specific for different immune cell sub-populations. Infiltrate of predominantly macrophages (CD68) and dendritic cells (CD11c) were observed in all analyzed samples (Fig 1a). Only few T-cells (CD3) and B-cells (CD20) could be visualized in the inflamed tissue (Fig 1b). Most of the cellular infiltrates were organized as multinuclear giant cells surrounding the UHMWPE

particles (which appear birefringent under polarized light) (Fig: 1c).To further confirm the nature of the infiltrates FACS analysis was performed on collagenase digested peri-prosthetic tissue. Analysis confirmed the previously documented immuno-histochemical findings that the majority of the infiltrates were myelomonocytic in nature with most of cells expressing DC markers (CD11c and CD83) or monocytes/macrophages markers (CD11c, CD14, and CD16) (Fig 1d).

**Lysosomal damage and inflammasome activation by UHMWPE wear debris** Ultrastructural analysis of inflammatory infiltrates indicated phagocytosis of nanometer-sized particles of UHMWPE (Fig 2a,b). In every cell endosomal compartments were completely engorged by the alkane particles (Fig2c). The failure of the endosomal enzymes to degrade UHMWPE resulted in a significant increase in the number and size of the compartments (Fig 2d- f) as well as increased fusion between compartments (Fig:2f-g). Finally several compartments underlying the plasma membrane were also observed, some undergoing the process of exocytosis (Fig2h).The endosomal engorgement induced physical damage to the limiting membrane of the compartments with subsequent cytosolic release of endosomal enzymes. (Fig:3a) The integrity of endosomal compartments was assessed following endocytosis of the lysosensor DND 189, as well as a Cathepsin B,S,L specific activity probe. Confocal analysis performed on control cells detected the presence of intact endosomal compartments (Fig 3b). On the other hand DC cultured for 72 hours with UHMWPE demonstrated extensive damage of the endosomal compartments with release of the fluorescent tracer in the cytosol and the extracellular milieu (Fig 3c). To further confirm presence of endosomal enzymes extracellularly the culture supernatant was collected and assayed for presence of lysosomal enzymes. A statistically significant increase of beta-hexosaminidase as well as cathepsin S and B was observed in the supernatant of DC cultured with UHMWPE (Fig 3d & e).
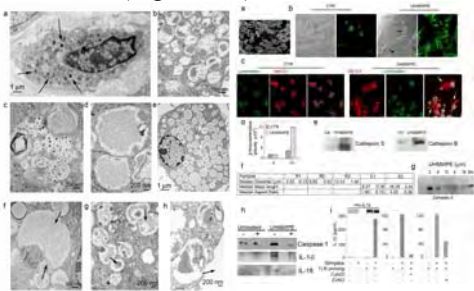
Fig2

Fig3

Supernatant collected after 72 hours of culture indicated that smaller size particles induced more extensive endosomal damage as assessed by cathepsin S release into the supernatant Fig: 3f. Increased levels of Caspase 1 p10 Fragment (Fig: 3g) and active IL-1β and Il-18 (Fig: 3h) were observed in UHMWPE treated Caspase 1 cleavage and cytokine activation was down regulated in presence of cathepsin B specific inhibitor indicating that cytosolic release of cathepsin B following endosomal damage by UHMWPE particles is responsible for the inflammasome activation (Fig 3g & h). Similar results were found with other disease-relevant myeloid cell types and particles. TLR stimulation of human monocytes (Figure 3i).

**Alkane polymers induce TLR1/2 activation, myelomonocytic cell activation and Extracellular matrix degradation**
Significant increase in mRNA encoding for TLR1 and TLR2, was observed in UHMWPE treated DC (Fig 4a). RNA hybridization assay showed an up-regulation of the different NF-KB/ Rel subunits(Fig 4c) TLR1/2 activation by UHMWPE polymers was further confirmed by a luciferase assay on stable HEK 3T3-TLR1/2 cell transfected with an NF-KB enhancer element (Fig4b). After 48 hours of UHMWPE incubation DC, Macrophages and osteoclasts were harvested and stained for surface activation markers. A significant up-regulation of surface MHC II, B7-1, B7-2 and CD40 was observed in dendritic cells and macrophages and to a lesser extent in monocytes and osteoclast upon incubation with oxidized alkane but not in control treated cells (Fig 4d). Supernatant from DC cell cultures was also harvested to measure cytokine production. Up-regulation of several pro-inflammatory cytokines including IL-6, IL-10, IL-12, TNF-α, also observed (Fig 4e).
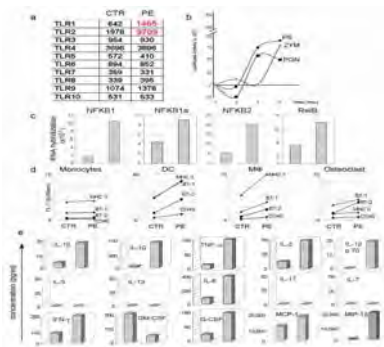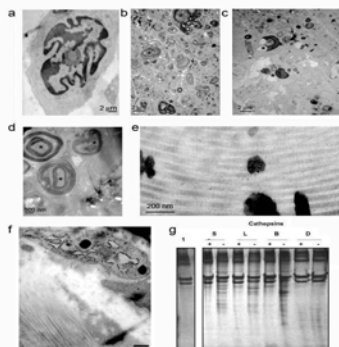
Fig 4

Fig 5

In periprosthetic inflamed tissue several necrotic cells with pyknotic and fragmented nuclei could be observed (Fig 5a). Also several myelin figures, characteristic of protein/lipid precipitation observed in necrotic tissue, were evident both intra and extracellularly (Fig 5b, c & d). Numerous micron and nanometer size particles could be detected in the extracellular collagen matrix (Figure 5e). vitro digestion by endosomal cathepsins (Fig 5g).

**Conclusion** It was recognized that aseptic necrosis is the typical outcome associated with implant failure and that size of the particles was important in determining the severity of the inflammatory process. Herein we determine the molecular basis for this phenomenon.TLR1/2 engagement by polymeric UHMWPE debris induces a pro-inflammatory transcription program mediated by NFkB signaling pathways, inducing the expression of pro-IL-1β and pro-IL-18. As second step UHMWPE particles, readily phagocyted by local cells, induce endosomal destabilization. Consequent cathepsin release is perceived by the immune system as an endogenous danger signals inducing NALP3 inflammasome activation. Thus a multidimensional cascade of immune response is initiated. Important implications in UHMWPE designing can be gathered from this analysis.

# DIFFERENCES BETWEEN HOST RESPONSES IN ASEPTIC AND SEPTIC LOOSENING OF METAL-ON-POLYETHYLENE TOTAL HIP REPLACEMENT IMPLANTS

Yrjö T. Konttinen*[1,2,3], Jukka Pajarinen[1], Elisabetta Cenni[4], Lucia Savarino[4], Enrique Gomez-Barrena[5], Yasunobu Tamaki[6], Michiaki Takagi[6], Jari Salo[7]

[1]Institute of Clinical Medicine, Department of Medicin, Biomedicum, PO Box 700, FIN-00029 HUS, Finland, yrjo.konttinen@helsinki.fi (*corresponding author), [2]ORTON Orthopaedic Hospital of the ORTON Foundation, Helsinki, Finland, [3]COXA Hospital for the Joint Replacement, Tampere, Finland, [4]Istituti Ortopedici Rizzoli, Bologna, Italy, 5Universidad Autónoma de Madrid, Fundación "Jiménez Díaz" Hospital, Madrid, Spain, [6]Yamagata University School of Medicine, Yamagata, Japan, [7]Helsinki University Central Hospital, Helsinki, Finland

## Introduction

In a global perspective, metal-on-conventional polyethylene is the most popular gliding pair in total hip replacement. This gliding couple leads to formation UHMWPE wear debris. This wear debris is in part phagocytosed by macrophages in the peri-implant tissues. This provokes chronic foreign body inflammation. Phagolysosomal enzymes do not have the capability to degrade the phagocytozed polyethylene debris. Chronic inflammation stimulated fibroblast- and osteoblast-mediated synthesis of osteoclastogeneic receptor activator of nuclear factor kappa B ligand (RANKL). This again stimulates osteoclast formation leading to either linear but often aggressive granulomatous peri-implant bone lysis.

It has long been suspected that some type or more or less evident infections could also contribute to the same end. It could be a relatively acute, productive and purulent infection causing local and even systemic symptoms, but apparently often is a local and indolent infection maintained by biofilm hidden microbes. In the biofilm bacteria live vita minima and are relatively insensitive to antibiotics, which affect active metabolic processes. Second, biofilm forms a physical diffusion barrier hampering entrance of host leukocytes, antibodies, complement, antibiotics and other host defense factors and drugs.

The aim of the present study was to evaluate how the presence of a septic component modulates the host response compared to particle disease alone, without an infection.

## Materials and Methods

Peri-implant tissue samples were collected from patients (3 women and 2 men) with non-infectious aseptic loosening undergoing revision operation. They were 71.2 (range 64-78) years old.

They were compared to peri-implant tissue samples (8 women and 2 men) with bacterial culture positive septic loosening cases also undergoing revision. 10 tissue samples from osteoarthritis were used as comparators.

First, cells participating in the host response were characterized by using the following antibodies in immunohistochemical staining:
a) T lymphocytes = CD3
b) B lymphocytes = CD20
c) Macrophages = CD68 and CD163
d) Plasma cells = CD138
e) Fibroblasts = HSP47
f) Neutrophils = neutrophil elastase

Second, the armament used by these cells for both pathogen-associated molecular patterns (PAMPs) and endogenous alarmins (which together form danger- or damage-associated molecular patterns or DAMPs) was characterized as to the expression of Toll-like receptor (TLR) 4 and 9.

## Results and discussion

Interesting differences in the cellular composition between these three conditions (Table).

1) Controls were characterized by loose connective tissue consisting of vascularized connective tissue matrix with some infiltrating macrophages and T and B lymphocytes.
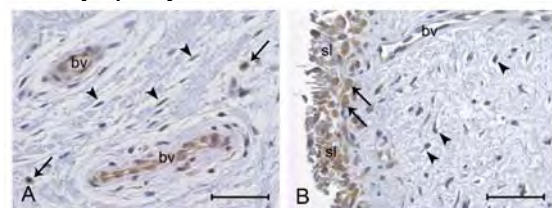


*Figure 1. TLR in control samples in the endothelium (A) and synovial lining (B).*
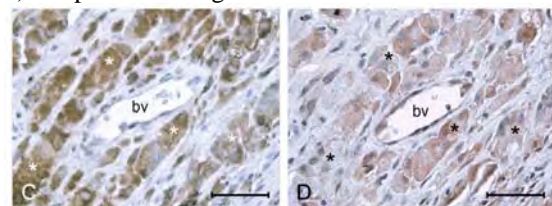
2) Aseptic loosening



*Figure 2. Macrophages and TLR4 in a chronic foreign body reaction (also foreign body giant cells and granulomas were seen, with some infiltrating T cells).*

3) In septic loosening two more cells types took more prominent positions, namely neutrophils in same samples and areas and T and B cells as well as plasma cells in other areas.
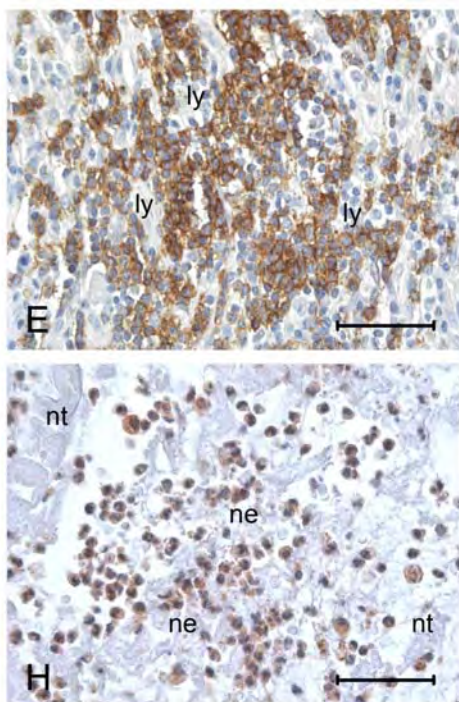


*Figure 3. Above B lymphocyte infiltrate and below neutrophils in septic loosening.*

| Cell type | Contr | Aseptic | Septic |
|---|---|---|---|
| Fibroblasts | ++ | + | ++ |
| Neutrophils | - | - | ++ |
| Macrophages | + | +++ | ++ |
| T cells | ± | + | ++ |
| B cells | + | - | ++ |
| Plasma cells | - | - | + |

I

Interestingly, the cells were in controls and in aseptic and septic loosening equipped with TLRs as shown in the tables below for TLR4 and TLR9. It is clear that
1) In controls particularly the internal vascular (endothelium) and synovial fluid (lining, with fibroblasts and macrophages) interface was equipped.
2) In aseptic loosening the infiltrating macrophages formed a major population.
3) In septic loosening the addition neutrophils and to some extent lymphocytes with TLRs were also seen.

| TLR4 | Contr | Aseptic | Septic |
|---|---|---|---|
| Endothelium | ++ | + | +++ |
| Fibroblasts | + | + | +++ |
| Neutrophils | - | - | ++ |
| Macrophages | + | +++ | +++ |
| Lymphocytes | - | - | + |

| TLR9 | OA | Aseptic | Septic |
|---|---|---|---|
| Endothelium | + | + | ++ |
| Fibroblasts | ± | + | ++ |
| Neutrophils | - | - | ++ |
| Macrophages | + | ++ | ++ |
| Lymphocytes | - | - | + |

**Conclusion**
1) In control tissue samples (osteoarthritic synovium) TLR positive cells were restricted to surface tissues and only few inflammatory cells were detected.
2) In aseptic interface was heavily infiltrated with monocyte/macrophages, which were also the major TLR positive cell type rendering the tissue reactive to TLR ligands.
3) Interestingly, septic cases contained also neutrophil and lymphocyte infiltrates, of which especially B cell infiltrates might be clinically useful in discriminating the two major complications of the joint replacement surgery.

To avoid aseptic loosening, it would be beneficial to improve the material properties of the UHMWPE, perhaps preferably by cross-linking and anti-oxidants to improve wear resistance and tolerance against oxidative stress.

**References**

Santavirta S, Konttinen YT, Nordström D, Bergroth V, Antti-Poika I, Eskola A: Immune-inflammatory response in infected arthroplasties. Acta Orthop Scand 60:116-118, 1989
Santavirta S, Konttinen YT, Bergroth V, Eskola A, Tallroth K, Lindholm TS: Aggressive granulomatous lesions associated with hip arthroplasty. Immunopathological studies. J Bone Joint Surg (Am) 72-A:252-258, 1990
Tamaki Y, Takakubo Y, Goto K, Hirayama T, Sasaki K, Konttinen YT, Goodman SB, Takagi M: Increased expression of toll-like receptors in aseptic loose periprosthetic tissues and septic synovial membranes around total hip implants. J Rheumatol 36:598-608, 2009

# Long-Term In-Vitro Wear Results of New Thermo-Compressed Cross-Linked Polyethylene

Saverio Affatato[1], Michele Spinelli[1], Pierangiola Bracco[2], Luigi Costa[2]

1) Department Laboratorio di Tecnologia Medica, Istituto Ortopedico Rizzoli, Bologna-Italy
2) IFM Chemistry Department, University of Turin, Italy
Corresponding author: affatato@tecno.ior.it

## 1. Introduction

Ultra-high-weight-molecular-PE (UHMWPE) used in orthopaedic implants presents serious clinical problems. The scientist are focussing to improve the wear performance of conventional UHMWPE and increase its mechanical properties. To this end, increasing the cross-linked density is well established as a promising solution to improve the wear resistance and durability of polyethylene [1]. The goal of the present work was to compare the wear behaviour of a new thermo-compressed cross-linked PE with standard cross-linked and conventional UHMWPE.

## 2. Materials & Methods

The wear behaviour of five different polyethylenes (conventional and cross-linked, dimensional cups = 28-mm inner x 44-mm outer; 4 specimens for each batch) coupled with 28-mm CoCrMo femoral heads were investigated using a hip joint simulator (Table 1).

Table 1 – Polyethylenes description.

| PE-type | Description |
| --- | --- |
| PE-A | PE GUR-1020 (EtO-sterilized) |
| PE-B | PE GUR-1020 (γ-sterilized) |
| PE-C | PE GUR-1050 (γ-sterilized) |
| XLPE | Cross linked PE GUR-1020 (EtO-sterilized) |
| XLPE-RT | Thermo-compressed cross-linked PE GUR-1050 (EtO-sterilized) |

Wear test was performed using a 12-station hip joint simulator (Shore Western, USA). The simulator set-up followed is described in details elsewhere [2]. Each articulating station was subjected to a sinusoidal loading (max 2 kN) with a frequency of 1.1 Hz, according to the rotation test frequency. Weight loss of the cups was determined every 0.5 Mc. A microbalance (Sartorius AG, Germany) with a precision of ±0.1 mg was used to measure the weight loss during the experiments.

An FTIR Microscope (Spectrum Spotlight 300, Perkin-Elmer, Shelton, Connecticut, USA) was used to map the oxidation. For collecting the line-scan spectra, the area of analysis was set at $100 \times 100 \ \mu m^2$ and the spectra were recorded every 100 μm along the mapping direction, starting from the articulating surface towards the bulk.

## 3. Results

All the specimens completed the planned 10 Mc. Compared to the different cup configurations, the XLPE-RT combination wore more than the XLPE but maintained a lower weight loss than the other conventional PE during the whole test (Fig. 1).
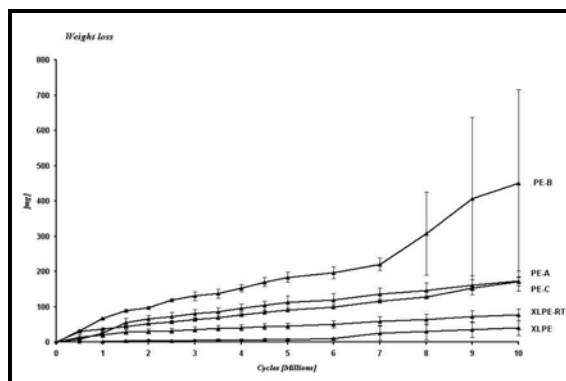


Fig. 1 - Weight loss (± S.D.) for five different PE.

Significant statistical differences ($p < 0.0001$) were observed between all the polyethylene cups using the *Kolmogorov-Smirnov* non-parametric statistical.

All samples showed diffusion of apolar products from the bovine serum, as indicated by the ester absorption at 1740 cm-1 found in all spectra.

## 4. Discussion

We found a reduced wear rate for the XLPE configurations in comparison to the conventional PE. In particular, the XLPE and XLPE-RT cups showed a significant wear reduction compared with the conventional PE (Fig. 1). XLPE-RT acetabular cups showed higher weight losses than XLPE (50%); for the tested specimens, the process of machining the specimens does not influence the wear performance of the XLPE. All the acetabular cups (cross-linked and conventional PE) showed significant differences between them in respect to the wear behavior. Weight loss was found to decrease for the XLPE than the other configurations.

## 5. References

[1] Jacob JJ. The UHMWPE handbook: ultra-high molecular weight polyethylene in total joint replacement. J Bone Joint Surg [Am] 2005:87-1906.

[2] Affatato S and al. Comparative study on the wear behaviour of different conventional and cross-linked PE for total hip replacement. Tribology International 2008; 41:813-822

# DIFFUSION OF VITAMIN E INTO UHMPWE: INFLUENCES OF VITAMIN E, AND OF HEAT, UPON FREE RADICAL ACTIVITIES DURING THE DIFFUSION PROCESS AND POST-DIFFUSION FREE RADICAL OBSERVATIONS

Benjamin M. Walters*[1], M. Shah Jahan[1], Sarah N. Johnson[1], Allyson A. Boyer[1]

[1] 216 Manning Hall, Dept. of Physics, The University of Memphis, Memphis, TN 38152. bwalters@memphis.edu

## Introduction

Free radicals are believed to be precursors to oxidation. The major problems which limit the life of UHMWPE prostheses are due mainly to chemical oxidation. Cross-linking by high-energy irradiation followed by melting is one method used to reduce the problem of wear. Cross-links are formed between the polyethylene chains by the free radicals formed from ionizing radiation in the amorphous region of UHMWPE. The free radicals formed in the crystalline phases of the polymer network do not recombine, and remain trapped and react with oxygen to form peroxy radicals. These peroxy radicals may attack other polyethylene chains, initiating an oxidative chain-reaction.

Melting has been used as a method to remove the free radicals which remain after cross-linking. Melting releases the trapped free radicals from the crystalline region of the UHMWPE; these released free radicals are then available to from more cross-links [5]. However, melting decreases the crystallinity, and therefore the fatigue strength and mechanical properties, of the UHMWPE [1]. It has been proposed that the step of melting can be done away with by using another method to eliminate the radicals remaining after cross-linking; this alternative method is the addition of vitamin E (alpha-tocopherol) to the UHMWPE [1]. Vitamin E is believed to remove any free radicals that do not form crosslinks after irradiation [1-3], and has been shown to effectively stabilize medical grade UHMWPE from oxidation [1,4-6].

One method used to add vitamin E to the UHMWPE is by diffusion – heating the UHMWPE while submerged in vitamin E so that the vitamin E diffuses into the UHMWPE. Heating the UHMWPE at below melting temperatures reduces the number of free radicals in UHMWPE, although not to the same extent as melting. It is therefore difficult to determine whether a reduction of free radicals in vitamin E-diffused UHMWPE can be contributed to the vitamin E's presence alone, or to the fact that the UHMWPE has been heated. In our study, we have diffused vitamin E into 30kGy gamma-irradiated UHMWPE at 100°C – a temperature well below the melting point of UHMWPE - in order to observe the general process of vitamin E being diffused into gamma-irradiated UHMWPE. While previous studies have evaluated vitamin E-diffused UHMWPE [1,6,7], our study investigates the free radical reactions going on during diffusion – at various time periods of the diffusion process – using ESR (electron spin resonance) techniques to directly detect the free radicals of the material. In addition, as the free radical activity does continue after diffusion, we also investigate these reactions at various time periods following diffusion.

## Materials and Methods

$2.5 \times 2.5 \times 8$ mm³ blocks of consolidated UHMWPE (GUR 1050) bar stock were cleaned and sealed in a nitrogen environment and gamma-irradiated (30.1-33.9 kGy) at room temperature. The samples were subsequently kept in liquid nitrogen during non-experimentation periods. The irradiated UHMWPE samples were separated into three groups: Those to be vitamin E-diffused (heated in the presence of vitamin E), those to be only heated (same heat exposure, but without vitamin E), those to be exposed to vitamin E but not heated, and those to be left alone (neither heated nor exposed to vitamin E). In addition, there was a group of vitamin E-only (no UHMWPE) samples tested similarly.

Samples to be heated were done so at 100°C, one group in nitrogen and one in air. Unless being heated or ESR-tested, samples were kept in liquid nitrogen in order to preserve free radical activity.
ESR Measurements and Data Analysis: Free radicals in each sample were analyzed in a nitrogen environment at 23°C using an X-band spectrometer (Bruker, EMX 300) operating at 9.8 GHz microwave frequency and 100 kHz magnetic field modulation frequency. UHMWPE samples which involved vitamin E exposure remained in vitamin E throughout the treatments and measurements.

## Results and discussion

ESR data from the experiment did differ among the groups of samples. Except for the group of UHMWPE samples which were not exposed to vitamin E or heat, all groups showed free radical decrease at various stages of diffusion; the decreases of free radical concentrations, those exposed to heat alone and those heated in the presence of vitamin E, as seen in Figures 1 and 2, showed the greatest reduction in free radicals.
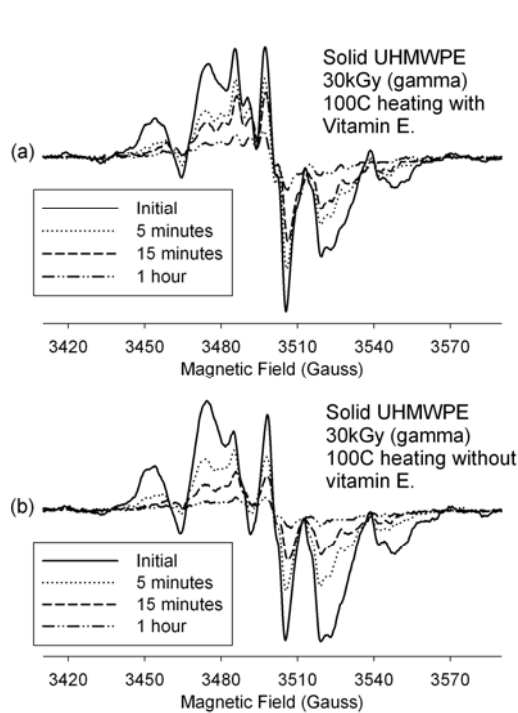
Fig. 1. ESR spectra of (a) gamma-irradiated UHMWPE heated with vitamin E (diffused), and gamma-irradiated UHMWPE heated alone (no vitamin E).
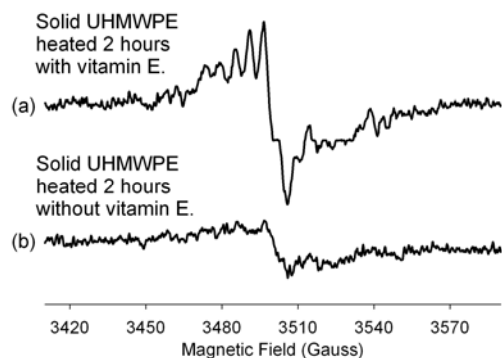


Fig. 2. (a) ) UHMWPE after 2 hours of heating at 100C in the presence of vitamin E. (b) UHMWPE (without vitamin E) after 2 hours of 100C heating.

As seen in figure 2, after two hours of heating, it appears that the sample containing vitamin E contains more radicals than that without vitamin E. However, the radicals represented by the spectrum of figure 2(a) are those primarily due to vitamin E, not the UHMWPE. Shown in figure 3 is a spectrum of vitamin E alone.

The rate of decrease of radicals in heated samples was greatest within the first hour. In addition, all samples have shown further decrease, although at a decreased rate, in total free radical concentrations at time periods subsequent to diffusion.
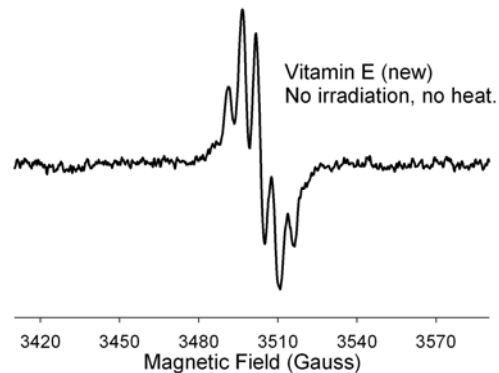


Fig. 3. Vitamin E. New, unirradiated, unheated.

## Conclusion

While in some instances the factor of heat alone appeared to have a greater contribution to the reduction of free radicals, we were unable to show conclusively that the greatest reductions of free radicals in the samples were due to heat or to vitamin E. Further measurements are underway to determine the extent to which heat and/or vitamin E have upon future free radical activity, including the formation of long-lived, oxygen induced radicals (OIR) which have been previously observed to form after long time periods in UHMWPE [8,9].

## References
[1] Oral E, Wannomae KK, et al. Biomaterials 2004;25:5515-22.
[2] Oral, E, Rowell S, Muratoglu O. Biomaterials 2006;27: 5580-7.
[3] Shibata N, Kurtz S, Tomita N. Journal of Biomechanical Science and Engineering; 2006:1(1):107-123.
[4] Oral E, Greenbaum E, Malhi A, et al. Biomaterials 2005;26:6657.
[5] Shibata N, Tomita N. Biomaterials 2005; 26(29):5755–5762.
[6] Oral E, Christensen SD, et. Al. Journal of Arthroplasty 2006; 21:580-591
[7] Oral E, Rowell S, Wannomae K, Muratoglu O. Biomaterials 2006; 27(11):2434–9.
[8] Jahan MS, King MC, Haggard WO, Sevo KL, Parr JE. Radiation Physics and Chemistry 2001;62:141–4.
[9] Jahan MS, Fusail M. Nuclear Instruments and Methods in Physics Research Section B: Beam Interactions with Materials and Atoms 2007; 265(1):67-71.

# SURFACE FUNCTIONALIZATION OF UHMWPE BY PLASMA PROCESSES

M.C. López*[1], F. Yubero[1], A.R. González-Elipe[1], J. Esteban[2], E. Gómez-Barrena[2], J.A. Puertolas[3]

[1*] *Instituto de Ciencia de Materiales de Sevilla. (CSIC- U. Sevilla) C/ Américo Vespucio 49 , E-41092 Sevilla, Spain (mclopez@icmse.csic.es), [2]Hospital Fundación Jiménez Díaz, Madrid, Spain, [3] Instituto de Ciencia de Materiales de Aragón (CSIC-U. Zaragoza), Zaragoza, Spain,*

## Introduction

The biological activity of UHMWPE surfaces (susceptibility to bacterial adherence) or the improvement of wear resistance of this material with suitable hard coatings are strongly correlated with the ability of setting appropriate functional groups at the surface of this polymer.

Incorporation of functional groups at polymer surfaces is commonly achieved by plasma activation. This is a current technology to increase their surface reactivity to, among other effects, favour the adhesion of coatings on their surface, enhance their wettability or modify their biocompatibility by grafting on their surface specific chemical groups. Low pressure as well as atmospheric pressure have been extensively used for that purpose. Among the latter processes, those based on a dielectric barrier discharge (DBD), are widely used.

Ultra high molecular weight polyethylene (UHMWPE) is daily subjected to several sterilization processes that may incorporate functional groups to its surface. Among them, the use of ethylene oxide (EO) and gas plasma (GP) are the most commonly used surface treatments. Other sterilization processes may also influence the characteristics of the surface of this material such as gamma irradiation (GI).

In this study, we have investigated the influence of three of the most used sterilization methods of UHMWPE (EO, GP and GI) and other commonly used surface plasma treatments (low pressure MW plasma and atmospheric DBD plasma) on the formation of specific functional groups at the surface and on their wetting behaviour. This is a preliminary study to be correlated by others where the presence of specific functional groups at the surface of UHMWPE will be correlated to bacterial adherence studies and on the performance of hard and antiseptic coatings on UHMWPE.

## Materials and Methods

The raw UHMWPE material used in this study was a ram extrusion rod GUR 1050 (Perplas Medical Ltd., Lancashire, UK). Discs 3 mm thick and 20 mm in diameter were machined from the rod. All discs were grounded and polished using SiC papers to obtain a average surface roughness of 0.8 $\mu$m. The polished specimens were cleaned by a standard procedure, which includes three steps of soap solution, distilled water, and ethanol in ultrasonic bath tank. Finally a vacuum chamber was used to dry the substrates. The average surface roughness Ra was measured by using confocal microscope Sensofar PLm 230D (Sensofar, Barcelona, Spain).

Contact angle measurements were performed using deionized water. Each contact angle measurement was taken five times in different zones of the surface to obtain an averaged value for the entire surface. The drops (5 μl) were placed manually onto the polymer surface.

Identification of the functional groups at the surface of the UHMWPE samples after each sterilization or surface plasma treatment was performed by means of X-ray Photoelectron Spectroscopy (XPS).

EO sterilization was performed in the facilities of the Hospital Clínico de San Carlos (Madrid, Spain). GP sterilization was performed in a Sterrad® system (Johnson & Johnson, Irvine, CA, U.S.A.) at the Hospital Fundación Jiménez Díaz (Madrid, Spain). EO and GP sterilizations were made following the standardized protocols used in clinical settings. After exposure to EO the samples were aerated during 24 hours. Gamma irradiation was performed with a dose of 25 kGy at Aragogamma SA (Barcelona, Spain)

Treatments by low pressure MW plasma were carried out in a reactor consisting of a quartz tube with a funnel shape termination attached to a stainless-steel chamber where the samples were placed. The reactor has a remote configuration and the samples were exposed downstream to the plasmas species generated in the quartz tube by a surfatron launcher that was supplied with a MW power of 60W. A typical working pressure of 0.3 Torr was used for the experiments. The plasma gas mixtures consisted of Ar as the majority component (25 sscm) and $O_2$ (0.7 sscm) as minority component. Exposure times of 1 min were used for these experiments. The DBD reactor consisted of two active metallic electrodes made of stainless steel. On the bottom electrode was placed

the polymer to be treated acting as a dielectric barrier. The rear part of the polymer was in contact with the metal piece by means of conductive silver paste. Mixtures of Ar (76 sscm) and $O_2$ (2 sscm) were used for these treatments. Typical treatment times of 30 s were used for this procedure.

## Results and discussion

Figure 1 shows survey XPS spectra corresponding to UHMWPE samples after EO, GP and GI sterilization processes and MW and DBD plasma treatments.
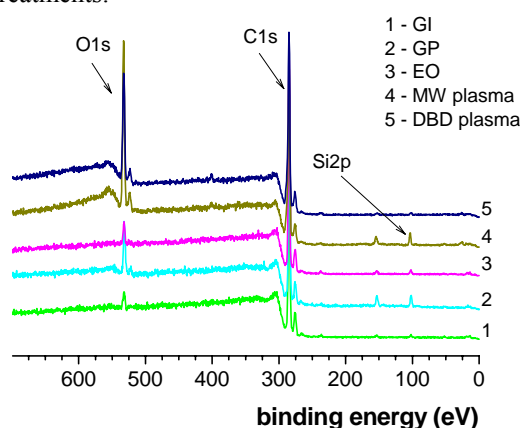


*Figure 1. XPS survey spectra from UHMWPE surface after several sterilization (GI, GP, EO) and plasma (MW, DBD) treatments*

Quantitative surface chemical analysis did not show any significant difference between the GI, EO y GP sterilized surfaces. We observe signal coming from C, O, and Si atoms at the sample surfaces. The main contribution to all the spectra corresponds to the C 1s signal. The Si content at the surface of the samples is about 3-5 atomic %. The binding energy of the Si 2p peak is about 102.3 eV, consistent with a $Si^{4+}$ oxidation state of Si in silica. Some O content was observed after the sterilization processes (10-12% atomic %). Samples with highest Si content coincide with those with highest O content. The binding energy of the O 1s signal (~532.0 eV) is consistent with oxygen atoms linked to Si and with the presence of hydroxyl (-OH) groups at the polymer surface. It is worth to stress that no residues of EO were observed on the EO sterilized surfaces. The most significant difference is the amount of O incorporated to the polymer after the MW and DBD plasma treatments, that is significantly higher than that observed with the standard sterilization processes. In fact it can be observed that the incorporation of oxygen species penetrates significantly inside the polymer surface, as it is suggested by the increase of background in the low kinetic energy side of the O 1s signal. Similar spectra were observed 1 month after the different treatments.

Figure 2 shows detail of the C1s signal. It is formed by a main peak at 285.0 eV binding energy (BE) that is ascribed to C-C and C-H bonds of the UHMWPE structure. Besides, it is evidence the presence of other more oxidise groups such as –COH/–C– O–C– (BE at 286.0 eV), –CO (BE at 287.5 eV) and –COOH/– COOR (BE at 288.6 eV) after MW and DBD plasma treatment
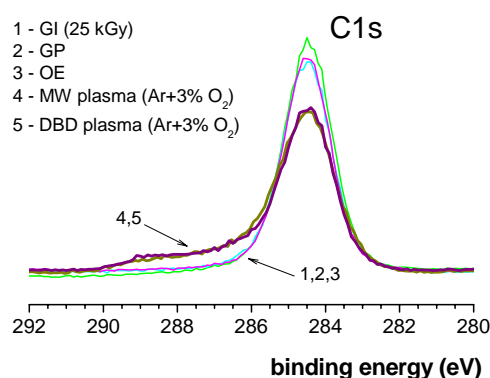


*Figure 2. C 1s signal from UHMWPE surface after several surface treatments*

The results obtained by XPS are corroborated by water contact angles (WCA) measurements after each surface treatment. It is observed that the MW and DBD plasma treatments induce low values of WCA (about 60º-70º) at the UHMWPE samples compared with those obtained after GI, GP and EO sterilization processes (about 110º). Thus, MW and DBD treatments significantly reduce the WCA (produce more hydrophilic surfaces). This property remains even 1 month after treatment.

## Conclusion

Standard sterilization processes do not affect significantly the functional groups present at the surface of UHMWPE, samples. However, the use of suitable cold MW and DBD plasmas do modify the surface chemistry of the polymer. In fact, a significant amount of hydrophilic groups are incorporated at the polymer surface after these plasma processes. These groups remain at the surface of the polymer one month after the plasma treatment. Thus, this kind of surface activation processes can easily be used to modify the biological activity of this polymer (i.e., bacterial adherence) or to improve adhesion of coatings on UHMWPE.

# A REVIEW OF THE ISSUES SURROUNDING UHMWPE

## Richard Treharne*[1], Emanuele Nocco, and Alex Greene

[1]5865 Ridgeway Center Parkway, Suite 218, Memphis, TN 38120  Rick.Treharne@ActiveImplants.com
* Corresponding Author at Active Implants Corporation

## Abstract
UHMWPE, although widely used in orthopaedics, has numerous issues surrounding its use. Wear debris have been reported to be in cysts, as has its association with osteolysis. This paper reviews the issues associated with UHMWPE and concludes that a new type of plastic bearing material is needed.

## Introduction
Ultrahigh molecular weight polyethylene (UHMWPE) was first used by Sir John Charnley for acetabular prosthetic cups. Although many people assume it to be a natural material since it only contains hydrogen and oxygen, it is actually unnatural in that it does not normally appear in nature. Ethylene is actually a colorless gas and when the first inventor of polyethylene tried to make it in the 1930's he was told that his attempt was impossible. The ultrahigh molecular weight version was found to have "low friction" and therefore assumed excellent wear characteristics. In this abstract we will review the issues surrounding UHMWPE and examine why so many attempts have been made to improve it.

## Materials and Methods
The medical and scientific literature concerning UHMWPE was reviewed and the references to those references examined for further literature.

## Results and Discussion
Morrison et al 1997 found UHMWPE in an iIliopsoas cyst after total hip replacement. The conclusion was that "The intense inflammatory response…was most likely secondary to…polyethylene debris…" Wang et al 1996 found UHMWPE in a pelvic mass after total hip replacement and concluded that the reason was the "…foreign body reaction to polyethylene…" Hing et al in 2001 found "broken polyethylene fragments" in an intrapelvic mass in a patient after total hip replacement. Finally Chavda et al in 1994 found "Polyethylene debris and reactive synovium…indicating a cause-effect relationship of polyethylene wear debris and failure.."
In addition to finding UHMWPE in cysts and masses after being worn UHMWPE components have also fractured in use. Numerous reports of fracture are in the literature.
Most troubling of all are the reports concerning osteolysis. At least 23 major clinical studies have shown that UHMWPE debris can cause osteolysis.

Because of all these reported problems numerous attempts have been made over the years to try to lower the wear rate. The literature shows that attempts have been made to increase the molecular weight, adding carbon fibers, packaging in nitrogen, eliminating free radicals, changing sterilization techniques, adding Vitamin E, and the most recent research has been involved with crosslinking the polymer. Crosslinking, however, has been reported to lower other mechanical properties of UHMWPE. See Table 1.
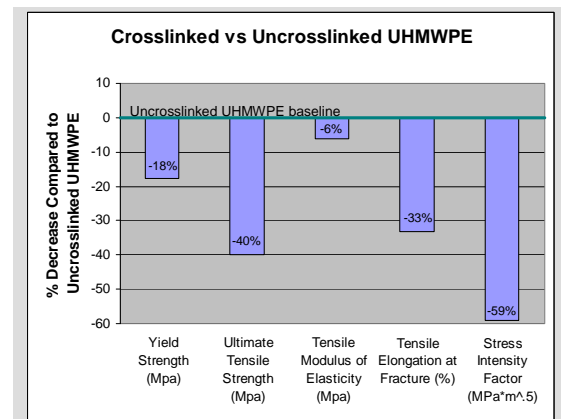


Table 1 Reported decrease in mechanical properties as a result of crosslinking UHMWPE

While all of these attempts may help lower the wear rate, the end result may not be sufficient to reduce the overall problem of osteolysis, but to delay it.

Researchers and surgeons appreciate the low modulus properties of UHMWPE and plastics in general because they are perceived as being more physiologic. The reality is that despite claims in the literature, UHMWPE is not near the properties of cartilage, it is just perceived as such because it is so much closer to natural materials than cobalt-chrome alloy or ceramics.

## Conclusion
UHMWPE has many issues. Many different attempts by many researchers have occurred over the years to try to improve it. In the end though, it might be concluded that the best way to eliminate the issues surrounding UHWMPE is to eliminate it and search for alternative plastics that are equal to or better than UHMWPE in regard to biocompatibility, biostability, and wear.

# ACCELERATED AGEING BY OXIDATIVE DEGRADATION OF UHMWPE: AN ASCORBIC ACID INHIBITION STUDY

Magda Rocha[1], Alexandra Mansur[2], and Herman Mansur[*3]

[1] *Department of Metallurgical and Materials Engineering, Laboratory of Biomaterials and Tissue Engineering, Federal University of Minas Gerais / R. Espírito Santo 35, 30160-030, Belo Horizonte, Brazil; * Author to whom correspondence should be addressed; E-Mail: hmansur@demet.ufmg.br; Tel. +55-31-3409-1843; Fax: +55-31-3409-1815.*

## Abstract

In the present study, an accelerated ageing by oxidative degradation of UHMWPE in hydrogen peroxide solution was performed and the inhibition with ascorbic acid (known as vitamin C) was analyzed. Both systems were extensively characterized by Fourier Transformed Infrared Spectroscopy (FTIR). Different chemical groups of UHMWPE associated with the degradation reaction were monitored for over 120 days in order to evaluate the possible oxidation mechanisms involved and the inhibitory behavior of vitamin C. The results have provided strong evidence that the oxidation mechanism is rather complex, and 2 stages with their own particular first-order kinetics reaction patterns have been clearly identified. Furthermore, the vitamin C has proven to be an efficient antioxidant of UHMWPE.

## Introduction

Ultra-high molecular weight polyethylene (UHMWPE) is a biomaterial widely used as part of prostheses that require articulating surfaces for its excellent mechanical qualities. Two major problems limit the life of UHMWPE prosthesis-wear and delamination, with both phenomena being mainly the result of chemical oxidation of polymer. It has also been well established that these UHMWPE components are susceptible to oxidative degradation through consolidation of the resin at high temperatures and pressures, sterilization by gamma irradiation, storage of the irradiated UHMWPE components and the implantation environment. The oxidation of UHMWPE components has been linked to changes in the mechanical properties of the material, such as decreased fatigue strength and the production of wear particles around the site of the implant. Despite the large number of works in recent years that seem to indicate a satisfactory behavior of UHMWPE for bearing applications, further research needs to be carried out in order to properly predict lifetime of these prostheses when implanted. The oxidation of UHMWPE is in reality a complex sequence of various cascading reactions which is not fully understood. Hence, α-Tocopherol also called as vitamin E has been used in order to minimize the oxidation and degradation of UHMWPE, which has recently been approved by

ASTM standards in biomedical applications. Vitamin C or ascorbic acid is a natural and powerful reducing agent and its effectiveness as antioxidant widely known and it is a promising alternative for inhibiting the oxidation of UHMWPE.

The aim of this research was to investigate and characterize the accelerated degradation of UHMWPE under exposure to an aggressive hydrogen peroxide medium as well as to assess the antioxidant potential of vitamin C for this polymer. Both mechanisms oxidation and inhibition were chemically evaluated by FTIR spectroscopy.

## Materials and Methods

Experiments were conducted with ram-extruded UHMWPE bar stock GUR 1020, commercial grade approved for surgical implants (ISO 5834-2/2005), kindly donated by Ticona Engineering Polymer (USA). The UHMWPE bar stock was sectioned into 5 cm × 5 cm × 5 cm blocks and then samples were sliced with thickness of 150-250 μm. They were cleaned in ethanol and distilled water ultrasound bath, and dried in air.. The experiments were divided into two groups: The group-1, where non-oxidized slices triplicates (n=3) of UHMWPE were immersed in 30 mL of hydrogen peroxide 30 v/v% and incubated at 37ºC. In the group-2, non-oxidized slices (n=3) of UHMWPE were immersed in 30mL of hydrogen peroxide and vitamin C solution at 0.3 e 1.0 w/v% and incubated at 37ºC. All solutions were replaced every five days, in order to maintain the activity of the solution. The accelerated aging intervals were monitored at 0, 7, 14, 21, 28, 45, 60, and 120 days. Fourier Transformed Infrared Spectroscopy (FTIR) spectra were collected in transmission mode with wavenumber ranging from 4,000 to 400 $cm^{-1}$ during 64 scans, with 2 $cm^{-1}$ resolution (Paragon 1,000, Perkin-Elmer, USA). The FTIR spectra were normalized and major vibration bands were identified and associated with the main chemical groups. The total level of oxidation (Iox) was determined by FTIR according to ISO 5834-2 as showed in Equation 1 where $A_O$ = Integrated area from 1,650 $cm^{-1}$ to 1,850 $cm^{-1}$ and $A_R$ = Integrated area from 1,330 $cm^{-1}$ to 1,396 $cm^{-1}$. The areas were calculated through Origin Program®, version 7.0.

$$I_{Ox} = A_O/A_R \quad \text{(Equation 1)}$$

**Results and discussion**

Initially, the FTIR spectrum from UHMWPE (not shown) was obtained before and after 28, 60, 120 days of accelerated aging in hydrogen peroxide. The main changes in the FTIR spectrum upon oxidation of polyethylene samples involved the formation of typical products such as isolated hydroperoxides $(3,550 \text{ cm}^{-1})$, hydrogen bonded hydroxyls including hydroperoxides $(3,410 \text{ cm}^{-1})$, lactones $(1,860 \text{ cm}^{-1})$, esters $(1,740 \text{ cm}^{-1})$, acids and ketones $(1,710 - 1,720 \text{ cm}^{-1})$. In addition, an increase in the absorbance in the $1,400 - 1,180 \text{ cm}^{-1}$ region associated with –C-O-C vibrations and in the region from $800 - 1,100 \text{ cm}^{-1}$ mostly related to unsaturated C=C groups was noted. Fig. 1 refers to the main peak in the FTIR spectra in the $1,700 - 1,750 \text{ cm}^{-1}$ region, corresponding to the strong signal of carbonyl (C=O) groups, which is rather dependent of specimen degradation. A significant absorbance increase was observed in the test period from 7 up to 120 days. The carbonyl functional group is common to several chemical species, for instance ketones, esters, carboxylic acids and lactones, among others. Thus, such results provide strong evidence that UHMWPE oxidation has taken place via chemical reactions of the polyethylene chain with hydrogen peroxide from the aging solution.
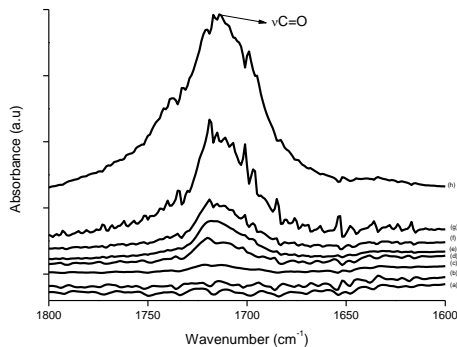


Fig. 1: (a) FTIR spectrum in the carbonyl (C=O) region of reference UHMWPE and UHMWPE submitted to peroxide accelerated ageing for different periods of time: (b) 7 days; (c) 14 days; (d) 21 days; (e) 28 days; (f) 60; (g) 45 days and (h) 120 days.

The results with data from 7, 14, 28, 45, 60 and 120 days test periods for oxidation degradation of UHMWPE are shown in Fig. 2. The curve obtained, based on the overall reaction (Iox), clearly indicated that oxidation of the UHMWPE has taken place, with a slow evolution up to approximately 28 days. Then, a steep rise could be observed up to 120 days of evaluation. In Fig. 3, it is showed the accelerated oxidation of UHMWPE under 3 different conditions, i.e., without vitamin-C (Fig.3a), with addition of 0.3% (Fig.3b) and 1.0% (Fig.3c). The results have indicated a significant

reduction on the oxidation index of UHMWPE attributed to the effective antioxidant vitamin C behavior. Moreover, it can also be noted that vitamin-C has shifted the curve to a longer time at the first stage of oxidation compared to the previous not inhibited $H_2O_2$ system.
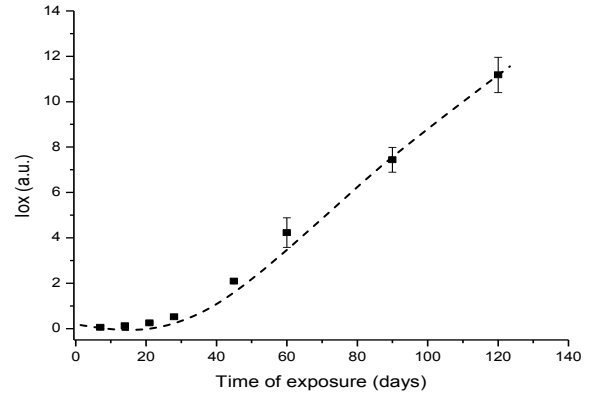


Fig. 2: Evolution of UHMWPE degradation in $H_2O_2$ estimated by FTIR using the Oxidation Index (Iox) at different aging times.
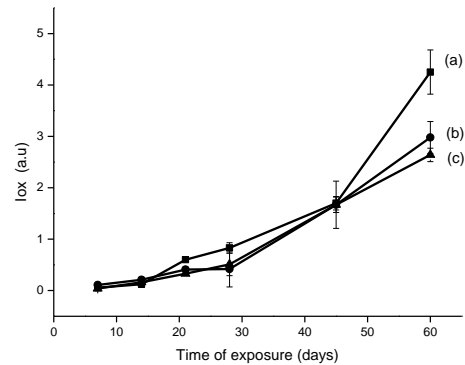


Fig. 3: Evolution of inhibitor of oxidation of UHMWPE with vitamin estimated by FTIR using the Oxidation Index at different times (a) oxidante, (b) vitamin C 3% and (c) vitamin C 5%.

In living organisms, vitamin C seems play a crucial role as an inhibitor of harmful free radicals. Thus, a similar mechanism associated with donation of H ions or interacting with hydrogen peroxide to capture OH radicals, protecting the UHMWPE.

**Conclusion**

This study has presented an accelerated aging procedure based on $H_2O_2$ for investigating the chemical stability of UHMWPE. Relevant and new information concerning to the oxidation of UHMWPE is showed, with two main stages been verified. Moreover, vitamin C has proven to be effective on reducing the oxidation of UHMWPE and modifying the kinetics of the first stage at slow reaction rate. Both mechanisms of oxidation and its inhibition by natural antioxidants are still largely unknown and need to be more in-depth investigated in order to minimize or ideally prevent it from occurring under clinical usage in orthopedic implants.

# OXIDATION AND VITAMIN E CONTENT OF VITAMIN E BLENDED CONVENTIONAL UHMWPE AFTER 9 YEARS STORAGE

W. Schneider*[1], D. Zurbrügg[2], M. Shen[3], R. Klabunde[1]

[1]*Zimmer GmbH, Sulzerallee 8/PO Box, CH-8404 Winterthur, Switzerland,*
*werner.schneider@zimmer.com (*), [2]Niutec AG, Else Züblinstr. 11/PO Box, CH-8404 Winterthur, Switzerland, [3]Zimmer Inc., P.O.Box 708, Warsaw, IN 46580-0708, USA*

## Introduction

Gamma sterilization of ultra-high molecular weight polyethylene (UHMWPE) under nitrogen has been well-established for conventional polyethylene in hip and knee applications [1, 2]. During irradiation, according to long-established theory, free radicals are generated in the UHMWPE, known to cause oxidation which weakens the material [1, 2]. To reduce oxidation, UHMWPE can be stabilized against through vitamin E for stabilization of the polymer [3, 4]. This study investigates oxidation resistance and loss of vitamin E after 9 years real time storage in blended conventional UHMWPE.

## Materials and Methods

GUR 1020 UHMWPE powder was blended with 0.1, 0.2, 0.4 and 0.8 w.t. % vitamin E. From the compression molded bar stocks, specimen were machined with cross-section of 10 x 15 mm, packaged like an implant under nitrogen in sealed pouches and exposed to γ-irradiation of 25-40 kGy (Leoni Studer, Switzerland). Part of the specimens was subjected to accelerated aging according to ASTM F 2003 for 120 days in an oxygen bomb (5 bar $O_2$, 70°C). Subsequently all specimen were put on storage for 9 years. Fourier Transformed Infrared Spectroscopy (FTIR) was used to evaluate vitamin E content and Oxidation Index (OI). OI was evaluated after heptane extraction (12h, 98°C) to avoid misinterpretation due to oxidized vitamin E. Specimens were measured as line-scans from the surface towards the core. Spectra were analysed using scans 1275-1245 $cm^{-1}$ and normalized to 1900 $cm^{-1}$ for vitamin E content. OI was measured according to ASTM F 2102. For calibration of the FTIR absolute quantification of vitamin E content was measured by Gas Chromatography/Mass Spectrometry (GC/MS).

## Results

Table 1 shows the measure-ments of OI and vitamin E content of UHMWPE as a function of the original vitamin E content used for blending. After γ-irradiation and 9 years shelf storage the samples show a decrease in vitamin E content of about 50 %. A further significant decrease is caused by the harsh aging protocol of 120 days in oxygen bombs. None of the vitamin E blended samples showed an OI above detection limit of the measurement method.

|  | Vitamin E blending content [w.t. %] | | | |
|---|---|---|---|---|
|  | 0.1 | 0.2 | 0.4 | 0.8 |
| VE (w/o 120 d) | < D.L. | 0.07 | 0.21 | 0.44 |
| VE (w 120 d) | < D.L. | 0.07 | 0.10 | 0.18 |
| OI (w 120 d) | < D.L. | < D.L. | < D.L. | n.a. |

*Table 1: OI and Vitamin E content of γ-sterilized Vitamin E blended UHMWPE after 9 years real time storage. (<D.L.: below detection limit of OI=0.025, Vit E=0.020)*

## Discussion

Results show no residual vitamin E was measured in the 0.1% vitamin E samples. Although vitamin E was consumed after γ-irradiation, aging and shelf storage, even 0.1% vitamin E was able to prevent polyethylene from oxidation. None of the γ irradiated and 9 years shelf aged samples showed an OI higher than detection limit.

## References

[1]   McKellop, H., et al. (2000). JBJS, 82-A (12):1708-1725.
[2]   Lu, S., et al. (2003). Biomaterials, 24(1):139-145.
[3]   Wolf, C., et al. (2002). J Mater Sci Mater Med, 13:185-189.
[4]   Shibata, N., et al. (2005). Biomaterials, 26(29) :5755-5762.

# EVALUATION OF UHMWPE AFTER SOLID-STATE DYNAMIC SHEAR DEFORMATION

Ambrósio, J.D.[1], Santos, R.E.[1], Belini, F., Bolfarini, C.[*1,2]

[1] *Center for Characterization and Development of Materials*
*CCDM/DEMa/UFSCar, CP 60, 13560-970 São Carlos, SP, Brazil*
[2] *Department of Materials Engineering / Federal University of São Carlos - (\*)* cbolfa@ufscar.br

## Introduction

Since the advent of hip arthroplasty, few polymeric materials have been used for this purpose. Today, the material employed for this application is ultra-high molecular weight polyethylene (UHMWPE), which was introduced in 1962 in this type of surgical procedure [1]. UHMWPE is widely used because of its excellent wear resistance and low friction coefficient. However, the wear of UHMWPE and the fragments resulting from this process are currently considered some of the most important factors in joint replacement failure, especially in the long term [2].

The tribological behavior of materials is strongly influenced by their microstructure, especially at the surface. Several methodologies have therefore been employed to increase their wear resistance through microstructural alterations, such as the use of irradiation to cause reticulation [3], ion implantation [4], mixture with other components [5], pressing [6], among others. Kurokawa *et al.* [7] demonstrated that the friction coefficient depends on the crystallinity of the sample, while Ohta *et al.* [3] presented results clearly demonstrating that chain orientation exerts considerable effects on wear resistance. However, the tribological behavior of semicrystalline polymers is still not entirely understood, and it is not known exactly which structural factor is determinant in the friction coefficient [8]. On the other hand, it is well established that the UHMWPE´structure is strongly dependent on the processing parameters.

Thus, the preliminary objective of this work was to ascertain the influence of solid-state shear on the deformation, hardness, density and degree of crystallinity of UHMWPE, aiming at subsequent studies of wear resistance in the longitudinal and transversal directions of shear.

## Materials and Methods

The UHMWPE samples were plate-shaped with dimensions of 100.0x50.0x4.5 mm. These plates were cut longitudinally from UHMWPE cylinders with a diameter of 60.0 mm. The plates were deformed by solid-state shear using two heated steel cylinders (200 mm diameter) rotating at constant speeds in opposite directions, allowing the opening between them to be regulated, as shown in Figure 01. The compression ratio (CR) was defined by equation 1, where T is the sample's thickness and D is the final aperture between the cylinders.
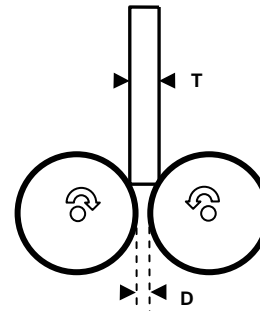
$$CR = (T - D) / T \qquad (1)$$



*Fig. 1 – Diagram of the device for solid-state shear deformation of UHMWPE*

The solid-state shear deformation was imposed gradually, in increments of 0.1 mm (2.2% of the plate's thickness), until the desired CR was attained. The plates were subjected to five consecutive steps of solid-state shear at each 0.1 mm increment of compression. After solid-state shear with a CR of 22%, 44% and 66% at temperatures of 50ºC and 90ºC, the three dimensions of the plates were measured again to evaluate their deformation.

The six deformed samples and one original sample were characterized by measuring their Shore D Hardness, density, and degree of crystallinity. The Shore D Hardness was evaluated with a Bareiss DigiTest hardness tester, according to the ASTM D2240 standard, while density was evaluated by pycnometry according to the ISO 1183-1 standard, and the degree of crystallinity was determined using a Mettler Toledo DSC 822E differential scanning calorimeter.

## Results and Discussion

As indicated in *Table 1*, shearing promoted a dimensional variation in the UHMWPE plates, and the higher the compression ratio the smaller the plate's thickness and the longer its final length. These variations were more intense at 50ºC than at 90ºC, which is probably due to the fact that at 90ºC the UHMWPE molecules are able to relax, thus leading to their elastic recovery. Considering the two temperatures for the 66% compression ratio, the thickness decreased by about 30%, the length increased by about 30%, and the width of the plates showed little alteration, indicating an almost pure

shear stress state leading to deformation of the material occurring preferentially along the shear direction in the cylinders.

Table 1 – Dimensional variation of the plates as a function of cylinder temperature and compression ratio

| Temperature of the Cylinders [°C] | Compression Ratio [%] | Dimensional Change | | |
|---|---|---|---|---|
| | | Thickness [%] | Width [%] | Lenght [%] |
| 50 | 22 | -9,1 | 1,5 | 5,4 |
| 90 | 22 | -6,9 | 0,4 | 2,8 |
| 50 | 44 | -19,1 | 5,3 | 14,9 |
| 90 | 44 | -16,2 | 3,4 | 12,0 |
| 50 | 66 | -32,6 | 5,8 | 36,1 |
| 90 | 66 | -30,3 | 8,9 | 27,5 |

The hardness of each plate was measured at 18 points along its surface. As illustrated in the graph in *Figure 2*, the hardness of the plates decreased as the compression ratio increased, and at the lowest cylinder temperature, for CRs of 22% and 44%, this decrease was more pronounced. The original UHMWPE showed the highest hardness value (64.5 Shore-D). The opposite effect was expected, i.e., that shear at a lower temperature and higher CR values would increase the hardness on the surface of the plates. An explanation for this apparently contradictory result might be related to a greater orientation that the molecular structure of UHMWPE could assume at the surface of the plates. Once they have been aligned in a preferential direction, the resistance to penetration of the needle of the durometer could be lower than that of entangled molecules.
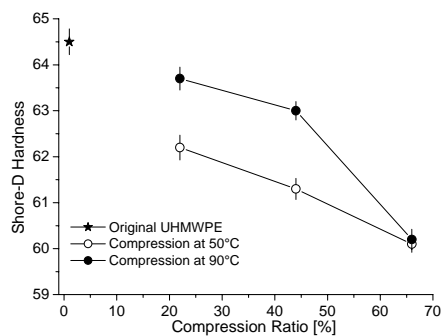


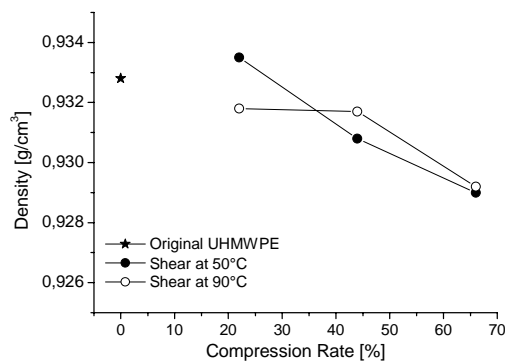Fig. 2 – Variation of Shore-D hardness as a function of the compression ratio and cylinder temperature



Fig. 3 – Variation of Density as a function of the compression ratio and cylinder temperature.

The density vs. compression ratio graph in *Figure 3* indicates that the density also decreased as the compression ratio increased at the two temperatures. Albeit small, this decrease in density as the compression ratio increased was a tendency found in all the samples. A comparison of these results with the graph in Figure 4, however, indicates that these results are coherent with an decrease in the degree of crystallinity. Therefore, the density and degree of crystallinity decreased as the compression ratio increased after the solid-state dynamic shear.
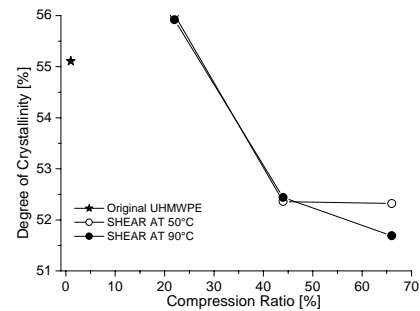


Fig. 4 – Variation of the Degree of Crystallinity as a function of the compression ratio and cylinder temperature

The degree of crystallinity was calculated based on 100% crystalline UHMWPE, whose melting enthalpy is 288.9 J/g [3]. Still with respect to the DSC tests, it should be noted that the melting temperature (Tm) of samples deformed by solid-state dynamic shear is 2-3°C higher than that of the original UHMWPE.

The hardness, density and degree of crystallinity decreased as the compression ratio increased. Another possibility for these apparently contradictory results may be due to the fact that the levels of pressure between the heated cylinders were lower than those used in RAM extrusion during fabrication of the raw material, which would have allowed for relaxation of the crystalline structure.

**Conclusions**

The solid-state dynamic shear deformation led to the following conclusions:
- The method proved very efficient in the deformation of UHMWPE plates in the direction of the principal shear component, as attested by the marked increase in the length of the plates.
- The next steps of this study will involve measuring the wear resistance and the degree of orientation in the directions longitudinal and transversal to the solid-state dynamic shear.

**References**
1 Charnley J.; Edited. Berlin: Springer; 1979.
2 A. Wang, et al., Wear, 1995
3 M. Ohta et al., Wear, 2001.
4 W. Shi et al., Wear, 2001.
5 N. Chang et al., Wear, 2000.
6 S. Wang et al., Wear, 2007.
7 M.Kurokawa et al., ASME J. Tribol., 2000.
8 T. Aoike et al., Wear , 2007.

# The effect of the consolidation process on structural parameters and micromechanical properties of PE-UHMW

Ruth Markut-Kohl*[1], Vasiliki-Maria Archodoulaki[1], Thomas Koch[1] and Sabine Seidler[1],

[1] Institute of Materials Science and Technology, Vienna University of Technology
Favoritenstraße 9-11, 1040 Vienna, Austria;
rmarkut@mail.tuwien.ac.at

## Introduction

Ultra high molecular weight polyethylene PE-UHMW is the golden standard as a bearing surface in total joint replacement [1]. Due to current standardization no antioxidants and processing additives are added [2].

The aim of this study is to investigate the influence of the consolidation process on the polymer. Ram extruded and compression molded medical grade PE-UHMW was investigated by means of Fourier transformed infrared spectroscopy (FTIR), differential scanning calorimetry (DSC) and instrumented nanoindentation. The chemical structure and the morphology of PE-UHMW are correlated to the micro-mechanical properties within different areas of the consolidated material.

## Materials and Methods

Medical grade PE-UHMW (GUR 1050) after consolidation was investigated. Ram extruded rods and compression molded sheets (from Orthoplastics) were analysed.

Oxidative degradation and effects of irradiation procedures were analyzed by means of local resolved FTIR. The spectra were base line corrected and normalized to a peak height of 0,05 at 2020 cm$^{-1}$ [3].

The morphology was investigated by DSC measurements. The non-isothermal crystallization behavior is discussed. Sample of 1 – 2 mg were heated (two runs) and cooled between 0 °C and 220 °C with rates of 10 K/min. Besides the degree of crystallinity, the distribution of the lamellae thickness was calculated from the DSC melting endotherms according to Eq. 1 and Eq. 2 [4-6].

$$L = \frac{2 * \sigma_e * T_m^0}{\Delta H_m * \left(T_m^0 - T_m\right) * \rho_c} \qquad \text{Equation 1}$$

$$\frac{1}{M} * \frac{dM}{dL} = \frac{\text{Heat Flow}}{\text{Heat Rate}} * \frac{\left(T_m^0 - T_m\right)^2 * \rho_c}{2 * \sigma_e * T_m^0} \qquad \text{Equation 2}$$

Instrumented nanoindentation was used for micro-mechanical, locally resolved characterization. The micro-hardness was determined along a line perpendicular to the surface of the consolidated material.

## Results and discussion

In the FTIR spectra of the outer layer of ram extruded PE-UHMW a peak at 1718 cm$^{-1}$ is present. On the contrary no peak at 1718 cm$^{-1}$ is present in the spectra of compression molded PE-UHMW. The peak at 1718 cm$^{-1}$ is associated with the carbonyl group which is formed within the polymer as a result of oxidation processes. Hence, in the outer layer of app. 0,85 mm thickness in the ram extruded material the polymer chains are oxidative degraded. This effect allows to suspect that ram extrusion process leads to oxidative degradation on the surface layer while compression molded materials shows no degradation induced by the consolidation process.

DSC experiments show that in these oxidized outer layers of the ram extruded material the degree of crystallinity is elevated compared with the centre layers and the compression molded material. This behavior is evident in both heating runs.

In general, the first heating run reflects the sum of thermo-mechanical history (e.g. during the manufacturing processes) and the chemical state of the material whereas in the second heating run only the chemical influences are visible.

In the first heating run the lamellae thickness distribution of the outer layers is shifted to higher lamellae thickness whereas in the second heating run the curve is shifted to lower lamellae thickness when compared to the centre layers (Fig. 1 and Fig. 2).
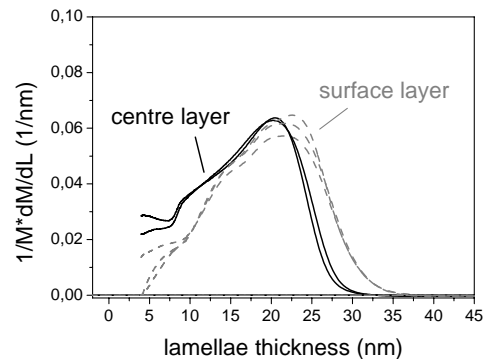


*Figure 1: Lamellae thickness distribution in ram extruded PE-UHMW, 1$^{st}$ heating run*
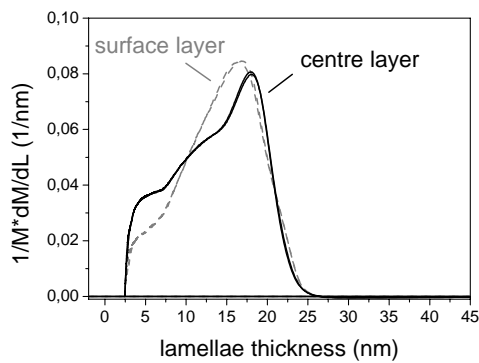
*Figure 2: Lamellae thickness distribution in ram extruded PE-UHMW, 2$^{nd}$ heating run*

Concerning the lamellae thickness distribution results calculated from first heating run it can be concluded that the shorter polymer chains in the oxidative degraded area are annealed during the extrusion process.

The lamellae thickness distribution calculated from second heating run shows a narrower distribution than in the first heating run. This can be attributed to the controlled non-isothermal crystallization during the DSC experiment. The crystallization of samples from the outer layers starts at lower temperatures (Fig. 3).
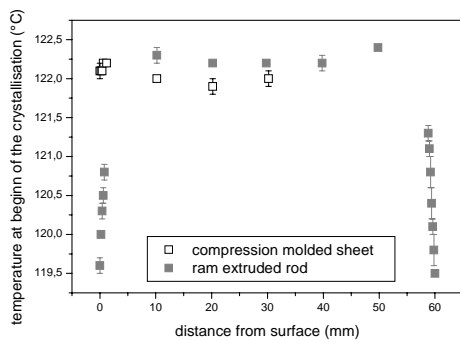


*Figure 3: Temperature at begin of the non-isothermal crystallization in the DSC experiments; ram extruded and compression molded material*

Crystallization at lower temperatures corresponds to a higher degree of supercooling. This results in the formation of smaller lamellae. Hence, the lamellae thickness distribution in the second DSC heating run is shifted to lower values.

In the compression molded material no local variation in the degree of crystallinity, the degree of supercooling and the lamellae thickness distribution is observed.

Nanoindentation experiments show values of higher hardness in the outer app. 0,9 mm layer of the ram extruded material. No such variations in the depth profile of micro-hardness were proven in the compression molded material. It is shown, the in oxidative degraded areas the degree of crystallinity is elevated and this results in higher values of micro-hardness.

**Conclusion**

Because of the complexity of the PE-UHMW material it is not sufficient to singly calculate the degree of crystallinity. Hence, the calculation of the lamellae thickness distribution gives more insight to the manufacturing and consolidation process. It is shown that the consolidation process leads to different oxidative degradation states in the material. In the ram extruded material the surface layer tends to degrade. Degradation during manufacturing process leads to a different degree of crystallinity and a different degree of supercooling is observed in non-isothermal crystallization. Furthermore, the oxidative degraded area in the ram extruded sample where the crystallinity is higher can be correlated to an area of elevated micro-hardness.

**References**
[1] S. M. Kurtz; The UHMWPE Handbook
[2] ISO 5834-2:1998 "Implants for surgery – Ultra-high molecular weight polyethylene – Part 2. Moulded forms"
[3] L. Costa et al.; *Polym Degr Stab*. 93 (2008) 1695-1703
[4] C. P. Stephens et al.; *Nucl. Instr. And Meth. In Phys. Res. B* 236 (2005) 540-545
[5] A. Romankiewicz e al.; *Macromol. Symp*. 180 (2002) 241 -256
[6] F.-W. Shen et al.; *J. Biomed Mater Res* 41 (1998) 71–78

# OBSERVATION OF ADSORBED PROTEIN FILM ON ULTRA HIGH MOLECULAR WEIGHT POLYETHYLENE AS BOUNDARY FILM

Kazuhiro Nakashima*[1], Yoshinori Sawae[1] and Teruo Murakami[1]

[1] nakaji@mech.kyushu-u.ac.jp, *Kyushu University, Japan*

**Abstract**
Effect of proteins contained in natural synovial fluid on friction property of Ultra high molecular weight polyethylene (UHMWPE) was investigated. Bovine serum albumin (BSA) and human γ-globulin (HGG) were used as additives in saline. Absorbed film of proteins was investigated using fluorescent technique. Protein additive ratio showed effect on friction property and formation of adsorbed film was changed by concentration of proteins.

**Introduction**
Joint prosthesis with UHMWPE was replaced from patients in some cases, when severe wear of UHMWPE occurred. Meanwhile, it is known that proteins or lipids contained in natural synovial fluid has effects on friction and wear property of UHMWPE for joint prosthesis. Proteins and lipids reduce friction and wear of UHMWPE, but also increase friction and wear in some rubbing conditions. For longevity of joint prosthesis it is needed to investigate the effect of adsorbed protein film on the surface. Authors has investigated protein film on poly vinyl alcohol (PVA) hydrogel, and clarified mechanisms of reduction of wear and friction in a rubbing pair of PVA hydrogel[1]. BSA and HGG contained in natural synovial fluid had a role of lowering friction and protecting from wear, respectively. Layered protein film composed of two proteins showed low friction and low wear of PVA hydrogel, but heterogeneous adsorbed film showed high friction and wear. Therefore, wear and friction property of UHMWPE can be improved by using ideal protein film. In this study friction property of UHMWPE and formation of protein film were investigated and discussed.

**Materials and Methods**
A rubbing pair of UHMWPE plate and zirconia ball with 26mm diameter was tested in a reciprocating friction tester. Load was 9.8N, sliding velocity was 20mm/s and sliding distance was 140m. Lubricants were saline solution with BSA and HGG. Additive ratio of BSA to HGG (A/G ratio) and protein content in saline solution was changed. BSA and HGG were labeled using RITC and FITC, respectively. Therefore adsorbed protein film can be observed and each protein can be distinguished respectively after friction test.

**Results and discussion**
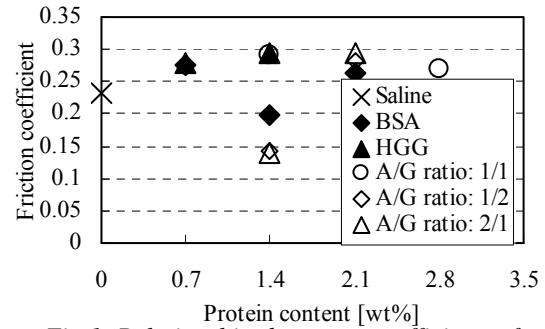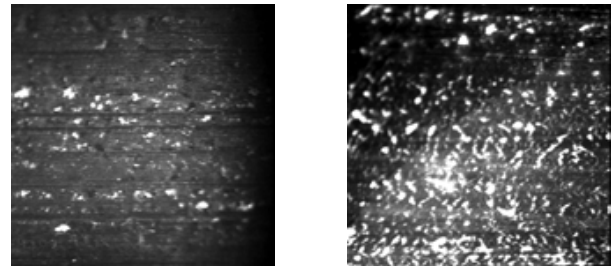Relationship between friction coefficient and


*Fig.1 Relationship between coefficient of friction and protein content*



(a) A/G ratio 1/2          (b) A/G ratio 1/1

*Fig.2 Fluorescent image of albumin on UHMWPE after reciprocating friction test in 1.4wt% protein solution*

protein content is shown in Fig.1. Lower friction coefficient was observed in 1/2 and 2/1 of A/G ratio of 1.4wt% total protein content. High protein content solution showed high friction coefficient. 1/1 of A/G ratio of 1.4wt% showed high friction coefficient. Thus, A/G ratio has effect on friction property. Figure 2 shows fluorescent microscope images of UHMWPE after wear test. Bright spots is adsorbed BSA and dark area is adsorbed HGG. BSA was adsorbed on HGG layer on UHMWPE in low friction coefficient condition shown in Fig.2 (a). In contrast, heterogeneous adsorbed protein film was formed in high friction conditions. Formation of adsorbed protein film is a key essence of friction property of UHMWPE.

**Conclusion**
Formation of protein adsorbed on UHMWPE was changed by A/G ratio and protein concentration. Low friction condition showed layered protein film with reduction of friction coefficient.

**References**
[1] K. Nakashima, et. al., JSME International Journal, Vol.48, No.4, pp.555, 2005

# DISTINCT PATHOPHYSIOLOGIC CHANGES IN PERIPROSTHETIC HIP TISSUES FROM HISTORICAL AND HIGHLY-CROSSLINKED UHMWPE IMPLANT RETRIEVALS

RM Baxter[1], A Ianuzzi[1,2], TA Freeman[3], SM Kurtz[1,2], MJ Steinbeck*[1]

*Corresponding Author: Dr. Marla J. Steinbeck, M.T. (ASCP), Ph.D.
3141 Chestnut Street, Biomedical Engineering Department, Drexel University Philadelphia, PA 19104.
mjs348@drexel.edu

[1]Drexel University, Philadelphia, PA 19104; [2]Exponent Inc., Philadelphia, PA 19104; [3]Thomas Jefferson University, Philadelphia, PA 19104

## Introduction

The assessment of the periprosthetic tissue reaction following total hip arthroplasty suggests that multiple factors contribute to the immunopathophysiologic responses directed toward implant wear debris. The current study investigated the histomorphologic changes and wear debris in tissue from two patient groups, those with historical (gamma air sterilized) or highly-crosslinked UHMWPE implant components.

## Materials and Methods

Histological sections were evaluated to determine the presence of histiocytes, giant cells, vascularization, fibrocartilage/bone and tissue morphology. To determine co-localization of histomorphologic changes and wear debris, overlapping full-field tissue arrays were collected in brightfield and polarized light. Both the incidence and degree of morphological changes and wear debris were described for periprosthetic tissues from nine patients in each cohort.

## Results and discussion

The predominant morphologic changes observed in the historical cohort were the presence of histiocytes in regions with significant amounts of small wear debris (0.35-2μm) and giant cells associated with large wear debris (>2μm) (Fig. 1). Frequent, focal regions of necrosis were also observed in association with wear debris. The dominant responses observed in the historical cohort were infrequently observed in tissues retrieved from the highly-crosslinked patient cohort. The major morphologic characteristics of the highly-crosslinked cohort tissues were the presence of fibrocartilage/bone with associated regions of necrosis (Fig. 2). For both the historical and highly-crosslinked cohorts, tissue responses were more extensive in the non-capsular tissues, which included the retroacetabular or proximal femoral regions (Fig. 3).

Our characterization of tissue histomorphology from historical and highly-crosslinked hip prostheses is unique in that it included a description of the incidence and degree to which the morphological changes and wear debris occurred. Based on the current findings, we suggest that the presence of wear debris-induced inflammation is only one contributor to loss of implant function, and the need for revision surgery is distinct for the two cohorts.

## Conclusion

This study emphasizes the need to quantify tissue responses in a more comprehensive manner to ascertain the predominant histomorphologic changes in localized areas, anatomical regions and individual patient tissues.

## Figures.



Figure 1: H&E-stained pseudocapsule tissues from historical UHMWPE THRs. Tissues from this location were frequently comprised of dense collagen; (A) brightfield and (B) polarized light, collagen fibers are visible (pink arrow). (C) Four of the nine pseudocapsular tissues contained large quantities of histiocytes (blue arrow) and giant cells (green arrow). (D) Large and small UHMWPE wear (yellow arrow) were consistently co-localized with giant cells and histiocytes, respectively. (200x)



Figure 2: H&E-stained retroacetabular tissue from a crosslinked UHMWPE THR. (A) A segment of bone (red

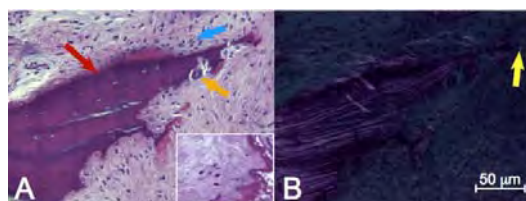*arrow) is embedded within a loose connective tissue. An osteoclast (orange arrow) is visible within a resorption lacuna, and necrosis is observed near fibrocartilage/bone (A, inset). Histiocytes (blue arrow) are visible near the top edge of the bone, and (B) a single small UHMWPE particle (yellow arrow) is visible. (200x)*
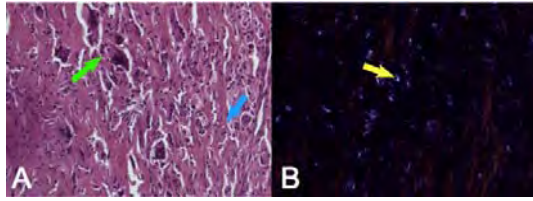


*Figure 1: H&E-stained proximal femoral tissue from a historical UHMWPE THR, patient # 2. (A) Five of the six non-capsular tissues contained large quantities of giant cells (2+, green arrow) and histiocytes (2+, blue arrow). (B) UHMWPE wear debris (yellow arrow) appears birefringent when imaged using polarized light microscopy. (200x)*

# PROBLEMS CONNECTED WITH PRECISE QUANTIFICATION OF UHMWPE WEAR DEBRIS

Monika Lapcikova*[1], Eva Zolotarevova[2], Miroslav Slouf[1], Petr Fulin[3], David Pokorny[3]

[1] *Institute of Macromolecular Chemistry AS CR, v.v.i; Heyrovsky Square 2, 162 06 Prague 6, Czech Republic; lapcik@imc.cas.cz*
[2] *Faculty of Sciences, Charles University, Hlavova 8, 128 40 Prague 2, Czech Republic*
[3] *Orthopedics Clinic, Hospital Motol, V Uvalu 84, 156 06 Prague 5, Czech Republic*

## Abstract

Some effects, which can influence results of the quantification of UHMWPE wear debris, were documented. The first set of experiments was focused on the influence sonication and pre-filtration through 10µm membranes, which are used to remove bigger, biologically less active wear particles. It was shown that sonication just before pre-filtration is necessary to limit agglomeration; polytetrafluoroethylene (PTFE, Teflon) membranes caused higher losses of the wear particles than polycarbonate (PC) membranes. The second set of experiments monitored losses during filtration on the membrane with pore size 0.1 µm. Scott et al. [1] studied similar effect on a membrane with pore size 0.2 µm. We confirmed that a high number of wear particles came even through 0.1µm filter.

## Introduction

The release of the wear debris from total joint replacements (TJR) based on ultrahigh molecular weight polyethylene (UHMWPE) results in osteolysis in human body [1, 2]. It has been accepted that the wear particles with equivalent diameter below 10 µm exhibit the highest biological activity [3] and that biological response of the UHMWPE particles depends on their number, size and shape.

In this study, we were interested in some rarely mentioned aspects influencing parameters of the isolated debris from tissue. We studied a common isolation procedure based on nitric acid digestion [2, 4]. For our experiments we used a mixed sample of debris obtained from periprosthetic tissues of several patients. This approach was selected for a better monitoring of events accompanying isolation and image analysis of the debris. More types of particles should be included in this sample than in those isolated from just one particular patient.

The first objective of our study was to clarify the influence of the sonication and type of the 10µm membrane used for pre-filtration on the amount of wear particles and their aggregates detected on final polycarbonate (PC) membranes with pore size 0.1 µm, used during the final isolation step.

The second objective was to quantify particles, which are able to penetrate through PC membrane with the pore size 0.1 µm and can be caught on the PC membrane with pore size 0.05 µm.

## Materials and Methods

*Isolation of wear particles.* UHMWPE debris came from periprosthetic tissues, obtained from revisions of TJRs in Faculty Hospital Motol, Czech Republic. Isolation of the debris was based on acid digestion [2, 4]. The final storage suspension of wear particles in isopropylalcohol (iPrOH) for subsequent experiments was a mix of 20 samples.

*Characterization of wear particle morphology by FESEM.* Field-emission gun scanning electron microscopy (FESEM; microscope Quanta 200 FEG; FEI company) was employed to visualize wear debris. The instrumental magnifications of FESEM micrographs were 3000× and 5000× (corresponding real widths of micrographs were 21 and 13 µm, respectively). Wear particle morphology (diameter, circularity etc.) was determined by the image analysis of FESEM micrographs (program NIS Elements; Laboratory imaging).

*Quantification of the wear particles by IRc method.* The IRc method, which was developed in our laboratory [4], determines the total volume of the isolated UHMWPE wear debris by means of FTIR spectra of the isolated UHMWPE particles on PC membrane.

## Results and discussion

*Influence of the membrane and sonication.* The same suspension of the debris was pre-filtered through PTFE and PC membrane with pore size 0.1 µm with and without sonication. This experiment confirmed that wear debris aggregates in iPrOH. The aggregates can pass through smooth circular holes in the PC membrane (Fig. 1a), but they are retained in the fibrous structure of the PTFE membranes (Fig. 1b). The sonication before filtration disassociated aggregates of the wear particles. Consequently, the single UHMWPE wear particles were able to pass through the membrane and even remain separated, on condition that the next filtration was applied immediately. The good disassociation of aggregates was verified for both types of membranes (micrographs in Figs. 1c,d). Surprisingly enough, PTFE membranes retained inside their porous structure a large portion of the wear particles, in particular those with filamentary shape (compare Figs. 1c and 1d). The FESEM

results were confirmed also by IRc method, which determines the total volume of UHMWPE wear particles smaller than 10 μm [4].
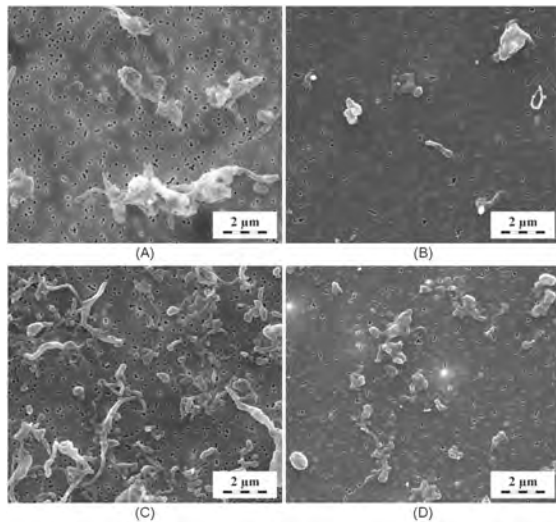


*Fig. 1 The representative FESEM micrographs of UHMWPE wear particles on PC membranes with pore size 0.1 μm. The original suspension of the debris was pre-filtered through different membrane filters with pore size 10 μm with or without previous sonication: (a) UHMEPE wear particles directly filtered trough PC membrane, (b) directly filtered trough PTFE membrane, (c) sonicated and filtered trough PC membrane, and (d) sonicated and filtered trough PTFE membrane.*

*Losses during filtration on membrane with pore size 0.1 μm.* The wear debris suspension was filtered through a PC membrane with pore size 0.1 μm and then through PC membrane with pore size 0.05 μm to catch particles smaller than 0.1 μm. The representative FESEM micrographs taken at the same magnification are compared in Fig. 2. It is clear that some of the particles, especially those with the filamentary shape, passed through the membrane with the 0.1μm pores and were retained on the membrane with the 0.05μm pores.
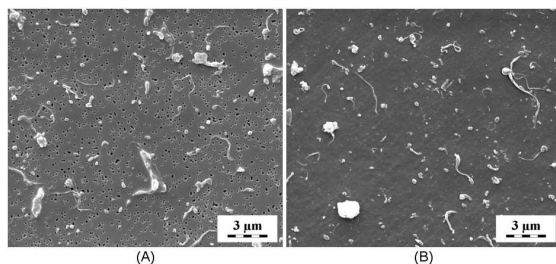


*Fig. 2 The representative FESEM micrographs of the PC membranes with pore size 0.1 μm (A) and 0.05 μm (B).*

Image analysis confirmed the qualitative FESEM results. The final histograms are given in Fig.3; aggregates were excluded from the image analysis. The average equivalent diameters of wear particles on the membranes with pore size 0.1 μm and 0.05 μm were 0.27 μm and 0.11 μm, respectively.
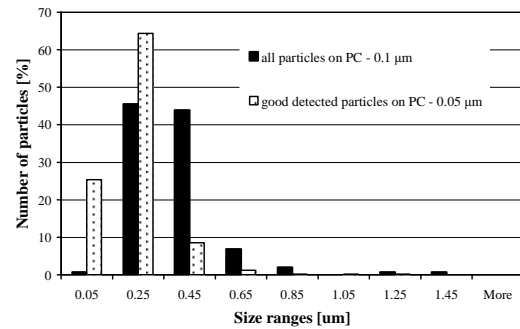


*Fig. 3. Histograms of the debris depicted in the micrographs in the Fig. 2.*

Our experience with 0.1μm membranes is similar to that of Scott et al. [1] who found that a substantial number of wear particles passed freely through the pores of the 0.2μm membranes, which resulted in an underestimation of particle number and an overestimation of particle size.

## Conclusion
1. We confirmed that sonication of the UHMWPE wear debris suspension and pre-filtration through PC membrane filter with pore size 10 μm is necessary in order to minimize aggregation and corresponding losses of the wear particles.
2. Pre-filtration through PTFE membranes was faster in comparison with PC membranes, but it resulted in higher losses of the wear particles.
3. The smaller average size of wear particles lead to higher losses during final filtration on PC membrane with 0.1μm pores, as proved by image analysis of PC membranes with 0.05μm pores.

## References
[1] Scott et al. (2001) Do current wear particle isolation procedures underestimate the number of particles generated by prosthetic bearing components? Wear, 250, 1213-1217.
[2] Slouf M et al. (2007) Isolation, characterization and quantification of polyethylene wear debris from periprosthetic tissues around total joint replacements. Wear, 262, 1171-1181.
[3] Matthews JB et al. (2000) Comparison of the response of primary human peripheral blood mononuclear phagocytes from different donors to challenge with model polyethylene particles of known size and dose. Biomaterials, 21, 2033-2044.
[4] Slouf M et al. (2008) Quantification of UHMWPE wear in periprosthetic tissues of hip arthroplasty: Description of a new method based on IR and comparison with radiographic appearance. Wear, 265, 674-684.

## Acknowledgement

# THERMAL AND MECHANICAL TREATMENTS TO OPTIMIZE THE MORPHOLOGY OF UHMWPE FOR RADIATION CROSSLINKING

Boffano Michele*[1,2], Bistolfi Alessandro[1,2], Bracco Pierangiola[3], Bellare Anuj[2], Costa Luigi[3], Brach del Prever Elena[1]

[1]Department of Orthopaedics and Traumatology and HM, CTO/M. Adelaide Hospital, Università degli Studi di Torino, Via Zuretti 29, 10126 Torino, Italy   *boffano@inwind.it
[2]Department of Orthopedic Surgery, Brigham & Women's Hospital Harvard Medical School, Boston, MA, USA
[3]IFM Chemistry Department, Università degli Studi di Torino, Torino, Italy

## Introduction

Radiation crosslinking imparts high wear resistance to ultra-high molecular weight polyethylene (UHMWPE). Irradiated UHMWPE is remelted to completely quench free radicals or annealed close to but below the melting temperature in order to avoid undesirable oxidative degradation. Various studies have shown that annealing is preferred over melting to retain mechanical properties. On the other hand, it has also been shown that only remelting is completely effective in preserving the material from oxidation. In this study, we uniaxially compressed UHMWPE prior to irradiation to alter its morphology. We hypothesized that compression would decrease crystallinity and thin down the crystalline lamellae. Low crystallinity and thin lamellae are desirable since they, when irradiated, lead to a higher crosslink density compared to high crystallinity UHMWPE with thick lamellae.

## Materials and Methods

GUR 1020 UHMWPE (Ticona, Bayport TX) compression molded sheets (MediTech Medical Polymers, Fort Wayne, IN) were sectioned into approximately 30mmx25mmx25mm blocks. Each block was preheated to 110ºC or 130ºC and compressed to various compression ratios (CR=Initial height/Final height) using a Carver hydraulic press. Samples were then cooled to room temperature and unloaded. A Perkin Elmer Pyris differential scanning calorimeter (DSC) was used to measure melting temperature and crystallinity (n = 3), using a heat of fusion, $dh_f$, of 293 J/g. Lamellar thickness (L) was calculated using the Gibb's Thomson equation: $L=2s_e T^0_m/[dh_f(T^0_m-T_m)]$ where $s_e$ ($=9x10^{-6}$ J/cm) is the lamellar surface free energy and $T^0_m$ is the equilibrium melting temperature for polyethylene ($=145.1ºC$) and $T_m$ is the observed melting temperature.

## Results and discussion

Uniaxial compression of UHMWPE at 110ºC led to a decrease in both peak melting temperature and crystallinity up to a compression ratio of 3.16, and then began to increase again at higher compression ratios. Both the crystallinity and lamellar thickness were significantly lower ($p<0.05$, ANOVA) in UHMWPE with a CR of 3.16 compared to uncompressed control. At 130°C, there was no statistically significant change in crystallinity with compression ratio but the lamellar thickness of UHMWPE at a compression ratio of 3.32 and 4.03 was significantly lower than that of the uncompressed control.

This study showed that uniaxial compression at elevated temperature significantly altered the morphology of UHMWPE. Compression at 110ºC led to a significant decrease in the crystallinity from 49.5% to 40.7% at a compression ratio of 3.16. This study is in agreement with previous studies, which showed that solid-state deformation leads to deformation in the crystalline regions via chain slip mechanisms followed by fragmentation of lamellae at higher strains, ultimately leading to the formation of relatively thin, oriented crystallites at very high strains. At 110ºC, the low crystallinity at a compression ratio of 3.16 indicates that extensive lamellar fragmentation must have occurred up to this compression ratio, followed by formation of oriented crystallites at higher compression ratios. At 130ºC, the lack of a significant decrease in crystallinity with compression is probably since there are fewer constraints to deformation in the partially melted state, and strain induced crystallization would compensate for any loss of crystallinity associated with fragmentation. It is preferable to perform the deformation at 110ºC than 130ºC, so that both lamellar thickness and degree of crystallinity decrease simultaneously. If the compressed UHMWPE is irradiated, there would be a higher degree of crosslinking and less trapped free radicals due to a larger amorphous fraction and a lower crystalline fraction. During post-irradiation annealing, free radicals associated with thin lamellae are more likely to be driven out and quenched compared to free radicals present in thick lamellae.

## Conclusion

In conclusion, uniaxial compression is an effective processing technique to decrease the crystallinity and lamellar thickness of UHMWPE, providing more amorphous content to maximize crosslinking

and minimize trapped free radicals during irradiation. Such a crosslinked UHMWPE would be more wear and oxidation resistant than UHMWPE irradiated without performing solid-state compression.

# Oxidative Stability Studies in UHMWPE

Venkat S. Narayan*[1], Richard King[1], and Askim Senyurt[1]

[1] *DePuy Orthopaedics Inc., PO Box 988, 700 Orthopaedic Drive, Warsaw, IN 46581, USA.*

## Introduction

The change in mechanical characteristics of UHMWPE with oxidation has been extensively reported [1]. This study characterizes the response different UHMWPE materials to oxidation using two different accelerated aging protocols. These include non-irradiated and gamma irradiated UHMWPE in air at 30 KGy, as well as UHMWPE that is stabilized with an antioxidant, Pentaerythritol tetrakis [3-(3,5-di-tert-butyl-4-hydroxyphenyl) propionate], hereafter referred to as **PBHP**.

## Materials and Methods

* Non-irradiated GUR 1020 (Ticona), hereafter referred to as **NI-1020**, that has been used in this study was consolidated by ram extrusion at MediTECH Medical Polymers.
* Ram extruded and gamma-irradiated GUR 1020, hereafter referred to as **GA-1020**, is generated by irradiation at a dose of 30 KGy in air.
* GUR 1020 that is stabilized with 0.075% (w/w) **PBHP** prior to consolidation by compression molding and gamma irradiation to 75 KGy is hereafter referred to as **AO-1020**.

Two accelerated aging protocols were undertaken in the current study:

1. ASTM F-2003 Protocol: This involved exposure of the UHMWPE materials being aged to a pressure of 5 atm. of $O_2$ at 70°C. While the standard protocol calls for a period of 2 weeks for the aging, the current study has been employed to generate materials at various periods of aging from 7 to 40 days.

2. The Dartmouth Aging Protocol: This involved exposure of the UHMWPE materials being aged to 3 atm. of $O_2$ at 63°C [2]. This protocol was employed for the same time period of aging as in the ASTM protocol.

Characterization of the non-aged and aged materials involved:
a. Oxidation Index by FTIR as described in ASTM F 2102
b. Crystallinity by DSC per ASTM F 2625
c. Tensile testing, Type IV, per ASTM F 638
d. Double Notched Impact per ASTM F 648

## Results and discussion

### A. Oxidation Behavior:

Based on extensive studies of various experimental conditions to simulate clinically observed oxidation behaviour, the conditions employed in the Dartmouth protocol were defined. The ASTM protocol conditions are more aggressive than those for the Dartmouth protocol. This is confirmed by the higher rate of increase in the oxidation index for non-stabilized systems (**NI-1020 & GA-1020**). At the same time, the antioxidant stabilized **AO-1020** shows no increase in oxidation index in either protocol. **NI-1020** has a slower rate of increase in oxidation index relative to **GA-1020.** This is consistent with the need for free radicals along with oxygen for the polymer to incur oxidation. It was also noted that the non-irradiated polymer undergoes high levels of oxidation by 40 days with the ASTM protocol. This is contrary to clinical experience where no significant *in-vivo* oxidation has been detected with non-irradiated polyethylene. The ASTM **(A)** and Dartmouth **(D)** Oxidation Indices for all the materials tested are summarized in **Table 1**.

| Sample Condition | Max Oxidation Index | | | | | |
| --- | --- | --- | --- | --- | --- | --- |
| | NI - 1020 | | GA - 1020 | | AO - 1020 | |
| | A | D | A | D | A | D |
| **Non-aged** | 0.043 | | 0.183 | | 0.343 | |
| **7 day aged** | 0.097 | 0.066 | 0.565 | 0.455 | 0.344 | 0.640 |
| **14 day aged** | 0.181 | 0.086 | 1.105 | 0.792 | 0.293 | 0.613 |
| **28 day aged** | 2.562 | 0.109 | 11.241 | 0.999 | 0.400 | 0.299 |
| **40 day aged** | 11.524 | 0.446 | 15.996 | 2.628 | 0.392 | 0.389 |

*Table 1 – Oxidation Index with Accelerated Aging*

The trend in oxidation with aging is displayed in **Figures 1a** & **1b** (ASTM & Dartmouth Aging protocols respectively).
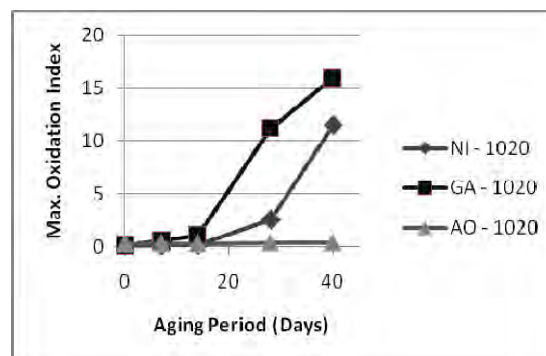


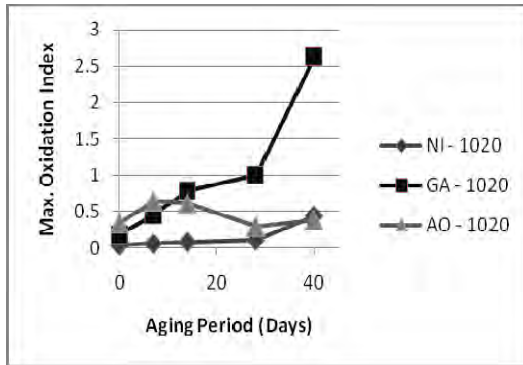*Figure 1a – Maximum Oxidation Index with ASTM Aging*

*Figure 1a – Maximum Oxidation Index with Dartmouth Aging*

**B.  Analysis of Crystallinity with Oxidation:**
The changes in percent crystallinity was monitored as a function of aging by each protocol and summarized in **Tables 2**.

| Sample Condition | % Crystallinity | | | | | |
|---|---|---|---|---|---|---|
| | NI - 1020 | | GA - 1020 | | AO - 1020 | |
| | A | D | A | D | A | D |
| Non-aged | 53.8 | | 56.5 | | 58.8 | |
| 7 day aged | 56.4 | 55.7 | 59.5 | 58.8 | 59.0 | 60.2 |
| 14 day aged | 56.9 | 55.1 | 61.1 | 60.6 | 58.0 | 60.2 |
| 28 day aged | 78.9 | 56.1 | 75.9 | 65.1 | 61.2 | 62.2 |
| 40 day aged | 73.3 | 60.2 | 75.7 | 69.7 | 60.1 | 59.6 |

*Table 2 – % Crystallinity with Accelerated Aging*

The percent crystallinity appears to be quite sensitive to the progression of oxidation for the non-stabilized polymers in that the change in percent crystallinity is higher in the ASTM protocol relative to the Dartmouth protocol. In case of the antioxidant-stabilized materials, on the other hand, the stabilization is clearly evidenced with no change in crystallinity by either protocol.

**C.  Tensile Property Response to Oxidation**
The changes in tensile properties, viz. yield strength **(YS)**, ultimate tensile strength **(UTS)** and % elongation at break **(%)** were monitored as a function of aging by each protocol. For both protocols, the properties are summarized in **Tables 3a** & **3b**.

| Aging Period (Days) | Tensile Properties with ASTM Aging | | | | | | | | |
|---|---|---|---|---|---|---|---|---|---|
| | NI – 1020 | | | GA – 1020 | | | AO - 1020 | | |
| | YS MPa | UTS MPa | % | YS MPa | UTS MPa | % | YS MPa | UTS MPa | % |
| 0 | 22 | 42 | 416 | 22 | 42 | 397 | 23 | 46 | 336 |
| 7 | 22 | 44 | 434 | 24 | 45 | 508 | 24 | 47 | 324 |
| 14 | 23 | 39 | 427 | 27 | 27 | 578 | 24 | 49 | 329 |
| 28 | 6 | 24 | 4 | * | * | 0 | 24 | 49 | 347 |
| 40 | 2 | 4 | 0 | * | * | * | 25 | 50 | 342 |

*Table 3a – Tensile Properties with ASTM Aging*
 *  *Too brittle to measure*

| Aging Period (Days) | Tensile Properties with Dartmouth Aging | | | | | | | | |
|---|---|---|---|---|---|---|---|---|---|
| | NI - 1020 | | | GA – 1020 | | | AO - 1020 | | |
| | YS MPa | UTS MPa | % | YS MPa | UTS MPa | % | YS MPa | UTS MPa | % |
| 0 | 22 | 42 | 426 | 22 | 42 | 397 | 23 | 46 | 336 |
| 7 | 22 | 47 | 433 | 24 | 45 | 481 | 24 | 47 | 338 |
| 14 | 23 | 48 | 446 | 26 | 40 | 587 | 24 | 48 | 341 |
| 28 | 23 | 36 | 411 | 11 | 22 | 60 | 24 | 49 | 328 |
| 40 | 23 | 33 | 405 | 7 | 22 | 2 | 25 | 50 | 347 |

*Table 3b – Tensile Properties with Dartmouth Aging*

For **NI-1020** and **GA-1020**, the change in UTS and % elongation is suggestive of disentanglement and chain scission in the early stages of the oxidation process, leading to increased ductility initially. At higher aging periods, the chains are cleaved to significant levels causing a complete loss of the polymer viscoelastic properties.

**D.  Double Notched Izod (DNI) Impact Toughness Response to Oxidation**
The changes in double notched Izod impact toughness was monitored as a function of aging by each protocol and summarized in **Tables 4**.

| Sample Condition | DNI Toughness (kJ/m$^2$) | | | | | |
|---|---|---|---|---|---|---|
| | NI - 1020 | | GA - 1020 | | AO - 1020 | |
| | A | D | A | D | A | D |
| Non-aged | 126 | | 101 | | 74 | |
| 7 day aged | 136 | 136 | 103 | 105 | 74 | 73 |
| 14 day aged | 143 | 140 | 36 | 88 | 73 | 74 |
| 28 day aged | 10 | 131 | 1 | 10 | 74 | 75 |
| 40 day aged | 7 | 39 | 2 | 4 | 74 | 75 |

*Table 4 – DNI Toughness with Accelerated Aging*

Tracking with the oxidation behavior, both, **NI-1020** and **GA-1020** show a complete loss of impact toughness in 40 days of aging per the ASTM protocol.
The milder Dartmouth protocol shows a more gradual drop in the impact toughness for **NI-1020** while **GA-1020** shows a complete loss of toughness in 40 days.
**AO-1020**, on the other hand, maintains its toughness throughout both aging protocols.

**Conclusion**
- The antioxidant-stabilized UHMWPE is resistant to oxidation by either protocol.
- Chain scission and disentanglement is manifested by an increase in crystallinity upon oxidation.
- Initial mechanical response to accelerated aging is increase in ductility before embrittlement.

**References**
[1]  C.M.Rimnac *et al.,* J. Bone Joint Surg., **76A**, pp 1052-56, (1994).
[2]  J.P.Collier *et al.*, CORR, **414**, pp. 289-304, (2003).

# EPR STUDY OF IRRADIATED UHMWPE

## M.Cristina Paganini*, Valentina Brunella, Mario Chiesa

*[1]* *Dipartimento di Chimica IFM, Università degli Studi di Torino e NIS Centre of excellence, via Giuria 7 – 10125 Torino- Italy. E-mail: mariacristina.paganini@unito.it*

**Introduction**

UHMWPE is widely used in orthopedic technologies since several years. At the present the sterilization process with high energy radiations is spreading more and more. [1] With the expression "high energy radiations" we indicate γ radiation as well as electron beams. UHMWPE (Ultra High Molecular Weight Poly-Ethylene) has been irradiated with electron beam at different doses. Irradiation generates radicals in the material. [2] EPR technique has been used to detect radicals and to give a final assignment to these radical species. EPR spectra of the trapped intermediates generated by irradiation have been deeply studied in the past [3] because it can provide detailed information about the nature of the radicals and also about their concentration.

**Materials and Methods**

Medical grade UHMWPE (Gur 1050, Poly Hi Solidur – MediTECH Division, Fort Wayne, USA) with a molecular mass higher than $5 \cdot 10^6$ u was used as resin powder (Pe-1). The sample has been e-beam irradiated at 60 kGy, at RT, under vacuum, and has been kept in liquid nitrogen until the measurement began.

Irradiated samples were characterized by EPR spectroscopy to investigate the radicals evolution and their modification.

EPR spectra were recorded in the temperature range 77 – 370 K on a Bruker EMX operating in the X band mode. Experimental settings were as follows: microwave power range from 0.1 to 100 mW, scan width 300 gauss, modulation amplitude 2.0 Gauss. All the obtained EPR signals showed g values around the g value for free electron, g ≈ 2.000. All EPR spectra were reported in magnetic field (B) units of Gauss. Few experiments have been performed with a pulse EPR machine, Bruker Elexys.

**Results and discussion**

UHMWPE samples have been irradiated in vacuo at room temperature (RT) with a radiation dose of 60 kGy) and then kept frozen in liquid nitrogen (77K). In Figure 1 two spectra recorded at different microwave power (0.1 mW and 100 mW) are reported. Due to different power saturation behaviour it is possible to observe an evolution of the spectrum increasing the microwave power and,

in this case, two different species have been isolated.

The signal at 0.1 mW is a sextet (species named A), on the contrary the signal recorded at 100 mW is a septet (named B). In the range between 1 and 100 mW the observed spectra are a superimposition of both components A and B. This, of course, can complicate the spectrum and it affects an easy interpretation of the signals.

Species A, observed soon after irradiation, show a six line EPR spectrum centred at g = 2.0002 very close to the value of the free electron with a hyperfine coupling constant of about 30 Gauss.
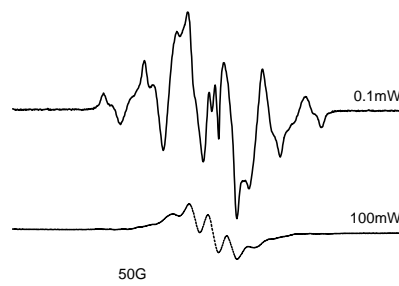


*Fig.1 EPR signal of irradiated UHMWPE recorded at different microwave power (species A and species B).*

Species B shows a seven line spectrum centred again at g = 2.0002 and with a hyperfine line of about 16 Gauss. Double integration of signal A and B evidenced a deep difference in spin concentration of the two species.

In the time after irradiation, both signals decay but with different rate. Signal A, decays faster than the other and almost disappears in the first 20 hours. After 24 hours species A is gone and a new signal, much less intense appears (named C) as reported in figure 2. Signal C proceeds to decay and 2 days after irradiation no more EPR signals can be recorded. Signal C is again a septet centred at g = 2.000 and with a coupling constant of about 20 Gauss. On the contrary signal B decays very slowly and one month later it is still evident and with the same shape.
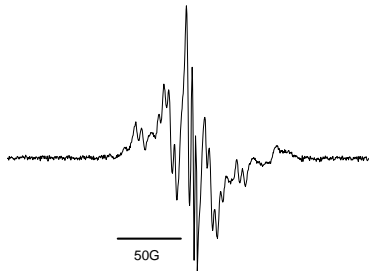
*Fig.2 EPR signal of irradiated UHMWPE recorded after 24 hour. A new species appear power (species C)*

ENDOR experiment and also measurements with a pulse EPR machine have been performed to confirm the results obtained with CW-EPR. The presence of species A and C have been confirmed, in addition pulse experiments showed up that species C is already present immediately after irradiation, but it is not observable by CW-EPR because of its very low intensity and also because of the presence of species A in the same field region. Species B, on the contrary has not been observed, probably because of its very fast relaxation time that doesn't allow the detection of the species.

As reported in literature species A can be attributed to alkyl radicals and species C to allyl radicals. The attribution of species B is not straightforward yet, especially because, it is not observable with pulse EPR. Further investigations are necessary to understand its nature and its role in the solid polymer.

**Conclusion**

After irradiation with high dose of radiation (60 kGy) UHMWPE shows the presence of radicals. These radicals can be observed by EPR technique. Three different families pf species have been recorded, alkyl species, allyl species and a new species, still not assigned.

**References**

[1] Durant J, Jahan M.S., Nuclear Instruments and Methods in Physics Research B 236, 160-165 (2005).

[2] Costa L., Brunella V., Paganini M.C., Baccaro S., Cecilia A., Nuclear Instruments and Methods in Physics Research B 215, 471-478 (2004)

[3] Onishi S, Ikeda Y., Kashiwagi M., Nitta I., Polymer 2 (C) 119-141 (1961).

# CHARACTERIZATION OF A POLYCARBONATE-URETHANE ELASTOMER FOR ORTHOPEDIC APPLICATIONS.

Bracco, P[*1], Zanetti, M[1], Cipriani, E[1], Costa, L[1]

[1]*University of Torino, Italy*

*pierangiola.bracco@unito.it*

## Introduction

Polyurethane (PU) elastomers are used in a wide range of medical devices thanks to their versatility and peculiar mechanical properties. PUs are a heterogeneous family of polymers, their molecular structure affect the physical behavior, so they could cover a great range of application. In the recent past, Polycarbonate urethane (PCU) has also been proposed as a suitable candidate to substitute UHMWPE as a bearing material in arthroplasty, thanks to the presumed superior physical and mechanical properties of the material. [1,2]

PUs are characterized by a more complex chemical structure than many of the most widely produced polymers, such as polyethylene. They typically comprise three reactive components: a hard segment (diisocyanate), a soft segment (aliphatic polycarbonate in PCU) and a chain extender. These segments are partially immiscible setting biphasic morphology, in which hard segment microdomains are dispersed in a matrix of soft segments. There is some degree of mixing thanks to hydrogen bonding between the two segments, so these microdomains act as thermally labile physical cross-linking sites as well as fillers for the rubbery soft-segment matrix. This peculiar structure is responsible for the versatility in physical and mechanical properties.

Nevertheless, small changes to this structural organization (induced for example as a consequence of processing, sterilization, fluids absorption, etc.) can result in significant variations in the mechanical and chemical properties and affecting the material performances.

The objective of this study was the characterization of a commercial PCU, with a special attention to the changes induced to its chemical structure by thermal treatments.

## Materials and Methods

The investigated PCU was Bionate® 80A (The Polymer Technology Group, Berkley, CA) in the form of pellets and was analyzed as-received. Two Bionate® 80A new acetabular component (Active Implant Corporation, Memphis, TN) were also tested for comparison. The first (P1) was not sterilized; the second (P2) was a prosthesis implanted for four month.

Thermogravimetry (TG) experiments were conducted in air and nitrogen, from room temperature to 800 ºC at a heating rate of 10ºC/min.

Differential scanning calorimetry (DSC) experiments were conducted in nitrogen atmosphere, from -75°C to various temperatures, up to 250°C, at a heating rate of 20°C/min.

Attenuated Total Reflectance Fourier Transform Infrared (ATR-FTIR) spectra were collected with a diamond crystal, using a resolution of 4 cm$^{-1}$ and 16 scans per spectrum.

## Results and discussion

Thermogravimetric curves obtained from Bionate® 80A, Fig. 1, exhibit a quite simple decomposition path: the material starts to decompose at about 230°C, both in nitrogen and in air. A black residue is observed in the sample pan after the treatment in nitrogen atmosphere. It must be pointed out that the onset of decomposition is not too far from the suggested processing conditions (180-210°C).
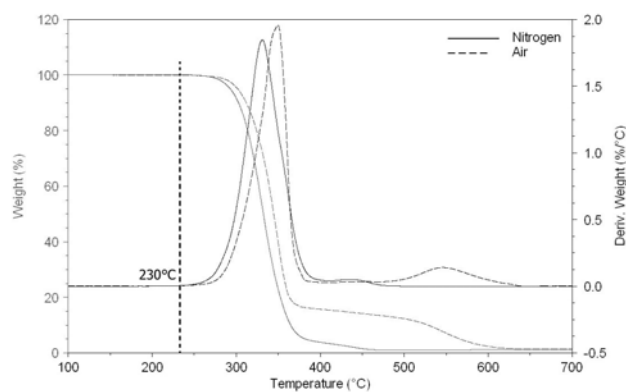


*Figure 1*

Thermogravimetric analyses (not showed) of the two prostheses display the same behavior of Bionate 80A in air, instead the experiments conducted in nitrogen show a different behavior. In fact the negligible signal at 450°C in Fig. 1 is amplified in the case of prostheses.

Fig. 2, curve a shows the DSC thermogram of the as-received Bionate® 80A. Three signals can be identified and, according to literature [3], have been attributed as follows:

- at -21°C: the glass transition temperature ($T_g$) of the soft, polycarbonate-based segment,
- at 120°C: an endothermic phenomenon due to disruption of the short-range ordered domains of the hard-phase,
- at 160°C: an endothermic peak resulting from the mixing of hard and soft phases.

During the cooling ramp there is only a signal at –25°C, which could be attributed to the glass transition of the soft phase.

Since the structural organization of the polymer changes as a function of the temperature, some

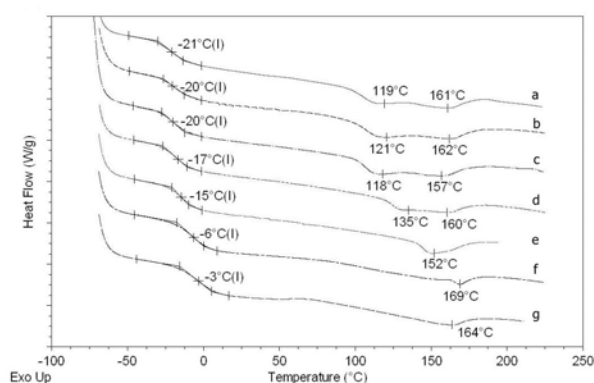thermal treatments were performed in order to understand this behavior.



*Figure 2*

DSC experiments, Fig. 2, were conducted on samples previously heated under nitrogen to: b) 80°C, c) 100°C, d) 120°C, e) 140°C, f) 160°C, g) 180°C. It was found that the $T_g$ of the soft phase shifts to progressively higher temperatures, increasing the temperature of the thermal treatment, indicating a "stiffening" effect due to incomplete recovery of the original structure after the first heating, this suggests a higher degree of hard-soft segment mixing. Also the first endothermic peak shifts to higher temperature, suggesting an increase in the average length of the hard segments involved.
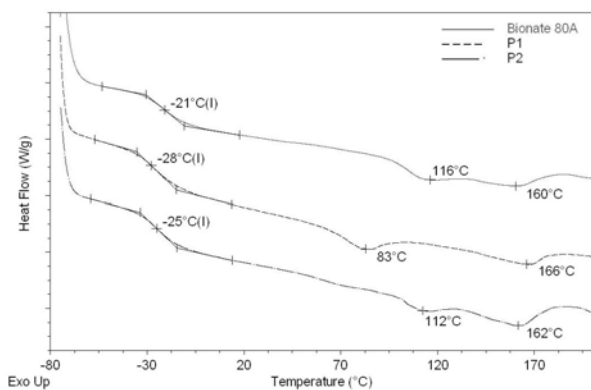


*Figure 3*

Fig. 3 shows the DSC thermogram of the acetabular component. For the P1 both the $T_g$ and the first endothermic process are shifted, compared with those of the original material. Instead for the P2 the signal are more similar to the background material.

Fig. 4 shows the FTIR spectra of the original material and those of the same sample heated to 200°C and allowed to cool on the ATR crystal. Spectra have been recorded up to 60 hours after the thermal treatment. The absorption peak at 1737 cm$^{-1}$ is characteristic of the soft polycarbonate-based segment (νC=O carbonate), while that at 1700 cm$^{-1}$ can be attributed to the ordered, hard polyurethane-based segment (νC=O urethane, hydrogen bonded). The shoulder appearing at 1720 cm$^{-1}$ after heating can be attributed to a shift of the latter, due to disruption of the short-range order (including H-

bonding). It was observed that the subsequent spectra evolved towards that of the original material, but the equilibrium was not reached during the time-span of the experiment.
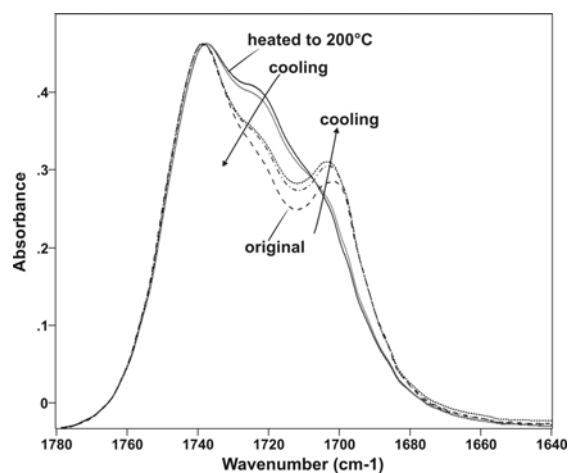


*Figure 4*

The measurements performed suggest that, once perturbed the equilibrium-structure (i.e. by heating), the material tends to re-form a structure similar to the initial one, but with a very slow kinetic.

In addition, a residue was found on the ATR crystal once removed the original, unheated, sample. The same residue was observed after extraction of the sample in cyclohexane. Further experiments are in progress in order to investigate the nature of this residue.

## Conclusion

Basically, these results indicate that the structural organization of this material appears to be very sensitive to the thermal history previously given to the material itself (for example during processing). In particular, the acetabular component exhibits quite different characteristics from the pristine material, possibly as a consequence of the manufacturing process and/or storage conditions.

It can be concluded that, even though PCU elastomers seem to be promising materials for arthroplasty, they exhibit a strongly significant thermal sensitivity. These preliminary results suggest that, in order to preserve the original properties, a particular care must be observed during processing, sterilization and storage of PCU devices.

## Acknowledgment

## References
[1] Geary et al, J Mater Sci: Mater Med 2008 (19):3355–3363,
[2] Kurtz et al. ORS 2009, 471.
[3] Martin et al, J Appli Polym Sci 1997 (64): 803-817

# EFFECTS OF ELASTOMER BLENDING ON THE DUCTILITY AND COMPLIANCE OF UHMWPE

Boffano Michele*[1,2], Bistolfi Alessandro[1,2], Bracco Pierangiola[3], Carpentieri, Ilenia[3], Bellare Anuj[2], Brach del Prever Elena[1]

[1]Department of Orthopaedics and Traumatology and HM, CTO/M. Adelaide Hospital, Università degli Studi di Torino, Via Zuretti 29, 10126 Torino, Italy   *boffano@inwind.it
[2]Department of Orthopedic Surgery, Brigham & Women's Hospital Harvard Medical School, Boston, MA, USA
[3]IFM Chemistry Department, Università degli Studi di Torino, Torino, Italy

## Introduction

Ultra-high molecular weight polyethylene (UHMWPE) has been used, for over four decades, as a bearing material in total joint replacement prostheses. Its resistance to wear and high fracture toughness make it preferable compared to other polymers. Historically, rim cracking of misaligned acetabular cups due to impingement with metallic stem, fatigue related damage in tibial components of knees and fracture of metal-backed patellar components have determined catastrophic failures. Conformal implant have been designed in total knee arthroplasties to a decrease in contact stresses, but it is preferable utilize a materials design approach to prevent fracture since conformity is often achieved by sacrificing range of motion.

In this study, UHMWPE was blended with an ethylene-octene elastomer which possesses rubber-like characteristics. We tried to obtain a new material substantially more ductile (large maximum strain) and with higher compliance (or low modulus) so that it would not fracture easily, compared to pure UHMWPE.

## Materials and Methods

UHMWPE powder type GUR 1050 (Ticona, Oberhausen, Germany) and ENGAGE™ 8200 ethylene-octene elastomer pellets (Dow Chemical Company, Midland, MI) were blended using a Thermo Haake Minilab (Thermo Fisher Scientific, Karlsruhe Germany) Compounder at a temperature of 160°C. Extruded rods (2mm diameter) of the blends were placed in a mold to obtain 2mm thick discs using a Carver hydraulic press (180 °C temperature). Three different blends were prepared: 5%, 10% and 25% of weight fractions of UHMWPE. Control samples were obtained from compression molded discs of 100% UHMWPE and 100% elastomer. From the discs, tensile specimens were cut out (type V ASTM D638). Tensile tests were conducted on each group (n=3) using a Adamel Lhomargy DY22 dynamometer (crosshead speed of 10mm/min) and controlled with Labview 7.0 Express software (National Instruments). Melting temperature and crystallinity (n = 3) using a heat of fusion, $dh_f$, of 293 J/g were measured using a differential scanning calorimeter (DSC, Perkin Elmer Pyris). Lamellar thickness (L) was calculated using the Gibb's Thomson equation: $L=2s_e T^0_m/[dh_f(T^0_m-T_m)]$ where $s_e$ (=$9\times10^{-6}$J/cm) is the lamellar surface free energy, $T^0_m$ is the equilibrium melting temperature for polyethylene (=145.1°C) and $T_m$ is the observed melting temperature.

## Results and discussion

The modulus of the 100% UHMWPE, revealed by tensile tests, was substantially higher than the modulus of the blends as well as the pure elastomer ($p<0.05$, ANOVA, Fisher's PLSD test), as shown in Table 1. No statistically significant difference ($p>0.05$, ANOVA) was observed either in the modulus between the blends and the elastomer or in the maximum stress was observed when comparing the following pairs: 0% and 5% UHMWPE blend, 5% and 10% UHMWPE blends, and 10% and 25% UHMWPE blends. Only the maximum stress was significantly higher for pure UHMWPE compared to any of the blends and pure elastomer. Except for the maximum strain between the 0% and 5% UHMWPE blends, all other maximum strains were significantly different from each other ($p<0.05$, ANOVA). The general trend of the samples showed that the blends and pure elastomer had substantially higher maximum strain compared to the pure UHMWPE (Figure 1). A monotonical decrease of crystallinity, melting temperature and lamellar thickness was observed with decreasing weight fraction of UHMWPE (Table 2) and the differences were statistically significant for all groups of samples.

This study shows that blending UHMWPE with a polyethylene-like elastomeric copolymer can increase the ductility (maximum strain) and the compliance (inverse of modulus). The initial strain was dominated by stretching of the elastomeric region and this fact can explain the lack of statistically significant difference in the modulus of the elastomer and blends up to 25 weight percentage UHMWPE. It also implies that the blends of UHMWPE and elastomer were immiscible. The modulus did not increase with weight fraction of UHMWPE up to 25 weight

percent, indicating that there must be regions in the blend that are UHMWPE rich and the majority of the region was elastomer-rich. Probably the UHMWPE was segregated in the blend, acting as flaws in the elastomeric matrix, and it can explain why the maximum stress decreased with increasing UHMWPE weight fraction. The fracture at low stress may be overcome by radiation crosslinking of the UHMWPE-elastomer blend in order to bond chemically UHMWPE to the elastomeric macromolecules.

**Conclusion**

In order to decrease or even prevent catastrophic failure blending of UHMWPE with a polyethylene-like elastomer may be an attractive alternative. An UHMWPE with rubber-like properties would have higher ductility and compliance.

| Sample ID | Modulus (MPa) | Maximum strain (%) | Maximum stress (MPa) |
|---|---|---|---|
| 100% UHMWPE | 225.2 ± 26.4 | 740 ± 32 | 55.4 ± 1.7 |
| 25% UHMWPE | 3.1 ± 0.6 | 1069 ± 126 | 2.8 ± 0.3 |
| 10% UHMWPE | 0.7 ± 0.6 | 2376 ± 37 | 5.6 ± 0.6 |
| 5% UHMWPE | 1.0 ± 0.3 | 2928 ± 66 | 7.1 ± 0.2 |
| 0% UHMWPE | 2.0 ± 0.5 | 2920 ± 248 | 9.4 ± 1.1 |

*Table 1. Modulus, maximum strain and maximum stress for various weight fractions of UHMWPE in the blend obtained from tensile tests.*

| Sample ID | X [%] | $T_m[^{\circ}C]$ | L [nm] |
|---|---|---|---|
| 100% UHMWPE | 48.3 ± 0.2 | 136.4 ± 0.2 | 29.5 ± 0.5 |
| 25% UHMWPE | 9.5 ± 0.2 | 134.3 ± 0.3 | 23.7 ± 0.8 |
| 10% UHMWPE | 3.4 ± 0.1 | 133.3 ± 0.3 | 21.8 ± 0.5 |
| 5% UHMWPE | 1.7 ± 0.4 | 132.7 ± 0.2 | 20.7 ± 0.3 |
| 0% UHMWPE | - | - | - |

*Table 2. Degree of crystallinity, X, melting temperature, Tm, and lamellar thickness, L, versus weight percentage UHMWPE in the blend*
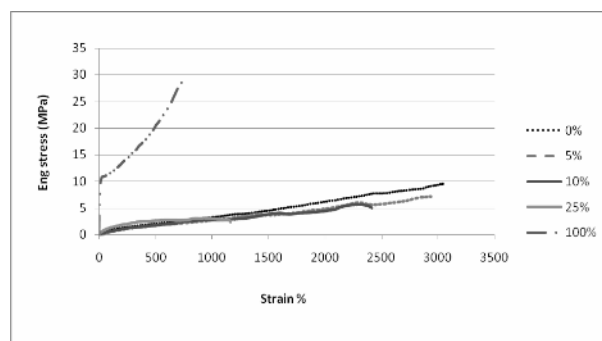


*Figure 1. Stress-strain curves for different weight fractions of UHMWPE in the samples*

# A NEW GENERATION OF EASILY CROSSLINKABLE POLYETHYLENE COPOLYMERS

Eva Wisse*[1], Nileshkumar Kukalyekar[1], Rob Janssen[1], Tim Kidd[1], Micha Mulders[1], Harold Smelt[2], Jan Stolk[1].

[1] DSM Research, SRU PM, P.O. Box 18, 6160 MD Geleen, The Netherlands,
e-mail: eva.wisse@dsm.com
[2] DSM Dyneema, P.O. Box 1163, 6160 BD Geleen , The Netherlands

## Introduction

Ultra High Molecular Weight Polyethylene (UHMWPE) has been successfully used in total joint arthroplasty for more than 50 years. However, implant lifetime improvement is still an issue. The current paradigm of UHMWPE is threefold: good wear resistance and oxidative stability whilst maintaining mechanical properties [1]. Today's state-of-the-art material is highly crosslinked polyethylene (HXLPE), a high wear resistant material. However, the remaining free radicals after irradiation crosslinking can initiate *in vivo* oxidation and reduce the implant lifetime [2, 3]. Remelting can significantly reduce the amount of remaining free radicals, but will also lower the crystallinity and therefore affect the mechanical properties [4]. Annealing does not influence the properties but also does not remove all free radicals [5].

In this paper we present a new generation of UHMWPE based on copolymerization of ethylene and a diene that forms a highly crosslinked network after only a sterilization dose of gamma-radiation (Fig. 1).
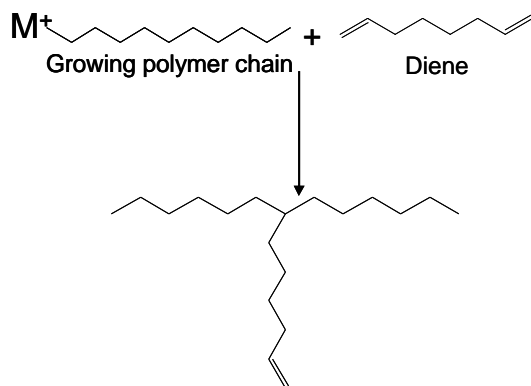


*Fig. 1. Chemistry of a new generation of easily crosslinkable polyethylene copolymer.*

## Experimental

All samples were prepared by copolymerizing ethylene and octadiene. The resulting materials were analyzed with IR and NMR to determine the amount of vinyl double bonds. Two polymers were used as linear reference materials: 1) PEs synthesized under the same conditions as the diene-copolymers but without the addition of diene comonomer and 2) MG003 (DSM).

All powders were compression moulded into blocks of 15 mm thickness. These blocks were irradiated with 25 or 75 kGy (at Beta-Gamma-Services GmbH). The sample dimensions needed for analyses were machined from the corresponding blocks. Swell ratio testing was done according to ASTM F2214-02 to determine the network density and calculate the molecular weight between effective crosslinks (Mc). Wear testing was performed in a Pin-on-Disc wear tester using water/serum lubrication [6].

## Results and discussion

Vinyl double bonds are known to readily react with macroradicals to form Y-crosslinks upon irradiation of (UHMW)PE [7]. By introducing more pendant vinyl bonds in the PE chains, the crosslink efficiency could be increased. A lower number of radicals could be required, thus reducing the oxidative degradation *in vivo*.

To prove this concept various copolymers with increasing amounts of incorporated pendant double bonds were synthesized. Their swell ratio and wear resistance were measured after irradiating them with a sterilization dose (25 kGy of gamma-radiation). The data was compared to reference samples (both linear UHMWPEs) where no diene was added to the reaction vessel (2 – 25 kGy) and to MG003 irradiated with 25 or 75 kGy (Fig. 2). The diene-copolymers show an increasing network density with increasing residual double bond content at the low radiation dose. The sample with 12 C=C per 100.000 C-atoms shows a comparable, even slightly higher, network density than the linear UHMWPE irradiated with 75 kGy. The wear factor is known to be directly related to the network density [8], which is also what was observed for this series of materials.

ESR measurements performed on the diene copolymers and linear UHMWPEs, showed that the amount of remaining (stable) free radicals is 2-3 times lower for samples irradiated with 25 kGy as compared to samples irradiated with 75 kGy (Fig. 3). This shows that this new generation PE has indeed a reduced free radical content due to the lower irradiation dose, whilst maintaining the same degree of crosslinking. Moreover, this suggests that

the irradiated diene-copolymers are more oxidatively stable than conventional HXLPE. Oxidation levels after ageing should confirm this in the near future.
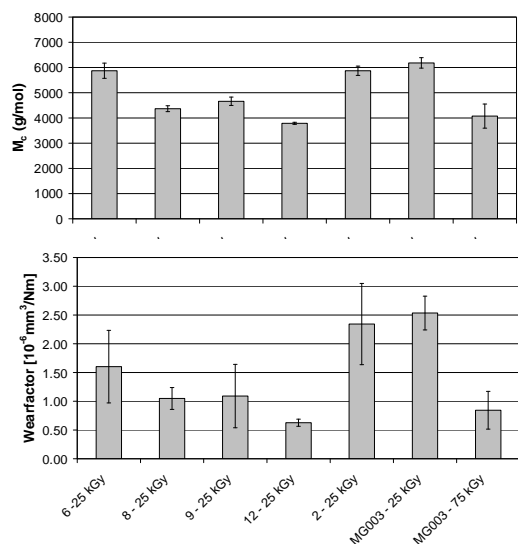


*Fig. 2. Molecular Weight between effective crosslinks (top) and wearfactor (bottom) for copolymers with indicated amount of unsaturations (amount of pendant double bonds per 100.000 C-atoms) and indicated gamma radiation dose (kGy).*
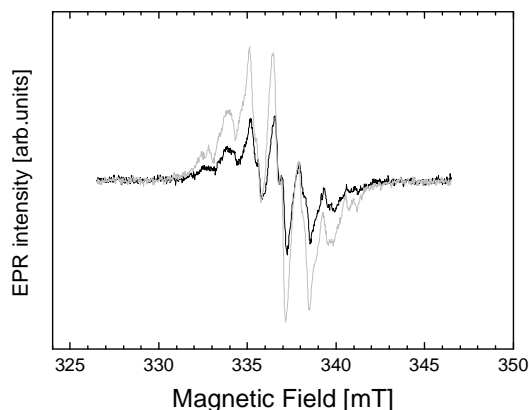


*Fig. 3. ESR spectra on octadiene copolymer with 9 vinyldouble bonds per 100.000 C-atoms after irradiation with 25 (black) or 75 kGy (grey).*

## Conclusion

A new (UHMW)PE grade with low wear levels at 25 kGy & higher oxidative stability was developed by copolymerizing ethylene and octadiene.

These new diene-copolymers show a similar network density and wear resistance as highly crosslinked material (75 kGy) after only a sterilization dosage (25 kGy) of gamma radiation. The reduced remaining free radical content will most probably result in a more oxidatively stable material, which potentially eliminates the need for remelting after crosslinking. This should also give the copolymers improved mechanical properties as compared to current HXLPE grades after remelting. The mechanical properties and the oxidative stability are currently being studied in more detail.

## References

[1] Gomez-Barrena, E.; Puertolas, J.-A.; Munuera, L.; Konttinen, Y. T. Acta Orthopaedica **2008**, *79 (6)*, 832

[2] L. Costa, I. Carpentieri, P. Bracco, Polymer Degaradation and Stability **2008**, 93, 1695

[3] P. Bracco, V. Brunella, M.P. Luda, E.M. Brach del Prever, M. Zanetti, L. Costa, Polymer Degradation and Stability **2006**, 91, 3057

[4] Oral, E.; Malhi, A.; Muratoglu, O. Biomaterials **2006**, 27, 917

[5] Wannomae, K.; Bhattacharyya, S.; Freiberg, A.; Estok, D.; Harris, W.; Muratoglu, O. Journal of Arthroplasty **2006**, 21(7), 1005

[6] Saikko, V. Proc. IMechE **2005**, 219 Part H:J. Engineering in Medicine, 309

[7] a) Bracco, P.; Brunella, V.; Luda, M. P.; Zanetti, M.; Costa, L. Polymer **2005**, 46, 10648; b) Kurtz, S. M. The UHMWPE handbook, Elsevier, **2004**, ISBN 0-12-429851-6; Chapter 11 by L. Costa and P. Bracco.

[8] a) Wang, A. Wear **2001**, 248, 38; b) O.K. Muratoglu; Bragdon, C. R.; O'Connor, D. O.; Jasty, M.; Harris, W. H.; Gul, R.; McGarry, F. Biomaterials **1999**, 20, 1463